INFORMATION TO USERS

This was produced from a copy of a document sent to us for microfilming. While the most advanced technological means to photograph and reproduce this document have been used, the quality is heavily dependent upon the quality of the material submitted.

The following explanation of techniques is provided to help you understand markings or notations which may appear on this reproduction.

1. The sign or "target" for pages apparently lacking from the document photographed is "Missing Page(s)". If it was possible to obtain the missing page(s) or section, they are spliced into the film along with adjacent pages. This may have necessitated cutting through an image and duplicating adjacent pages to assure you of complete continuity.

2. When an image on the film is obliterated with a round black mark it is an indication that the film inspector noticed either blurred copy because of movement during exposure, or duplicate copy. Unless we meant to delete copyrighted materials that should not have been filmed, you will find a good image of the page in the adjacent frame.

3. When a map, drawing or chart, etc., is part of the material being photographed the photographer has followed a definite method in "sectioning" the material. It is customary to begin filming at the upper left hand corner of a large sheet and to continue from left to right in equal sections with small overlaps. If necessary, sectioning is continued again–beginning below the first row and continuing on until complete.

4. For any illustrations that cannot be reproduced satisfactorily by xerography, photographic prints can be purchased at additional cost and tipped into your xerographic copy. Requests can be made to our Dissertations Customer Services Department.

5. Some pages in any document may have indistinct print. In all cases we have filmed the best available copy.

University Microfilms International

300 N. ZEEB ROAD, ANN ARBOR, MI 48106
18 BEDFORD ROW, LONDON WC1R 4EJ, ENGLAND

TZUO, PI-FONG LIN

EFFECTS OF DURATION OF FRINGE OF NOISE AND FRINGE OF SILENCE ON DETECTION OF BRIEF SIGNALS MASKED BY NOISE

City University of New York PH.D. 1980

EFFECTS

OF

DURATION OF FRINGE OF NOISE AND FRINGE OF SILENCE

ON

DETECTION OF BRIEF SIGNALS MASKED BY NOISE

by

Pi-fong Lin Tzuo

A dissertation submitted to the Graduate Faculty in Psychology in partial fulfillment of the requirements for the degree of Doctor of Philosophy, The City University of New York.

1980

This manuscript has been read and accepted for the Graduate Faculty in Psychology in satisfaction of the dissertation requirement for the degree of Doctor of Philosophy.

8/11/80
date

Chairman of Examinating Committee

August 12, 1980
date

Executive Officer

Dr. Eli Osman

Dr. David H. Raab

Dr. Eric Heinemann
Supervisory Committee

The City University of New York

ABSTRACT

EFFECTS

OF

DURATION OF FRINGE OF NOISE AND FRINGE OF SILENCE

ON

DETECTION OF BRIEF SIGNALS MASKED BY NOISE

by

Pi-fong Lin Tzuo

Adviser: Professor Eli Osman

This dissertation is an attempt to further our understanding of the temporal processes involved in the masking of brief signals by noise. The masker was broadband white noise of constant spectrum level (about 46 dB SPL), and its temporal character in relation to the signal was the main independent variable. The signal was either a 400-Hz tone-burst or a broadband noise-burst. Its duration was fixed at 11.5 msec with 2.5 msec rise/fall times. The masking noise was always presented throughout the 11.5 msec signal interval and was otherwise manipulated as follows. In the 'noise-fringe' conditions the masker was symmetrically extended forwards and backwards in time with respect to the signal interval. In the 'gap-fringe' conditions, silent gaps were similarly introduced symmetrically in time on the two sides of the signal interval, in the otherwise continuously

presented masker. Special attention is commanded by the two extreme conditions, usually referred to as 'gated' and 'continuous' masking. Nine one-sided fringe durations ranging from 0 to 95 msec were chosen for the masker settings for each type of fringe and each of the two signals. Psychometric functions were obtained from each of three listeners using a single interval Yes-No procedure. Each psychometric function was converted to a plot of an index of detection (d') in log units vs. signal-to-noise ratio in dB. Regression analysis then yielded threshold (at d'=1) and slope parameters for each such function. Analysis of the joint pattern of changes in threshold and slope is the basis for interpretation of the study.

A brief summary of the results follows. Continuous masking is more effective than gated masking for the tonal signal, but not for the noise signal. For both signals, as the noise-fringe is increased from the gated condition, the threshold first rises along a negatively accelerated course to peak in the vicinity of 25 to 45 msec. Subsequently it drops gradually out to 95 msec, and drops again for the continuous masking condition. As the gap-fringe is introduced the threshold first remains stable, then drops to a minimum at 15 msec, and shows smaller changes thereafter. Slope functions of noise-fringe duration and gap-fringe duration are also similar for both signals. For noise-fringe durations of 0 to 15 msec, the slope remains stable somewhere between .60 to .85, after which it begins to rise gradually, soon crosses unity, and keeps increasing to a maximum less than 2. As the gap-fringe is introduced and expanded, the slope drops smoothly,

crosses unity between 10 to 15 msec, then drops to around .90, and finally decreases to the level of the gated condition.

A general statistical decision theoretic model of a leaky power integrator was derived and applied for the special case of an exponential weighting function. The model provides a reasonable explanation of the data for short noise-fringe and long gap-fringe durations, but generally must be supplemented by other detection processes. Thus, at very brief noise-fringe durations for tones, results may be due to phase-delays. For relatively long noise-fringe durations, results may be consequences of increasing temporal uncertainty (which soon saturates) and decreasing masking of large signal peaks, both of which are consequences of masker transients. Selected parameters of the model and particular features of the results were related to the concept of a 'temporal critical masking interval'.

One major contribution of this research is the demonstration that important restrictions on theoretical interpretations of psychophysical results are implied by analysis of complete psychometric functions.

ACKNOWLEDGEMENTS

I would like to express my deepest appreciation to Professor Eli Osman for serving as my dissertation adviser. Dr. Osman, as my best teacher and one of my best friends, has provided me with invaluable experiences throughout my graduate studies and has undertaken the supervision of this project with unlimited guidance and encouragement.

Sincere graditude is also acknowledged to Dr. David H. Raab and Dr. Eric Heinemann for their support and assistance during the completion of this dissertation.

This investigation was supported by grands (to Dr. Osman) from the United States Department of Health, Education and Welfare, Public Health Service and the PSC-BHE Research Award Progrem of the City University of New York.

TABLE OF CONTENTS

LIST OF TABLES

LIST OF FIGURES

I. INTRODUCTION

In the study of auditory perception, auditory stimuli are analyzed either in the frequency domain or in the time domain. Since Fletcher (1940) proposed the concept of the critical band, which is referred to as the band of nearby effective masking frequencies surrounding the tonal signal, a wealth of research has been generated in the study of auditory perception emphasizing frequency domain analysis. The measurement of the critical band and the maturation of its conceptualization have been heavily investigated, although much remains a mystery (Green and Swets, chapter 10, 1966).

In the literature, there is also a good deal of research in auditory perception dealing with the analysis of auditory stimuli in the time domain. Some have shown that the sensory effects of a stimulus persist for a while after it is terminated. This notion implies that the detectability of a tonal or a noise signal will be affected if it is preceded or followed by a masker. This is known as forward or backward masking. Based on this notion, and also by analogy with the concept of the critical band in the frequency domain, it may be possible to find a critical temporal band for a given signal, that is, a time period during which the masker is 'effective' in masking the signal. The measurement of such a critical temporal masking band should depend on the properties of the underlying 'temporal filtering.' Ideally, the problem would be simplest if the temporal filtering is

independent of the specific task requirements.

Based on this as a starting assumption, the main purpose of this dissertation is to study further properties of the 'temporal filtering' of the auditory system. It is designed to measure a 'critical temporal masking interval' and use it as an index of the effective temporal band of the temporal filter. Such measurement will be made from examinations of data showing changes not only in locations (thresholds) but also in shapes (slopes) of psychometric functions. These psychometric functions relate the percentage of a correct response to the signal level for the detection of either a brief tonal signal or a brief noise signal in a masking noise. The evaluation of some existing models of signal detection in terms of the threshold-slope relation will also be one of the purposes of this research work.

One approach to studying the temporal properties of the auditory system is to fix the signal parameters and manipulate only the properties of the masking noise. Two extreme modes of the manipulation of masker presentation yield the so-called gated and continuous masking paradigms. In one extreme, the gated condition, the masker is gated on and off synchronously with the signal. In the other extreme, the continuous condition, the masker is left on uninterrupted throughout an entire experimental session. The problem of differences between gated- and continuous-masking has received much attention in the literature recently (Green and Sewall, 1962; Green, 1964a, 1969; Campbell, 1966, 1969; Wightman and Green, 1966; Tucker et al., 1968; Leshowitz, 1969; Viemeister, 1974; Schacknow and Raab, 1976;

Wier et al., 1977), since it is important for understanding the dynamic properties of masking. Comparison of the effects of gated and continuous noise maskers is a reference issue for the detection paradigms studied in this research.

It is shown in some studies in the literature, that these two extreme modes of masker presentation, gated and continuous, yield different thresholds and also different slopes of psychometric functions. In order to investigate temporal filtering and the critical temporal masking interval, if it is a useful concept, it is reasonable to manipulate the mode of masker presentation in the following two different ways. One is to start with the gated condition and gradually approach the other extreme (continuous) by extending additional noise fringes on both sides of the signal. The other way is to start with continuous masking (in which the masker duration could be considered as virtually infinite), and gradually approach the other extreme (gated) by removing masking noise through the operation of introducing and gradually increasing silent gaps on both sides of the signal.

Consider a temporal filter with arbitrary shape, but fixed on the time axis. The temporal filter effectively describes the attenuation of noise power at different moments displaced in time from the signal. As the noise-fringe is expanded, we are 'filling the filter' in the sense of adding successively attenuated increments of noise power to the masking process. The sum is maximized for continuous noise. Then, as the silent gap is expanded, we are 'emptying the filter'

in the sense of subtracting successively attenuated increments of noise power from that masking process, until we have again returned to our minimal energy noise masker, the synchronously gated condition. For our particular stimulus paradigm, the mean of the difference in integrated power between signal-plus-noise and noise alone is independent of noise-fringe or gap-fringe duration, and so is that portion of its variance that is a function of stimulus energy in the signal interval. Only the variance is incremented or decremented as noise-fringe or gap-fringe durations are varied. There will be some common value of duration for noise-fringe and gap-fringe where the total variance will be the same, and since the psychometric function will then depend only on changes in signal energy, it will also be the same for the two cases. We will state the argument more carefully later on. It serves as a guideline for our study, where we determine whether there is a common duration of noise-fringe and gap-fringe for which the psychometric functions are identical.

A. Critical Bands in the Frequency Domain

Fletcher (1940) investigated detection in relation to masker frequency spectrum. The subject adjusted a continuous sinusoid until it was just detectable in the presence of the masking noise of variable bandwidth. Fletcher found that when the bandwidth of the noise is decreased while maintaining a constant spectral level, the threshold of the sinusoid located in the middle of the noise band will not be affected until a certain critical bandwidth is reached. From this

point, the signal level needed to hear the tone in the noise diminishes approximately linearly with further decreases in the bandwidth of the noise. This result led Fletcher to assume that the ear acts as a narrow filter with a width equal to that critical band. Only noise within the critical band is effective in masking the signal. If the signal energy needed to just hear the signal is assumed to be some constant proportion of the effective noise energy, the threshold of the signal will therefore be independent of the bandwidth if the masker bandwidth is wider than the critical band, and will vary inversely with the external bandwidth once the masking noise bandwidth is less than the critical band. Fletcher conducted experiments to measure such critical bands at a variety of center frequencies and found that the width of the critical band appeared to depend upon the frequency of the signal. Based on the assumption that the signal is just detectable when the signal power equals the total effective noise power, the critical bandwidth is also determinable by taking the signal energy to noise spectral level ratio needed to just hear the tone in broadband noise, and computing the implied bandwidth. This is known as the 'critical ratio method'. Green and Swets (1966) presented a table comparing estimates by the critical ratio method with Fletcher's original critical band measurements. Some estimates are in good agreement with Fletcher's (Hawkins and Stevens, 1950), but some show much larger values (Zwicker, Flotorp, and Stevens, 1957). Since Fletcher's work, much research has been reported dealing with various aspects of the problem of the critical band. In general, for

stimulus durations exceeding 150 to 200 msec, it is widely accepted that the width of the critical band is an increasing function of its center (signal) frequency and is largely independent of sound pressure level. However, when the stimulus duration is short, one problem is that the effective signal bandwidth itself increases with decreasing duration due to Fourier analytic energy spread. Results of various studies are not very consistent. Furthermore, it has been suggested that the critical band may need some time for development during the duration of signal presentation.

Two important approaches to the study of critical bands and filter evaluation are exemplified by the works of Greenwood (1961a, 1961b) and of Patterson and Henning (1977). Greenwood provided a different logical basis for determination of the critical band. He measured the masked threshold of pulsed tones, for different bandwidths, spectrum levels, and frequency locations of the masking noise, as a function of frequency. When the width of the noise band is subcritical or critical, the threshold of the pure tone should reach a maximum near the center of the masking noise and then decrease, providing a triangular function, while when the noise is supercritical, the threshold curve should have a flat top and appear trapezoidal. His results showed the expected patterns and the agreement of his data with others is very good. Some studies have been concerned with finding the precise shape of the presumed internal filter (e. g. Mathews and Pfafflin, 1965; Patterson, 1974; Patterson and Henning, 1977). The technique used for such analysis in recent work involves varying the width of an empty notch in

otherwise broadband noise (Patterson and Henning, 1977). Coupled with Fletcher's original method, it is somewhat analogous to the paradigms used in this study of temporal filtering.

B. Critical Temporal Masking Interval

If the auditory stimulus is analyzed in the time domain instead of in the frequency domain, it is not difficult to conceptualize the critical interval as the analogue of the critical band. If a signal is temporally placed in the center of a noise masker, as the duration of the noise masker diminishes, the detectability of the signal should not be much affected until a certain noise duration is reached. Any further decrease in the noise duration should result in enhancement of the detectability of the signal. Such a minimal noise duration equal in masking effectiveness to a much longer noise duration has been named the "critical masking interval" by Penner et al. (1972), Penner et al. (1973). Penner et al. (1972) measured the critical temporal masking interval for a click signal of 100-μsec duration in white noise using two different paradigms. The first paradigm was the temporal analogy of Fletcher's critical band study. A click was presented in the temporal center of a noise burst and its threshold was measured as the noise duration decreased. For sufficiently long durations the threshold of the click remained constant. As the noise duration was progressively shortened and less than a certain critical value, the threshold of the click was decreased. The critical value, that is, the critical temporal masking interval, was then determined empirically

as the noise duration at which the signal became easier to hear. Also by analogy with the concept of the "critical ratio method" in the frequency domain, the critical temporal masking interval was estimated using continuous noise by taking the ratio of threshold click energy to noise power density, since this yields the estimate of that duration for which total energy would be equated for click and noise. Penner et al. (1973) also measured the critical temporal masking interval using the temporal analogy of Greenwood's bandwidth experiments (Greenwood, 1961a, 1961b). The threshold of a click was measured in various temporal locations relative to a noise burst whose duration was varied. The critical temporal masking interval was determined as the noise duration at which the shapes of the temporal masking patterns, which showed the effect of the temporal location of the click on its threshold, changed from a trapezoid to a triangle as the noise duration was further decreased. The explanation is that when the masker duration is subcritical or critical and the location where the signal is presented is moved from the onset of the noise to the offset of the noise, the threshold gradually increases, reaches a maximum near the center and then begins to decrease, so that the temporal masking pattern becomes a triangular plot. When the noise is supercritical, the threshold curve has a flat top and is trapezoidal, since the click is surrounded by maximum effective masking energy for some span of position in the center of the noise. These various paradigms yielded similar numerical estimates of the critical temporal masking interval of about 6 to 20 msec for the detection of a click in white noise. The estimates were not greatly

affected by the bandwidth of the maskers, 100-600 Hz, 100-5000 Hz, and 3000-5000 Hz.

C. Critical Temporal Masking Interval and Integration Time in Detection

It has been generally assumed that the ear can accumulate sensory information over a period of time when the stimulus lasts for a while. The usual method for studying this integration time in detection experiments is to determine what combinations of signal duration and signal intensity are necessary to produce constant detectability. It is generally agreed that the longer a signal, the lower its required intensity for detection, up to a limit. As signal duration increases beyond the limit, the required intensity is independent of duration. Then, the duration of the signal at which the slope of the function representing the trading relation of duration and intensity becomes indistinguishable from zero can be estimated, and it is the estimate of the maximal integration time of the ear. It has been found to be on the order of 150 to 225 msec (Garner and Miller, 1947; Green, Birdsall, and Tanner, 1957; Green, 1960a, 1969; Zwislocki, 1960). For any stimulus duration greater than this maximal integration time, the sensory information is assumed to be only partially integrated. Within the maximal integration time, the temporal integration function, which shows how intensity trades with duration for constant detectability, has been studied by many investigators (e.g. Garner and Miller, 1947; Hamilton, 1957; Blodgett et al., 1958; Leshowitz and Raab, 1967; Jeffress, 1975).

In general, for a moderate signal duration of about 20 to 100 msec, this temporal integration is linear in the sense that the auditory threshold reduces 3 dB for each doubling of signal duration (or 10 dB for each decade increase of signal duration) (see e.g. Garner and Miller, 1947). For very short durations, temporal integration data yield an even steeper slope; about 4.6 dB for a doubling of signal duration for signals briefer than about 20 msec. For signal durations longer than 100 msec, the function produces a slope of 1.5 dB per doubling of signal duration. Therefore, Green et al. (1957) described the time-intensity trading relationship with three lines rather than one. Based on these empirical findings, Watson and Gengel (1969) argued that a negative exponential function proposed by Plomp and Bouman (1959) also provided an adquate description of temporal integration for human listeners, with the qualification that the time constant is a function of frequency. If signal duration is less than the maximal integration time (where threshold intensity becomes independent of duration), the assumption that the integration time for sensory information equals the signal duration does not necessarily hold (see e.g. Garner and Miller, 1947; Green, Birdsall, and Tanner, 1957). In their experiments with brief signals, Penner et al. (1972), Penner et al. (1973) found that the signal to noise ratio at threshold decreases as the constant spectrum level noise is increased in duration. This means that the actual integration proceeds for longer than the brief duration of the signal, and that there has to be a minimal limitation or lower bound for integration time. Such a minimal integration time for sensory

information is the critical temporal masking interval defined and discussed above. Note that most popular conceptualizations assume some time-weighted integration of energy as the relevant quantity.

D. Gated-Continuous Masker Comparisons

In recent years, a number of investigators have observed important differences between the effectiveness of continuous maskers and gated maskers. For example, Green (1969) found that when a 1200-Hz, 70-dB sinusoidal masker lasted for the entire listening session, it produced 30 dB less masking of a 10-msec, 1000-Hz signal than when gated on and off simultaneously with the signal. The gated masker is more effective by about 10 dB when signal and masker are of common frequency. For either tone-in-noise masking or noise-in-noise masking, gated maskers most often produce more masking of the signal (about 4 dB) than do continuous maskers. For the detection of a noise signal presented in a noise masker background, with common center frequency, Schacknow and Raab (1976) found that a 100-msec signal is easier to detect by about 4 dB in a continuous masker than in the gated condition when the masker bandwidth is broader than the signal bandwidth. However, there was no threshold difference between the two conditions when the signal and the masker had equal bandwidth. Wightman and Green (1966) and Viemeister (1974) are the only two studies involving variation of signal duration in the comparison of gated and continuous maskers of noise signals. They obtained similar signal threshold-duration functions but the intersection of the two functions

was as large as 70 msec in Viemeister's study, and between 3 and 10 msec in the Wightman and Green study. The gated-continuous relation is reversed so that continuous maskers are more effective when the signal is very brief. For 500-msec tonal signals masked by broadband noise, Tucker et al. (1968) found that when the signal is long, the gated masker produces more effective masking of the signal, while the reverse is true for a very brief signal; there was no difference for a moderate duration signal of 100 msec. These results are reflected in different slopes of intensity-duration reciprocity functions for gated and continuous masking conditions. However, where the two functions of threshold-duration intersect each other is not consistent among the studies. The results for brief signal conditions are also not very consistent among studies and the variability among subjects is greater than that for long duration signals (Wier et al., 1977). This dissertation will include a comparison of gated and continuous noise maskers which confirms the finding of Osman, Tzuo, and Tzuo (1980, unpublished), that for well practiced listeners with brief tonal signals in noise, continuous noise is clearly the more effective masker. Since that study was a follow-up to this one, and a partial replication, we shall not discuss it at this point.

Most investigators have emphasized the analysis of temporal masking threshold data, but paid little attention to the slope of the psychometric function. However, in addition to the gated-continuous differences for thresholds, there are also differences for slopes, and these are reasonably consistent. When Green (1960a) first proposed an

energy detection model for the noise signal masked by noise experiment, he compared his experimental data in a simple detection (continuous masker) task with the ideal observer. He found that the thresholds were consistently 5 or 6 dB higher for the real observers than for the ideal observer, and also that empirical psychometric functions appeared to be somewhat steeper for the real observers (the range for 60% to 90% correct responses was only 3 dB) than what was suggested by the model (a range of 7 dB). Green explained this phenomenon in terms of the observer being uncertain about either the starting time for the duration of the signal in such a detection task. To solve this problem, Green and Sewall (1962) introduced another paradigm in which noise bursts were added to either of the two intervals of a forced choice task, and served to mark the starting time and the duration of the signal. The psychometric function obtained through this method fit the energy detection model very well. Campbell (1966) studied a very long broadband noise signal of 1 sec presented in a continuous broadband noise masker and obtained the same narrow range of the psychometric function as did Green (1960a). However, De Boer (1966) gated a noise signal with a noise masker, both of 400-msec duration for a wide range of bandwidths of from 63 to 4000 Hz centered at 1000 Hz, and found the range to be 7 dB. In the study of tonal signals masked by continuous noise, all investigators (e.g. Green, 1966; McFadden, 1966; Campbell, 1969; Lewhowitz, 1969) obtained psychometric functions with slopes steeper than the maximum possible slope allowed by the original energy detection model. When the masker was gated on and off with the signal,

however, a slope significantly lower than the maximum for Green's energy detector was obtained for long or at least moderate duration signals, and it was even as low as the theoretical lower limit of Green's model for a very short signal (10 msec) (Osman, 1975). Such a very low slope (a range of 16 dB) was also found for a pedestal detection task (Leshowitz, 1969). These results are confirmed for brief tones in noise by Osman, Tzuo, and Tzuo (1980, unpublished), where, independent of listerner experience or locations of the psychometric functions as indexed by the threshold, psychometric functions are shallow for maskers gated synchronously with the signal in accordance with simple energy detection, and are quite steep for continuous maskers, necessitating the assumption of some process in place of or superimposed on the simple energy detector model, such as temporal uncertainty. Again, that study was an extension of some of the data of this dissertation, and will be discussed later.

One study in vision should be noted here. Leshowitz, Taub, and Raab (1968) compared the detection of pulsed signals in the presence of a continuous background and in the presence of a background pulsed (gated) simultaneously with the signal, using a two-alternative, temporal, forced-choice procedure. Differences were found in intensity-duration reciprocity relations, the form of the Weber function, and the shape of the psychometric function between continuous and pulsed detection conditions. Slopes of psychometric functions for the pulsed case were significantly less than those observed in the simple detection condition with a continuous masking background. The average value of

the range of the psychometric function was 3.5 dB for the simple case, and 10 dB for the pulsed case. Their results showed that an intersection of two constant detectability contours (one for the pulsed masker, the other for the continuous masker) was at around 6 msec of stimulus duration for the same level of background intensity. For longer signal durations, the threshold for the pulsed case was higher than that for the continuous background condition; but for short signal durations, the result was reversed.

E. Simultaneous, Backward, and Forward Masking Experiments in Auditory Detection

This dissertation is intended to explore the relation between two extreme modes of masker presentation, gated masker and continuous masker, in the context of temporal filtering. One methodological approach involves extending noise-fringes simultaneously on the two sides of the signal interval, and this design is similar to the paradigms of experiments on simultaneous masking. The simultaneous masking experiment is a masking experiment where the signal is presented during the masker and the onset of the signal may or may not be delayed relative to the onset of the masker. Since such an experiment usually uses a brief signal, it is also called a 'transient masking' experiment. The changes in masking as a function of the onset of the signal relative to the onset of the masker are used to determine the duration needed for the gated masker to reach an effective steady state.

In visual detection, Crawford (1947) measured the detectability

of a brief signal flash presented at various times during the presentation of a longer masking flash. He found a rather considerable (20 dB) elevation in the threshold for the signal flash near the onset of an intense masking flash and a smaller elevation in the amount of masking near the offset of such a masking flash. The large elevation of the threshold of the signal near the onset of the masker has been designated as a 'transient overshoot' effect. Osman and Raab (1963) were motivated by Crawford's finding and raised the question of whether the masking process is essentially homogeneous in time in auditory perception. They found the threshold for acoustic clicks to be remarkably independent of when the click is presented within an intense noise burst of either 10 or 500 msec, so that the temporal masking pattern was flat. There have also been a number of additional studies investigating one or another aspect of the problem (Miller, 1947; Samoilova, 1959; Scholl, 1962; Zwicker and Wright, 1963; Wright, 1964; Zwicker, 1965a, 1965b, 1972; Elliott, 1965, 1967; Leshowitz and Cudahy, 1972; Robinson and Trahiotis, 1972). The experimental data in audition are not very consistent. Some results show a transient overshoot effect as large as 15 dB, some are just about 6 dB, and some do not show any such overshoot effect. Although many parameters influencing the overshoot have not yet been studied, after extensive experiments on this problem, Zwicker and Fastl (1972) argued for the following trends: (1) The overshoot appears if the spectral properties of signal and masker are different. (2) The overshoot does not depend on masker level. (3) The overshoot disappears for signal durations

larger than 10 msec and grows to as much as 15 dB for signal durations as short as 2 msec. (4) The overshoot appears for a broadband masker with a spectral gap and a broadband signal in such a way as if the signal would pass through a "filter window" corresponding to the gap of the masker.

The first three points are relevant to the present study. The overshoot mechanism may be involved in masking of the tonal signal for brief noise-fringes where the duration of the signal is nominally 10 msec and the spectra of tone and masker are significantly different. The study most directly comparable to this one in the literature is reported by Elliott (1965), where thresholds for 10-msec tone-bursts masked by broadband noise of varying duration are reported. The published graphs can be examined to reveal the changes in masked threshold to be expected for a 10-msec or 5-msec 1000-Hz tone centered within a noise-burst, as a function of duration of the masker (30 to 100 msec). Subtracting 10 msec and dividing the remainder by 2 yields the duration of the noise-fringe. Interpolating Elliott's results yields a concave downward graph for threshold as a function of fringe duration. Further details of these results and arguments concerning mechanisms involved in the overshoot phenomenon will be discussed later in the context of interpreting the data of this dissertation.

With respect to the manipulation of presentation of the masking noise in time, masking noise preceding the onset of the signal in time yields forward masking, and masking by noise following the signal yields backward masking. Hence, the masker presentation in

this study may be thought of as the combination of backward, forward, and simultaneous masking, where we vary the "packaging" of the backward and forward masking jointly. In the literature, there are related investigations of either purely forward masking, or purely backward masking, or the combination of both (Elliott, 1962a, 1962b, 1964, 1969, 1971; Pickett, 1959; Raab, 1961, 1963; Pollack, 1964; Deatherage and Evans, 1969; Moore and Welsh, 1970; Dolan and Trahiotis, 1972; Smiarouski and Carhart, 1975; Fastl, 1976; Berg and Yost, 1976; Lynn and Small, 1977). Since, from the point of view of experimental design, backward and forward masking are not manipulated separately in this study, only certain results from the audition literature are deemed relevant. The typical paradigm in previous research is similar to our gap-fringe conditions, except that the segment of masker synchronously gated with the signal is absent. As the terms are used here, backward masking involves only noise following the signal while forward masking involves only noise preceding the signal, and the combination of forward and backward masking simply involves masking noise both before and after the signal. Major features of forward masking and backward masking in audition have been summarized by Elliott (1971) as the following: (1) The nearer in time to the masker that the auditory signal occurs, the more its threshold is elevated. (2) More backward than forward masking occurs at very short Δt, where Δt indicates the silent interval between signal and masker. (3) Although the temporal extent of the masking appears to be related to many variables of the experimental situation, most backward or forward masking occurs within about ± 100 msec.

(4) Duration of the masker does not affect backward masking but does influence forward masking at very brief Δt's. (5) Both backward and forward masking are influenced by the relation between the frequencies of signal and masker. (6) Amount of backward and forward masking, even at very short Δt's, is not a linear function of masker intensity. (7) When a signal is temporally positioned between two masker bursts or during a short silent gap in otherwise continuous noise, the observed masking exceeds what would be predicted on the basis of summing the independently determined amount of backward and forward masking. Again, work by Elliott (1962a) is most closely related to the present study. She studied backward and forward masking of 7-msec tone-bursts of 500 Hz (as well as 1000 and 4000 Hz). Her results conform to the above summary, and will be referred to again in relation to the interpretation of results for this study.

F. Theoretical Psychometric Functions Predicted by Models of Auditory Detection

The psychometric function, which provides the data base for this study, may be defined as the quantitative relation between level of signal intensity and measure of detection performance. Signal intensity level will be given in relative energy terms, as the decibel difference between tonal signal energy (E_s) [or signal power spectral density (S_o) if signal is noise] and noise power spectral density (N_o); that is, as 10 log (E_s/N_o) [or 10 log (S_o/N_o)]. Detection performance by the human listener is measured first as maximized

percent correct for a standard two-interval forced-choice (2IFC) psychophysical task, as transformed from performance in a one-interval yes-no (YN) task, and is also converted to the performance index d' using a transform proposed by Egan (1965): $d' = m(E_s/N_o)^k$. This transform is a purely empirical relation facilitating description of the data, and is used for three reasons. First, d' is an important theoretical quantity in the theory of signal detection, because it is readily understood as a measure of the separation of two Gaussian distributions of equal variance, and it can also be used to quantify the separation of the difference distributions of 2IFC, since these have equal variance even when the noise alone and signal-plus-noise distributions of the YN task do not. Second, the relation is easily applied in logarithmic form where best fits (maximum likelihood fits) of the function to data are accomplished by the method of least squares, and a position index (intercept or threshold) and a shape index (slope) are immediately obtained. Third, the relation provides very good to excellent fits for a great deal of empirically as well as theoretically derived psychometric functions.

In the modeling of the detection of signals in noise for a 2IFC task, let the relevant sensory variable be the difference between a measurement determined for interval I and a similar measurement determined for interval II: $X_D = X_I - X_{II}$. One of the two quantities X_I and X_{II} results from signal-plus-noise, and the other results from noise alone. Each has an associated conditional probability density function. The density for signal-plus-noise may be a function of

signal level, so that the two conditional densities will generally have unequal variances. Were they Gaussian with equal variances, then the ratio of their mean difference to their common standard deviation would define d'. The two conditional difference distributions for X_D, one for signal in interval I and the other for signal in interval II, have means symmetric about zero and a common variance. Identify one half of their mean difference to common standard deviation ratio as h. Then h would be $d'/\sqrt{2}$ if the conditional densities for X_I and X_{II} were normal with common variance. Assume the normality of these distributions to be well-approximated. Then the rate at which h grows with signal level is determined by the rate of growth of the mean relative to the variance for the signal-plus-noise distribution. This is implicit in the rate of growth of percent correct with signal level. Therefore, in addition to selecting some value of h to define threshold for E_s/N_o, the rate of growth of h with E_s/N_o determines the shape of the psychometric function. A good index of this shape is simply the range for two reference values of percent correct, say 60% and 90%. The associated values of h, h_a and h_b, would determine the shape of the psychometric function if Egan's equation provides a good fit. Specifically, let $h_a < h_b$, where h_a and h_b are the lower and upper limits of the chosen range of the psychometric function, and h_o is the value selected to define threshold.

Thus

$$10 \log(h\sqrt{2}) = 10 \log(d') = 10 \log(m) + k\ 10 \log(E_s/N_o), \qquad (1)$$

so that for threshold

$$10 \log(E_s/N_o) = [10 \log(h_o\sqrt{2}) - 10 \log(m)] / k \quad , \qquad (2)$$

and to estimate the slope, k, using two points of the psychometric function

$$k = 10 \log(h_b/h_a) / 10 \log(E_{s_b}/E_{s_a}). \qquad (3)$$

Some theoretical psychometric functions for a variety of detection models are presented in Figure 1 (from Green and Swets, 1966, p194). For convenience, the slope and the threshold at d' = 1 have been calculated for each, as shown in Table 1, by taking eight points in the range of 60% to 90% correct responses from each psychometric function and fitting them with the d' equation.

The most informed ideal observer is the cross-correlation detector which is an ideal observer for the signal known exactly. The observer is assumed to compare the observed waveform with the expected signal waveform and compute the cross product between the two. The observer's decision is based on the computed cross product. For the most ideal case there is only one expected signal and one cross product is computed. The two underlying distributions, one for noise alone and the other for signal-plus-noise, have been proved to be normal and of equal variance (Tanner and Birdsall, 1958) and the theoretical psychometric function is derived as

$$d' = (2E_s/N_o)^{\frac{1}{2}}, \qquad (4)$$

or

$$10 \log(d') = 1.5 + 0.5 [10 \log(E_s/N_o)] \quad . \qquad (5)$$

Stated in words, the cross-correlation detector always yields a

Figure 1. Theoretical psychometric functions for the cross-correlation model, the envelope detection model, and the uncertainty model for the case of one-of-M-orthogonal signals. The detector expects one of M equal-energy, orthogonal signals. The phase of the signal is either known or unknown. The curves give the expected percentage of correct responses in two-alternative forced choice as a function of 10 $\log(E_S/N_O)$, where E_S is the energy of the signal and N_O is the noise-power density. The parameter M is the number of potential signals. For M = 1, phase unknown, two calculations are shown. One is exact; the other is an approximation used to generate the curves for higher values of M. The difference between these two curves for M = 1 is an upper bound on the error involved in the approximation. (Taken from Green and Swets, 1966, p. 194.)

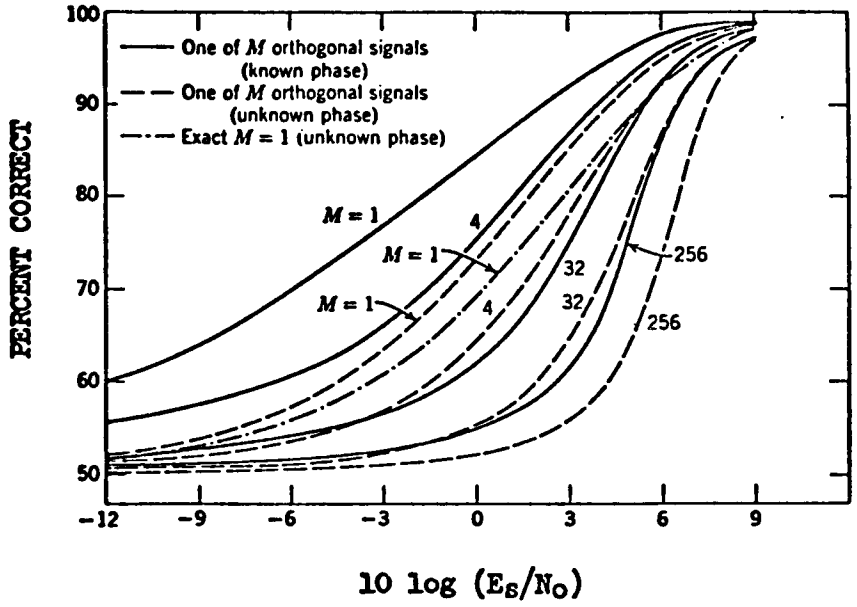
100
90
80
70
60
50
PERCENT CORRECT
One of M orthogonal signals (known phase)
One of M orthogonal signals (unknown phase)
Exact M = 1 (unknown phase)
M = 1
M = 1
M = 1
4
4
32
32
256
256
−12
−9
−6
−3
0
3
6
9
10 log (Es/No)

Table 1. Calculated slopes, thresholds at d' = 1, and ranges of theoretical psychometric functions in accordance with Egan's equation: $10 \log(d') = m (E_s/N_o)^k$ for the cross-correlation model, envelope detection model, and uncertainty model.

Uncertainty Level		Threshold	Slope	Range
M = 1	(known phase)	-3.23	0.50	14
M = 4	(known phase)	0.07	0.68	10
M = 1	(unknown phase)	0.82	0.80	9
M = 1*	(unknown phase)	1.87	0.82	9
M = 4	(unknown phase)	2.65	1.05	7
M = 32	(known phase)	3.14	1.14	6
M = 32	(unknown phase)	4.65	1.57	5
M = 256	(known phase	4.98	1.86	4
M = 256	(unknown phase)	6.21	2.18	3

* For M = 1, phase unknown, two calculations are shown. One is exact (threshold = 1.87 dB); the other is an approximation (threshold = 0.82 dB), which is used to generate the psychometric functions for higher values of M. The approximation is known to improve as M increases. The difference between these two psychometric functions for M = 1 is an upper bound on the error involved in the approximation.

psychometric function with a slope of 0.5 and a threshold of -3 dB for the case where only one signal is expected, all parameters of the signal are completely specified, and there are no free parameters.

More generally, the performance of human observers could be based on the addition of some degree of uncertainty, where the observer would have to compare the observed waveform with each of the M possible orthogonal signals. This is the so-called uncertainty model. The derived psychometric functions for the uncertainty model for several values of M are also presented in Figure 1 and Table 1. They tend to be steeper and move to the right, i.e. threshold increases, as M is increased. The larger the value of M, the greater the level of uncertainty about the signal. Once M exceeds 8 or so, these functions have similar shapes, independent of the amount of uncertainty about the signal parameters, and their threshold change is also very little.

Another model of auditory detection, the envelope detection model, which is for an ideal observer for signal known exactly except for phase, was first suggested by Marill (1956) and refined by Jeffress (1964, 1970). As suggested by Helmholtz (1885), the ear may be phase-deaf so that the decision of the ideal observer in a detection task is assumed to be based only on the envelope information provided by the stimulus. The distribution of the envelope given narrow band noise alone was proved to be a Rayleigh distribution (Rayleigh, 1945). When a signal is added to the noise, the momentary amplitude of the observed envelope depends on the phase angle difference between the signal and

the noise, where the absolute phase angle of the noise is immaterial. The distribution of the resultant envelope becomes a Rayleigh-Rice distribution. The variance of the signal-plus-noise distribution is generally larger than that of the noise alone distribution. Based on these two distributions, Marill formalized a simple expression for the psychometric function characterizing a 2IFC task as follows:

$$P(C) = 1 - \tfrac{1}{2}\exp(-E_s/2N_0). \qquad (6)$$

A set of psychometric functions for several values of M coupled with unknown phase were also derived and are also shown in Figure 1 and Table 1. Figure 1 also shows that, if more signal uncertainty is involved so that M is greater than 1, the psychometric functions shift to the right and become steeper. As M increases and reaches a certain level, the changes both in slope and threshold become very small and the psychometric functions tend to be parallel to each other. In this model, it is also assumed that the auditory system adjusts its filter bandwidth, W, according to the signal duration, T, so that the detector's bandwidth is reciprocally related to signal duration and yields WT = 1.

Yet another model is the energy detector (Green, 1960a; Pfafflin and Mathews, 1962; Green and Swets, 1966). This model consists of an initial bandpass filter followed by a square-law device and an integrator. The observer is assumed to base his decision on the output of the integrator, that is, on the energy in the observation interval (0, T). The distribution of the decision variable for noise alone is proved to be a chi-square distribution with 2WT degrees of freedom

and with a mean of N_0WT and a variance of N_0^2WT, where W indicates the effective rectangular bandwidth of the bandpass filter. For a tonal signal-plus-noise condition, the distribution of the energy tends to be a noncentral chi-square distribution with the same number of degrees of freedom but with mean of $N_0WT + E_s$ and variance of $N_0^2WT + 2E_sN_0$. If degrees of freedom is large and E_s is small relative to N_0, these two distributions may each be approximated by Gaussian distributions. Generally, the psychometric function is determined by

$$d' = \frac{E_s/N_0}{(WT + E_s/N_0)^{\frac{1}{2}}} . \tag{7}$$

It is very clear that, in addition to the signal parameters, the detectability of the observer depends on another important parameter, WT, the product of the effective bandwidth of the filter and the effective integration time of the integrator. If WT is much larger than E_s/N_0, equation (7) can be approximated very accurately by neglecting the term E_s/N_0 in the denominator, so that

$$d' \approx (WT)^{-\frac{1}{2}} (E_s/N_0) , \tag{8}$$

or, in log-log coordinates,

$$10 \log(d') \approx -10 \log(WT)^{\frac{1}{2}} + 10 \log(E_s/N_0) , \tag{9}$$

where the slope of the psychometric function as 10 log d' vs E_s/N_0 in dB is unity, and the threshold in dB (at d' = 1) is 10 log $(WT)^{\frac{1}{2}}$.

The measurement of the size of W varies as a function of frequency

of the tonal signal (Fletcher, 1953; Zwicker, Flottorp, and Stevens, 1957). This suggests that the detection process of the auditory system for a tonal signal depends heavily on the waveform characteristics of the signal. In addition to time span, to reduce possible observer uncertainty about some other aspect of the signal such as phase or frequency, Green and Sewall (1962) suggested use of wideband noise as the signal. Since wideband noise is of random character and the simple average of successive presentations of it will tend toward zero, the observer's task may be simplified to just comparing two energy quantities and selecting the more intense one as the one that contains the signal. In other words, such a task of detecting a noise signal in the noise background could be either treated as a signal detection task or as an intensity discrimination task.

For detecting a noise signal within a masking noise, based on the energy detection model which describes optimal performance for such a task, and assuming that the receiver matches its bandwidth to that of the noise signal and that stimulus energy outside the signal passband has no influence on the detection process (i.e. $W = W_s$, where W_s is the bandwidth of the signal), Green (1960a) derived an equation stating the relationship of d' and S_o/N_o, the ratio of the power density of the noise signal to that of the noise masker, as follows:

$$d' = (WT)^{\frac{1}{2}} (S_o/N_o) \frac{1}{\left[\frac{1}{2}(S_o/N_o)^2 + (S_o/N_o) + 1\right]^{\frac{1}{2}}}. \qquad (10)$$

The underlying distributions for both noise alone and signal-plus-

noise are chi-square distributions, with degrees of freedom of 2WT. These have also been approximated as normal distributions for large WT. For $S_o << N_o$, equation (10) becomes

$$d' \approx (WT)^{\frac{1}{2}} (S_o/N_o) , \tag{11}$$

or

$$10 \log(d') \approx 10 \log(WT)^{\frac{1}{2}} + 10 \log(S_o/N_o) , \tag{12}$$

where the slope is still unity for a dB scale and the threshold (at $d' = 1$) is $-10 \log (WT)^{\frac{1}{2}}$ (dB).

Comparing the obtained experimental data for a simple detection task with the results predicted by the model, Green (1960a) found that they differed by a constant. He then added an attentuation factor to the above mentioned equation. The resulting equation closely fit his experimental data except that the empirical psychometric function appeared to be somewhat steeper than what was suggested by the model. Green explained this phenomenon in terms of the observer being uncertain about either the starting time or the duration of the signal in such a detection task.

Green's constant attenuation factor actually can not be employed to fully account for the discrepancy (at a given level of detectability) between real and ideal observers because the discrepancy is not constant at all durations and at all bandwidths. In viewing this weakness, the original energy detection model has been revised or refined. For instance, De Boer (1966) involved a kind of internal noise in the

model, Schacknow and Raab (1976) extended it for noise intensity discrimination in which signal and masker are heterogeneous in bandwidth, and Treisman (1965), McGill (1968a, 1968b) and Luce and Green (1972) further developed their own models by combining stimulus fluctuations and neural fluctuations in specified ways.

McGill (McGill, 1967; Green and McGill, 1970) further related the envelope detection model and the energy detection model. By simply changing the variable of amplitude into energy in Marill's detection formula, he proved that the envelope detection model is actually an extreme case of the energy detection model where a narrow band noise centered on the signal frequency is assumed to exhibit a nominal bandwidth when the signal has a duration T, under the restriction of WT = 1.

Based on the assumption of energy fluctuations, McGill built a noise spectrum by adding up a specific number of Rayleigh narrow band noise sources spaced orthogonally in frequency. The convolution of these 2WT narrow band, short-duration noise sources, either with or without signal, yields noncentral or central chi-square energy distributions each with 2WT degrees of freedom. Based on these two distributions, Green and McGill (1970) derived and displayed a set of psychometric functions (see Figure 2) for pure noise intensity discrimination in a 2IFC task and another set of psychometric functions (see Figure 3) for detection of a sinusoid added to noise in a 2IFC task. The calculated slopes and thresholds at d' = 1 in accordance with Egan's equation are presented in Table 2. (Note that Egan's equation is also applied with S_o in place of E_s.)

Figure 2. Pure noise psychometric functions characterizing an energy detector in a two alternative forced-choice task derived by Green and McGill. (Background noise-power/unit-bandwidth indicated by N_o. Signal is a change in noise gain symbolized by S_o. Parameter $\nu = WT$ is the product of noise bandwidth and duration, which is one half of the degrees of freedom.) (Taken from Green and McGill, 1970, Figure 1.)

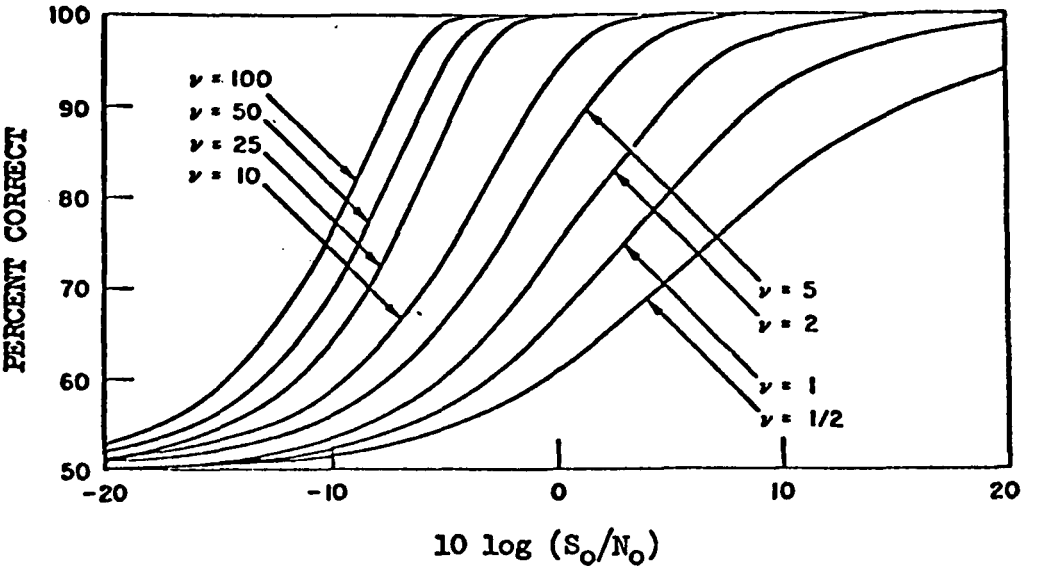
100
90
80
70
60
50
PERCENT CORRECT
ν = 100
ν = 50
ν = 25
ν = 10
ν = 5
ν = 2
ν = 1
ν = 1/2
-20
-10
0
10
20
10 log (S_o/N_o)

Figure 3. Theoretical psychometric functions for detection of a sinusoid (energy E_s) added to noise, discriminated from noise alone, characterizing an energy detector in a two alternative forced-choice task derived by Green and McGill. (Noise-power/unit-bandwidth indicated by N_o. Parameter $\gamma = WT$ is bandwidth-duration product characterizing noise samples. Function for $\gamma = \frac{1}{2}$ is limiting case generated by instantaneous sampling when signal phase is known.) (Taken from Green and McGill, 1970, Figure 2.)

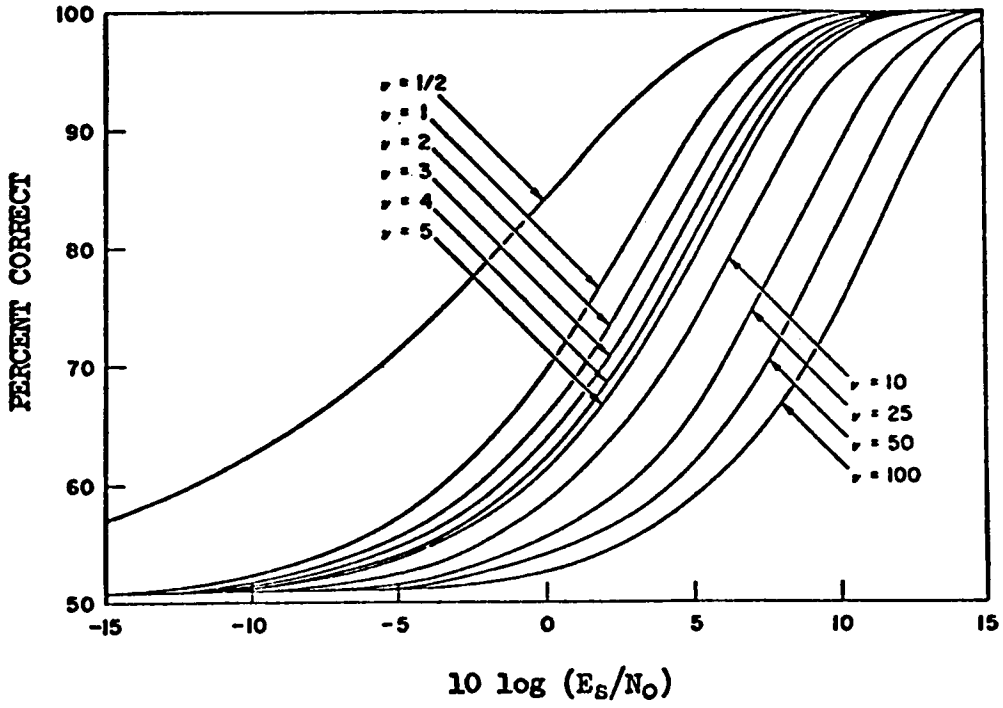
100
90
80
70
60
50
PERCENT CORRECT
-15
-10
-5
0
5
10
15
10 log (Es/No)
r = 1/2
r = 1
r = 2
r = 3
r = 4
r = 5
r = 10
r = 25
r = 50
r = 100

Table 2. Calculated slopes, thresholds at d' = 1, and ranges of theoretical psychometric functions in accordance with Egan's equations: $10 \log(d') = m (E_s/N_o)^k$ for tone in noise detection and $10 \log(d') = m (S_o/N_o)^k$ for noise in noise detection for energy detector derived by Green and McGill.

	Tone in Noise				Noise in Noise		
ν	Slope	Threshold	Range	ν	Slope	Threshold	Range
$\frac{1}{2}$	0.50	-3.15	14	$\frac{1}{2}$	0.44	8.35	16
1	0.82	1.73	9	1	0.59	3.93	12
2	0.84	2.84	8	2	0.69	0.83	10
3	0.87	3.49	8	5	0.79	-2.05	9
4	0.87	3.99	8	10	0.85	-4.17	8
5	0.87	4.37	8	25	0.97	-6.95	7
10	0.88	5.57	8	50	0.96	-8.45	7
25	0.88	7.04	8	100	0.97	-9.95	7
50	0.96	8.80	7				
100	0.95	10.14	7				

The above mentioned models of auditory detection do not differentiate whether the noise masker is gated with the signal or presented continuously. In other words, these models would predict the same psychometric function, equal in threshold and in slope, for the gated masking condition and the continuous masking condition, and also for any of the conditions of the present study. However, the gated-continuous difference is explicitly considered by Jeffress (1968). Three important aspects in his electrical model are: (1) He gated the signal ahead of the filter instead of after the filter as is usually done in the mathematical models, (2) He considered the rectifier as a half-wave rectifier rather than a square-law device since auditory neurons fire principally during the rarefaction half cycle of the input waveform, and (3) The postdetection filter is a leaky integrator or running averager (this feature is most relevant for the continuous-gated question). He concluded that the integration times and bandwidths estimated for human subjects appear to be within a reasonable range, with bandwidths of 50 to 70 Hz associated with integration times of 100 to 150 msec.

Since the leaky integrator or running averager may be represented as a time weighted integrator in the form of a convolution of the weighting function and the input, then if a square law device is assumed, the convolution integral is

$$\int_0^{\infty} w(\tau)x^2(t-\tau)d\tau = \int_{-\infty}^{t} w(t-\tau)x^2(\tau)d\tau \ . \qquad (13)$$

The psychoacoustics literature contains no detection theoretic analysis

of the leaky integrator model, with the exception of the simulation work of Green and Sewall (1962) and Jeffress (1968). Both used electrical analogues of the process to simulate frequency distribution data. Green and Sewall give a brief discussion of the results for energy integration. Jeffress presents an extensive and detailed discussion of the results for a leaky integrator where half-wave rectification is used in place of squaring. Both papers argue that whether energy, half-wave rectification, or full-wave rectification is employed will not greatly affect the statistics of the process. Jeffress presents psychometric functions for the chi and non-central chi distributions which are consequences of half-wave rectification. Other papers (Penner, 1974, 1975, 1978) analyze the leaky integrator simply in terms of signal-to-noise ratio, ignoring the variance of the process, and consequently do not yield predictions for psychometric functions. For example, Penner (1975) analyzed the temporal filter shape for the forward or backward masking of clicks by noise by beginning with the assumption that

$$E_S \propto \int N_0 \left| w(\tau) \right|^2 d\tau \ , \tag{14}$$

and estimated $w(\tau)$ to be of the form

$$w(\tau) = \frac{1}{\left[(\Delta\tau/\sigma)^2 + 1 \right]^2} \ , \tag{15}$$

from her masked click threshold data (Penner, 1974). Note that in Penner's work as well as others referred to in the related literature, the function $w(\tau)$ is treated as real rather than complex. This means

that the leaky integrator can not be regarded as a true postdetection filter, which would otherwise be the case, since a complex impulse response function is required to allow frequency dependent phase-shifts. A commonly assumed form for the weighting or impulse function is the exponential

$$w(t-\tau) = \exp\left[-(t-\tau)/\xi\right], \tag{16}$$

with ξ being evaluated as the time constant of the 'leaky' integrator (Munson, 1947; Jeffress, 1968; Zwislocki, 1969; Duifhuis, 1973; Penner, 1975, 1978; Lakey, 1976). If $w(t-\tau)$ were of rectangular shape ranging from 0 to T, the model would reduce to Green's original energy detector.

G. Signal Detection Model of a Leaky Power Integrator

The original energy detection model assumes the acoustic input to first pass through a rectangular band-pass filter with bandwidth W. The output of the filter is squared and the square is integrated for some time span (0, T) coinciding with the signal interval. The sampling analysis derivation of the model may be outlined as follows. Let the observed input waveform be designated y(t), and a particular sample waveform be designated x(t), for some finite duration. Then the likelihood:

$$p\left[y(t) = x(t)\right] = p\left[(y_1, \cdots, y_N) = (x_1, \cdots, x_N)\right], \tag{17}$$

for a time sequence of N sample values, where the values are spaced 1/2W seconds apart. It is argued that the sampled values are mutually

independent, and furthermore, that given any vector $(x_1, \cdots, x_N)$, the waveform x(t) can be precisely reconstructed using appropriate interpolation functions. (That is, there is a one-to-one correspondence between x(t) and the sequence $x_1, x_2, \cdots$) Similarily, the square-law device poses no difficulty since

$$p\left[y^2(t) = x^2(t)\right] = p\left[(y_1^2, \cdots, y_N^2) = (x_1^2, \cdots, x_N^2)\right]. \quad (18)$$

Integrated power for the filtered waveform is the derived quantity for the decision process, and it is found that

$$p\left[\int_0^T y^2(t)dt = \int_0^T x^2(t)dt\right] = p\left[\sum_i^{2WT} y_i^2 \Delta t = \sum_i^{2WT} x_i^2 \Delta t\right]. \quad (19)$$

This probability density for energy is readily derived under the assumption that the masking energy is due to a stationary Gaussian white-noise process (Fourier-series band-limited), using the fact that each y_i^2 is a squared Gaussian variable. Depending on whether the signal is deterministic (e.g. tonal) or stochastic (e.g. sample of noise), and conditional on presence or absence of signal, the standardized variate

$$(y_i^*)^2 = \left(\frac{y_i - \mu_i}{\sigma_i}\right)^2 \quad (20)$$

is distributed noncentral or central chi-sqaure with 1 degree of freedom (df). Then

$$\sum_i^{2WT} (y_i^*)^2$$

is noncentral or central chi-square with 2WT df. Therefore, adjusting

for means and variances, the distribution of

$$\sum_{1}^{2WT} y_i^2 \Delta t \approx \int_0^T y^2(t)dt \tag{22}$$

is that of a linear transform of chi-square, with known mean and variance. For $2WT \geq 10$, the distribution is sufficiently Gaussian to be regarded as such. Thus, the conditional distributions of

$$\int_0^T y^2(t)dt \tag{23}$$

are regarded as Gaussian and the means and variances are as shown in Table 3 for two cases: tonal signal and noise signal.

The following argument is presented as an attempt to arrive at a detection theoretic analysis of a leaky power integrator, which will then be considered in relation to the experimental results of this dissertation. The argument was provided by Osman (personal communication). The problem is to generalize the energy detection model to a leaky power integrator of the form

$$\int_{-\infty}^{t} w(t-\tau)x^2(\tau)d\tau \ , \tag{24}$$

where the $w(t-\tau)$ may be regarded as the impulse response of a post-detection filter with uniformly zero phase shift. Since $w(t-\tau)$ is deterministic,

if

$$p\ [y(t) = x(t)] = p\ [(y_1, \cdots, y_N) = (x_1, \cdots, x_N)], \tag{25}$$

then

Table 3. Means and variances of energy distributions, given various hypotheses, for tonal signal detection and noise signal detection.

Signal	Hypothesis	Mean	Variance
Tone	$y(t) = n(t)$	N_oWT	N_o^2WT
	$y(t) = n(t) + s(t)$	$N_oWT + E_s$	$N_o^2WT + 2N_oE_s$
Noise	$y(t) = n(t)$	N_oWT	N_o^2WT
	$y(t) = n(t) + s(t)$	$(N_o + S_o)WT$	$(N_o + S_o)^2WT$

$$p\,[w(t-\tau)y(\tau) = w(t-\tau)x(\tau)] =$$

$$p\,[(w_1y_1, \cdots, w_Ny_N) = (w_1x_1, \cdots, w_Nx_N)]\ , \quad (26)$$

where w_i is the value of $w(t-\tau)$ which multiplies $y(t)$ for the sample value y_i. Now it may not be that

$$p\left[\int_0^\infty w(t-\tau)y^2(\tau)d\tau = \int_0^\infty w(t-\tau)x^2(\tau)d\tau\right] =$$

$$p\left[\sum_i w_iy_i^2 = \sum_i w_ix_i^2\right]\ , \quad (27)$$

since the shape of $w(t-\tau)$ may produce complications. However, if we accept the approximation

$$D = \int_{-\infty}^{t} w(t-\tau)y^2(\tau)d\tau \approx \sum_i w_iy_i^2\Delta t\ , \quad (28)$$

then it is still a simple matter to determine the conditional means and variances of the variable D as a consequence of the independence of the sample points. (Furthermore, it might still be reasonable to assume the conditional distributions for D to be Gaussian.) Thus:

$$E(D) = E(\sum_i w_iy_i^2\Delta t) = \sum_i w_i\Delta t\ E(y_i^2), \quad (29)$$

$$Var(D) = Var(\sum_i w_iy_i^2\Delta t) = \sum_i w_i^2(\Delta t)^2\ Var(y_i^2). \quad (30)$$

using 'n' for noise and 's' for signal, the quantity

$$h = \frac{E(D \mid n+s) - E(D \mid s)}{\sqrt{Var(D \mid n+s) + Var(D \mid s)}}\ . \quad (31)$$

may be expressed as

$$h = \frac{\sum_i w_i \Delta t \left[E(y_i^2 \mid n+s) - E(y_i^2 \mid n) \right]}{\sqrt{\sum_i w_i^2 (\Delta t)^2 \left[\mathrm{Var}(y_i^2 \mid n+s) + \mathrm{Var}(y_i^2 \mid n) \right]}} \quad . \tag{32}$$

Now, for the sampling representation of the energy detection model in the case of a tonal signal:

$$\left(\frac{n_i + s_i}{\sigma_n} \right)^2 = \frac{(n_i + s_i)^2}{N_o W} \tag{33}$$

is distributed as non-central chi-squared with one-degree of freedom. The noncentrality vanishes as s_i vanishes. The mean is

$$1 + (s_i/\sigma_n)^2 \ , \tag{34}$$

and the variance is

$$2 + 4(s_i/\sigma_n)^2 \ . \tag{35}$$

Consequently,

$$E(y_i^2 \mid n+s) = N_o W + s_i^2 \tag{36}$$

and

$$\mathrm{Var}(y_i^2 \mid n+s) = 2N_o^2 W^2 + 4N_o W s_i^2 \ . \tag{37}$$

Note that if the signal is also a sample of noise, then

$$E(y_i^2 \mid n+s) = (N_o + S_o)W \tag{38}$$

and

$$\mathrm{Var}(y_i^2 \mid n+s) = 2(N_o + S_o)^2 W^2 \ . \tag{39}$$

Returning to h for the tonal signal,

$$h = \frac{\sum_i w_i \Delta\tau s_i^2}{\sqrt{\sum_i w_i^2 (\Delta\tau)^2 \left[4N_o^2 W^2 + 4N_o W s_i^2\right]}} \tag{40}$$

and since $\Delta\tau = 1/2W$,

$$h = \frac{\sum_i w_i \Delta\tau s_i^2}{\sqrt{\sum_i w_i^2 \Delta\tau \left[2N_o^2 W + 2N_o s_i^2\right]}} \ . \tag{41}$$

Now the summations are broken into three regions: before (b), during (d), and after (a) the observation interval (0, T), since the signal is nonexistent outside of (0, T), thus

$$h = \frac{\sum_d w_i \Delta\tau s_i^2}{\sqrt{\sum_b w_i^2 \Delta\tau (2N_{o_i}^2 W) + \sum_d w_i^2 \Delta\tau (2N_{o_i}^2 W) + \sum_a w_i^2 \Delta\tau (2N_{o_i}^2 W) + \sum_d w_i^2 \Delta\tau (2N_{o_i} s_i^2)}} \ . \tag{42}$$

During (0, T), $2N_o$ is constant and s_i^2 can be regarded as constant for present purposes. That is, for the numerator we can replace s_i^2 with

$$s_i^2 = s_n^2 = (\sum_i w_i s_i^2)/(\sum_i w_i) \ , \tag{43}$$

and for the denominator we can replace s_i^2 with

$$s_i^2 = cs_n^2 = (\sum_i w_i^2 s_i^2)/(\sum_i w_i^2), \tag{44}$$

where

$$c = \frac{(\sum_i w_i^2 s_i^2)(\sum_i w_i)}{(\sum_i w_i^2)(\sum_i w_i s_i^2)} . \tag{45}$$

Thus, signal energy after filtering is

$$E_1 = T(s_n^2), \tag{46}$$

or

$$s_i^2 = s_n^2 = E_1/T , \tag{47}$$

if s_i is constant for all i during (0, T). Therefore,

$$h = \frac{(E_1/T) \sum_d w_i \Delta\tau}{\sqrt{2W\left[\sum_b N_{o_i}^2 w_i^2 \Delta\tau + \sum_d N_{o_i}^2 w_i^2 \Delta\tau + \sum_a N_{o_i}^2 w_i^2 \Delta\tau\right] + \left[(2cE_1)/T\right]\left[\sum_d N_{o_i} w_i^2 \Delta\tau\right]}} . \tag{48}$$

For present purposes, since either $N_{oi} = N_o$ or $N_{oi} = 0$, with the stipulation that terms inside each summation are dropped where $N_{oi} = 0$, the expression can be rewritten as

$$h = \frac{(E_1/T)\sum_{d} w_i \Delta\tau}{\sqrt{2N_o^2 W\left[\sum_{b} w_i^2 \Delta\tau + \sum_{d} w_i^2 \Delta\tau + \sum_{a} w_i^2 \Delta\tau\right] + \left[(2cE_1N_o)/T\right]\left[\sum_{d} w_i^2 \Delta\tau\right]}} . \qquad (49)$$

Replacing the summation with integrals, again with the understanding that regions of integration will be restricted in accordance with those time intervals where $n(t) = 0$, the equation becomes:

$$h \approx \frac{(E_1/T)\int_0^T w(t-\tau)d\tau}{\sqrt{2N_o^2 W\left[\int_{-\infty}^{0} w^2(t-\tau)d\tau + \int_0^T w^2(t-\tau)d\tau + \int_T^t w^2(t-\tau)d\tau\right] + \left[(2cE_1N_o)/T\right]\left[\int_0^T w^2(t-\tau)d\tau\right]}} . \qquad (50)$$

This may be transformed into two equations, one for the threshold value of E_1/N_o, and one for the slope of the psychometric function. For the threshold defined at $h = h_o$,

$$10 \log(E_1/N_o) = 10 \log(T) + 10 \log \left\{ ch_o^2 \int_0^T w^2(t-\tau)d\tau + \right.$$

$$\left. \sqrt{c^2 h_o^4 \left[\int_0^T w^2(t-\tau)d\tau\right]^2 + 2Wh_o^2 \left[\int_0^T w(t-\tau)d\tau\right]^2 F} \right\}$$

$$- 20 \log \left[\int_0^T w(t-\tau)d\tau\right] \quad , \tag{51}$$

where

$$F = \int_{-\infty}^{0} w^2(t-\tau)d\tau + \int_0^T w^2(t-\tau)d\tau + \int_T^t w^2(t-\tau)d\tau \ . \tag{52}$$

For the slope, using the range between two values of h and taking $h_1 > h_2$ so that $E_{l_1} > E_{l_2}$,

$$k = \log(h_1/h_2) \ / \ \log(E_{l_1}/E_{l_2})$$

$$= 1 - \tfrac{1}{2} \left\{ \frac{\log \left\{ \dfrac{(WT)F + (cE_{l_1}/N_o) \int_0^T w^2(t-\tau)d\tau}{(WT)F + (cE_{l_2}/N_o) \int_0^T w^2(t-\tau)d\tau} \right\}}{\log(E_{l_1}/E_{l_2})} \right\} . \tag{53}$$

Note that since input signal energy is

$$E_s = \int_0^T s_i^2(t)dt \approx \sum_d s_i^2 \Delta\tau \ , \tag{54}$$

then

$$E_s \propto E_1 \ . \tag{55}$$

In fact

$$E_s = E_1 \ (\Delta\tau/T) \ \left[(\Sigma_i \ w_i \ \Sigma \ s_i^{\,2})/(\Sigma_i \ w_i s_i^{\,2})\right] \ . \tag{56}$$

Thus

$$10 \log(E_s/N_o) = 10 \log(E_1/N_o) + 10 \log(E_s/E_1). \tag{57}$$

For the case of signal being a sample of noise with spectral density S_o, the results are similar. Thus, for the noise signal threshold defined at $h = h_o$,

$$10 \log(S_o/N_o) = 5 \log(2h_o^{\,2}) + 5 \log[\,F\,]$$

$$- 5 \log\left\{W\left[\int_0^T w(t-\tau)d\tau\right]^2 - h_o^{\,2} \int_0^T w^2(t-\tau)d\tau\right\} \ , \tag{58}$$

where again,

$$F = \int_{-\infty}^{0} w^2(t-\tau)d\tau + \int_0^T w^2(t-\tau)d\tau + \int_T^t w^2(t-\tau)d\tau \ .$$

For the noise signal slope, using the range between two values of h and taking $h_1 > h_2$ so that $S_{o_1} > S_{o_2}$,

$$k = \log(h_1/h_2) \;/\; \log(S_{o_1}/S_{o_2})$$

$$= 1 - \tfrac{1}{2} \left\{ \frac{\log \left\{ \dfrac{(2F) + (S_{o_1}/N_o)^2 \int_0^T w^2(t-\tau)d\tau}{(2F) + (S_{o_2}/N_o)^2 \int_0^T w^2(t-\tau)d\tau} \right\}}{\log(S_{o_1}/S_{o_2})} \right\} . \qquad (59)$$

Now, with respect to the present noise-fringe/gap-fringe experiment, no matter what the form of $w(t-\tau)$, it can be seen that the threshold is a monotonically increasing function of

$$\int_{-\infty}^{0} w^2(t-\tau)d\tau + \int_{T}^{t} w^2(t-\tau)d\tau \; . \qquad (60)$$

The slope is also dependent on that quantity, and must lie between $\frac{1}{2}$ and 1. Let the locations of the fringe limits be t_1 and t_2, where

$$-\infty < t_1 < 0 < T < t_2 \qquad (61)$$

and

$$t_1 = T - t_2 \; . \qquad (62)$$

For noise-fringe:

$$\int_{-\infty}^{0} w^2(t-\tau)d\tau = \int_{t_1}^{0} w^2(t-\tau)d\tau \qquad (63)$$

and

$$\int_{T}^{t} w^2(t-\tau)d\tau = \int_{T}^{t_2} w^2(t-\tau)d\tau \ , \quad \text{if} \quad t_2 < t \tag{64}$$

$$\int_{T}^{t} w^2(t-\tau)d\tau \ , \quad \text{if} \quad t \leq t_2 \ . \tag{65}$$

For gap-fringe:

$$\int_{-\infty}^{0} w^2(t-\tau)d\tau = \int_{-\infty}^{t_1} w^2(t-\tau)d\tau \tag{66}$$

and

$$\int_{T}^{t} w^2(t-\tau)d\tau = \int_{t_2}^{t} w^2(t-\tau)d\tau \ , \text{ if } \quad t_2 \leq t \tag{67}$$

$$0 \ , \quad \text{if} \quad t < t_2 \ . \tag{68}$$

There must be a value of t_1 such that the noise-fringe and gap-fringe integrals are equal, that is, such that:

$$\int_{t_1}^{0} w^2(t-\tau)d\tau + \int_{T}^{t \text{ or } t_2} w^2(t-\tau)d\tau = \int_{-\infty}^{t_1} w^2(t-\tau)d\tau + \int_{t_2 \text{ or } t}^{t} w^2(t-\tau)d\tau \ , \tag{69}$$

because the left side of the equation increases and the right side decreases as $|t_1|$ increases. For that particular value of fringe duration the noise-fringe and gap-fringe psychometric functions must be identical.

This model provides a framework for the structure of the present experiment and the analysis of its results. Two popular forms of the

filtering process will be considered in the discussion later on, rectangular and exponential. The detail in which the model will be further specified and the precision with which parameter estimation will be attempted, will depend on relevant features of the results. When the model appears to be inapplicable, possible modifications will be discussed. In any case, the results will be compared to the most relevant work in the literature, and an attempt will be made to do so in proper theoretical context.

II. METHOD

The experiment was performed to study the monaural detection of a short signal burst in the presence of a wideband masking noise. The signal was either a 400-Hz tone burst or a wideband noise burst of 11.5-msec total duration. The masker was always present during the time span of the signal, and in addition had variable duration and pattern of the presentation outside of the signal interval, and this is our main independent variable. A single-interval "Yes-No" procedure was used to get psychometric functions for all stimulus conditions. Locations and slopes of psychometric functions were then determined. Specific details are given below.

A. Subjects

One male and two female graduate students (including the author, PT) served as subjects. All had normal hearing as judged by their absolute thresholds and received long term training (several weeks) for this experiment before the data were formally collected.

B. Apparatus

A block diagram of the apparatus is shown in Figure 4. Both noise signals and noise masker were generated independently by two noise generators (General Radio 1381) which were set to obtain noise with bandwidths as wide as possible (nominally 50 kHz). Thus, the frequency content of the noise was limited only by the earphone

Figure 4. Block diagram of the apparatus. (Labed as:
A attenuator, EP earphone, ES electronic switch,
M mixer, NG noise generator, OS oscillator,
OSC oscilloscope, RMS voltmeter, T transformer.)

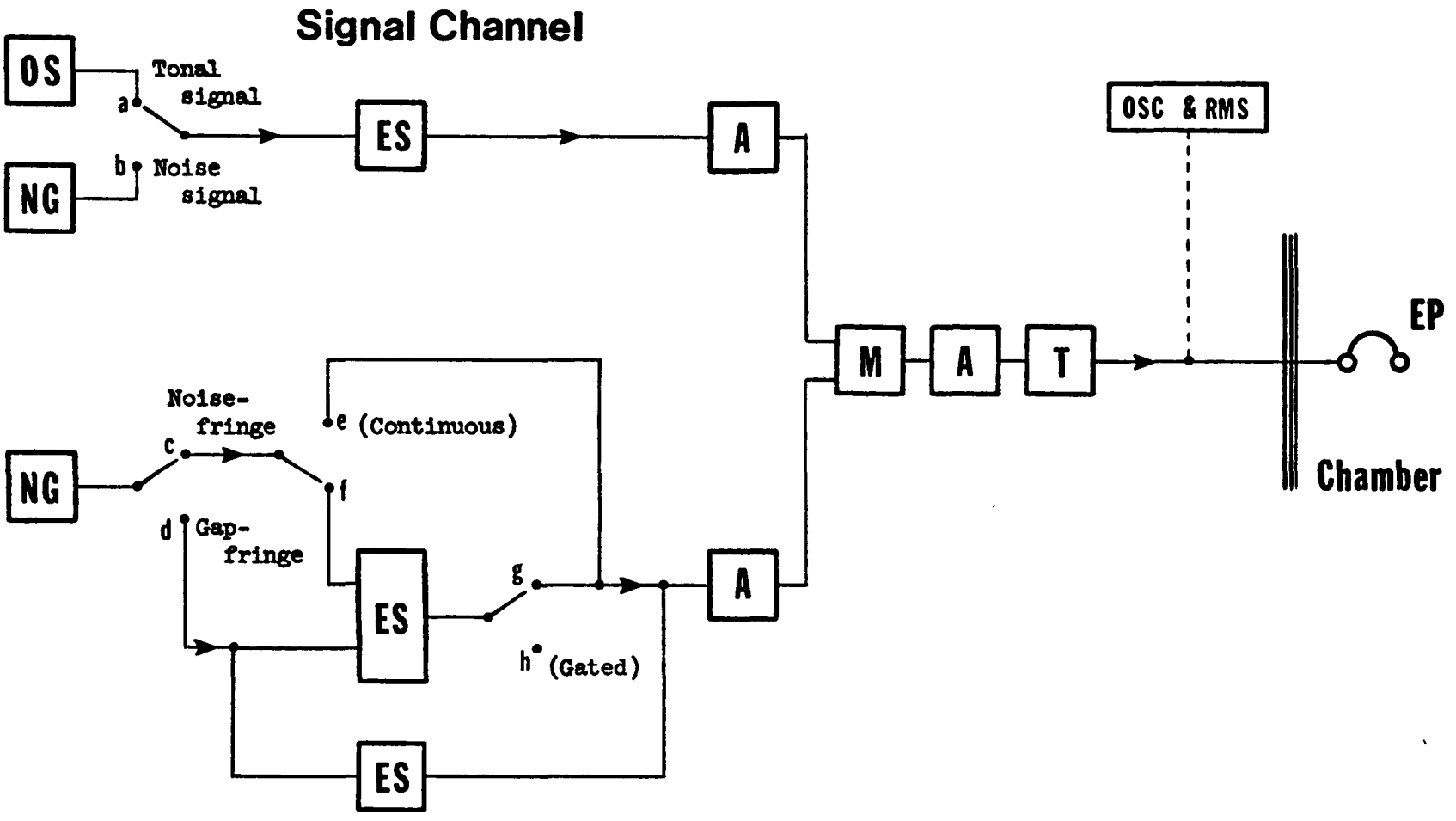
Signal Channel
OS
Tonal signal
a
ES
A
OSC & RMS
NG
b
Noise signal
M
A
T
EP
Noise-fringe
e (Continuous)
c
NG
f
Chamber
d
Gap-fringe
ES
g
A
h (Gated)
ES
Masker Channel

employed, a Telephonics TDH-39. Its frequency response curve is shown in Figure 5. The spectrum level of the noise masker was set at 46.1 dB SPL (see Appendix A) for all stimulus conditions. The 400-Hz tonal signal was generated by an audio oscillator (Hewlett Packard 200AB). The total duration of the signal to be detected, whether a tone or a noise burst, was 11.5 msec. The rise-fall time was always set to be 2.5 msec for tone or noise signals and also for the noise masker. The patterns of both tonal signal and noise signal as displayed on an oscilloscope are shown in Figure 6. The occurrence of the signal was controlled by a probability generator (BRS PP-1) with a fixed 0.50 probability of presentation in a given trial. Two electronic switches (Grason-Stadler 829E) and a series of BRS logic modules were used for determining which stimulus condition was in effect. After passing through two independent attenuators (General Radio 1450-TBR), the signal and the masker were mixed resistively and passed through a common attenuator (Daven 693), a transformer (Grason-Stadler E10589A), and then to the subject's right earphone. The subject was seated in s sound-proof chamber (Industrial Acoustics Company, Inc.). The intensity level of the signal was adjusted by the experimenter through the attenuator of the signal channel. Durations of the signal and the masker and their temporal relations were controlled and adjusted by two electronic timers (Grason-Stadler 471-1) and a series of BRS univibrators. Intensity levels of both signals and maskers were measured with an RMS voltmeter (Ballantine Laboratories 320A) outside the sound-proof chamber at the input to the earphone. A

Figure 5. The frequency response curve of the earphone (Telephonics TDH-39).

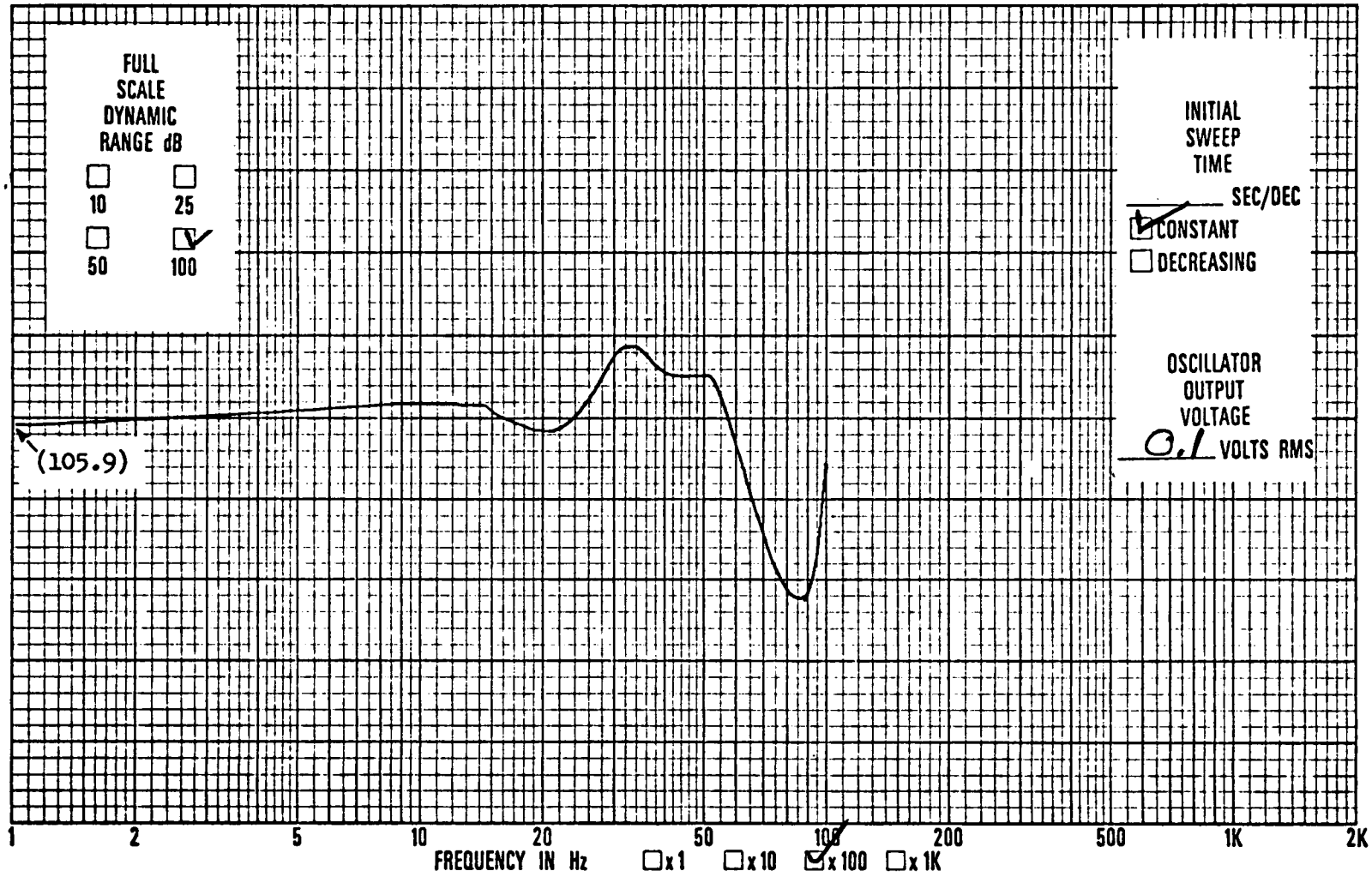
FULL
SCALE
DYNAMIC
RANGE dB
☐ 10
☐ 25
☐ 50
☑ 100
INITIAL
SWEEP
TIME
SEC/DEC
☑ CONSTANT
☐ DECREASING
OSCILLATOR
OUTPUT
VOLTAGE
0.1 VOLTS RMS
(105.9)
1
2
5
10
20
50
100
200
500
1K
2K
FREQUENCY IN Hz
☐ x 1
☐ x 10
☑ x 100
☐ x 1K

Figure 6. Patterns of tonal signal and noise signal shown as on the oscilloscope, both with durations of 11.5 msec.

Tonal Signal

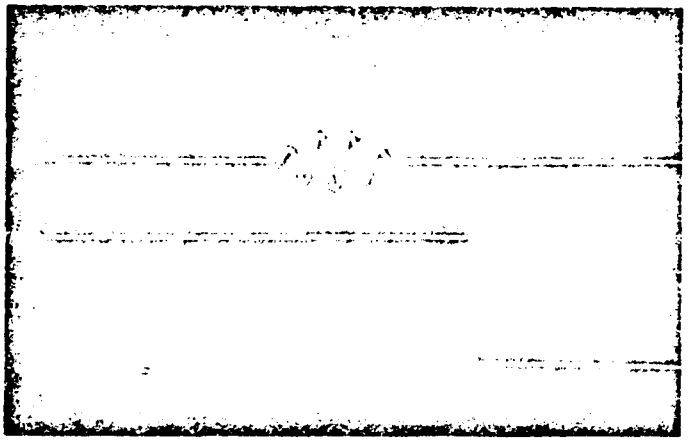

Noise Signal

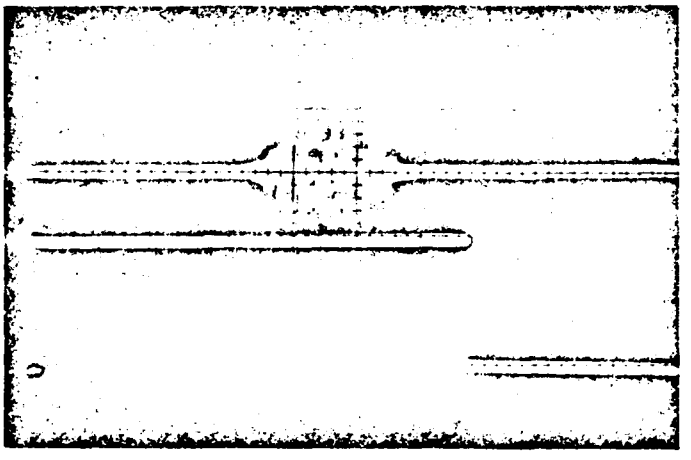

dual beam oscilloscope (Tektronix 502A) was always used by the experimenter for observing and checking the patterns of presentation of signals and maskers for all stimulus conditions. All subjects' responses for all conditions were made via pushbuttons and were recorded on electromechanical counters (BRS Decimal Counter CT-002). Subjects received feedback of results immediately after a given response on every trial in the form of a green light for a correct response or a red light for a incorrect response. The signal observation interval was approximately located for the listener by the onset and the offset of an orange light, pulsed by a 40-msec square wave whose midpoint was coincident with the midpoint of the signal interval. The signal interval occurred 1200 msec after the start of each trial. Each trial was started by the subject. The 'starting button', light indicators, and response buttons were mounted on a box which was put on a small desk just in front of the subject's seat.

C. Procedure

1. Experimental Design

The total duration of the signal was fixed at 11.5 msec. Two kinds of temporal arrangements of the masker were used. One of them was that, besides being simultaneously presented with the signal, the masker was extended symmetrically in time to produce a noise-fringe of selected duration before and after the signal - the noise-fringe condition. The other was that the masker was continuous in time

except for silent gaps of selected duration symmetrically surrounding the signal - the gap-fringe condition. One-sided durations of noise-fringe or gap-fringe were 0, 5, 10, 15, 25, 35, 45, 70, and 95 msec. The midpoint of the signal was always coincident with that of the noise masker. The 0-msec noise-fringe condition is usually referred to as the gated masking condition, and the 0-msec gap-fringe condition is usually designated as the continuous masking condition. As the noise-fringe increases, the condition approaches continuous masking. On the other hand, as durations of silent gaps in the continuously presented masker become longer, the gated masking condition is approached. For clarification, such timing relations of the signal and the masker for both the noise-fringe conditions and the gap-fringe conditions are depicted in Figure 7. A total of 2 (tonal signal, noise signal) x 2 (noise-fringe condition, gap-fringe condition) x 9 (fringe durations) or 36 stimulus conditions were included in the entire experiment. The order of data collection for the 36 stimulus conditions was randomized in the same way for all three subjects, with noise-fringe conditions and gap-fringe conditions presented alternately. For each stimulus condition, the set of signal intensity levels was chosen to yield listener performance in terms of percent correct in the approximate range of from 60% to 90%. Each experimental run always began with the signal at the strongest intensity level. Signal intensity was then decreased in steps of 2 dB for each block of trials, such that about 3 to 9 intensity levels were included in each given stimulus condition. A block consisted of 80 consecutive

Figure 7. Timing relations of the signal and the masker.

NOISE-FRINGE CONDITIONS:

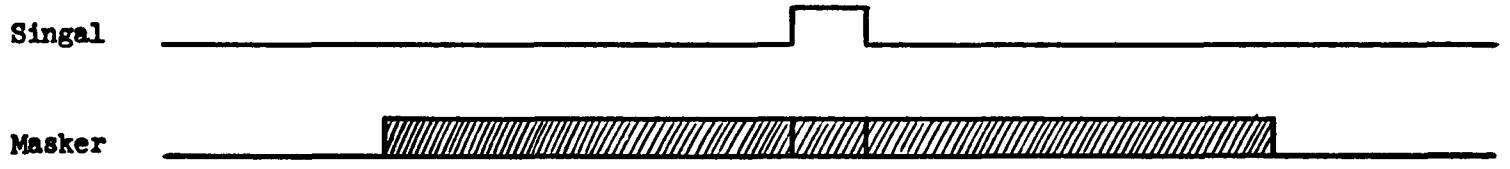

GAP-FRINGE CONDITIONS:

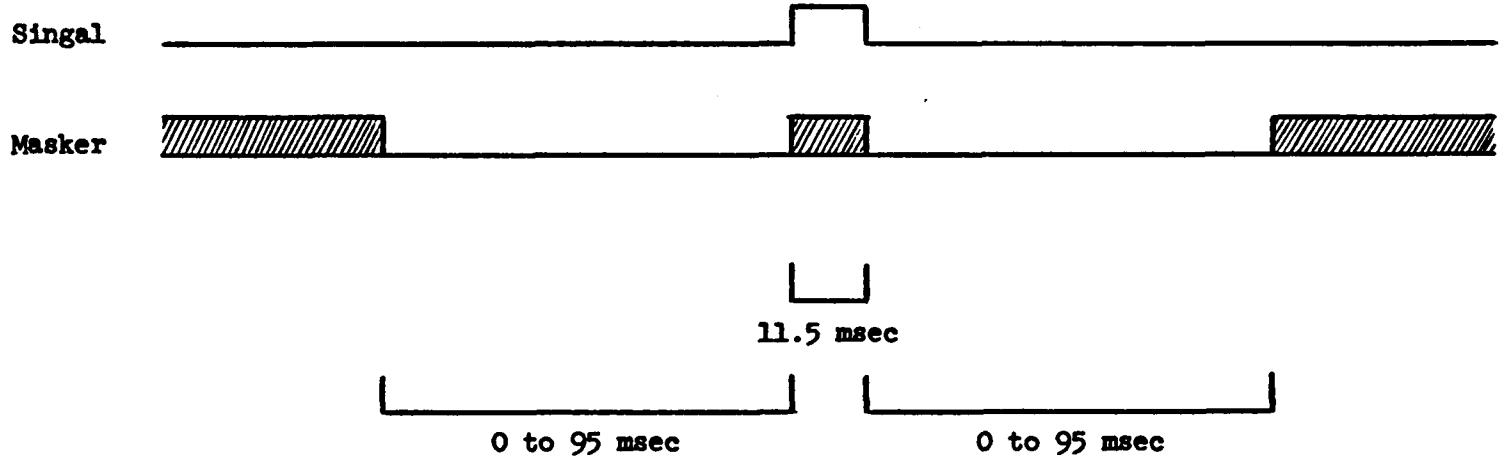

trials for a fixed signal level. Data collection for the entire set of 36 stimulus conditions at every signal level was repeated four times. Consequently, a total of 320 trials determined each data point on each psychometric function.

2. Psychophysical Methods

Listeners were verbally instructed as to task requirements and stimulus conditions. The subject was seated in the sound-proof chamber wearing the TDH-39 headset. Listening was self-paced, since the subject chose when to press the operate button which started each trial. Immediately after each stimulus presentation, the subject pressed the appropriate response button to indicate whether or not he judged the signal to be in the given noise background for that trial. The procedure is known as a single-interval or yes-no task. Feedback was given immediately after the subject's response for each trial by means of a green light for correct responses or a red light for incorrect responses. After the subject finished all 80 trials of an entire block, the experimenter adjusted the stimulus parameters and then signaled the subject to start the next block. For each stimulus condition, the range of intensity levels was chosen on the basis of each subject's performance in the preliminary training sessions. Subjects were allowed to take a rest between blocks for any two different stimulus conditions. The experiment was conducted, for each subject, for about 2 to 4 hours each day totalling about three months for the entire experiment. Before data were formally collected,

each subject received a minimum of about two weeks of preliminary training. Each subject was also allowed a few minutes of warm-up trials on each day.

3. Data Analysis

For each of the 36 stimulus conditions for each listener, the slope and the threshold of the psychometric function were estimated as follows. First, the hit rate and the false alarm rate across all four blocks of 80 trials were calculated. The measure d' was then determined by using those values to enter Elliott's Yes-No Table (Swets, 1964) and read the result. That d' was also converted into a maximum percentage of correct responses for 2IFC, $P_{max}(C)_2$, by consulting Elliott's Forced-Choice Table (Swets, 1964). Next, all data points for each stimulus condition for each subject were plotted by taking 10 log d' or $P_{max}(C)_2$ as ordinate values and pairing each with the corresponding stimulus intensity level in units of 10 $\log(E_s/N_o)$ for tonal signals and of 10 $\log(S_o/N_o)$ for noise signals as abscissa values where E_s is tonal signal energy, S_o is noise signal power density, and N_o is noise masker power density. These plots were fitted by the method of least-squares using Egan's formula: 10 log d' = m + k (10 log E_s/N_o) or 10 log d' = m + k (10 log S_o/N_o) (Egan, Lindner, and McFadden, 1969). The slope, k, and the threshold at d' = 1 (corresponding to $P_{max}(C)_2$ = 76%) were then estimated. Slopes and thresholds were each averaged for all three subjects for each stimulus condition. The variations of slopes and of thresholds as functions of noise-fringe and

of gap-fringe durations were studied for the individual listeners as well as for the averages across listeners.

III. RESULTS

The performances of all three listeners were similar to each others, so that their results were averaged for each stimulus condition. We will attend to the averaged data in our discussion. The individual data are presented along with the averaged to justify the argument that our presentation is fairly representative of each individual data set.

Thresholds for d' = 1 on the psychometric functions for the three individual subjects and the averages over subjects for detection of the tonal signal are shown in Table 4 and for detection of the noise signal in Table 5. Slopes of the psychometric functions for individual subjects and the averaged slopes for detection of the tonal signal are shown in Table 6, and for detection of the noise signal in Table 7.

Figures 8 and 9 depict the values of averaged thresholds as a function of duration of either the 'fringe of noise' or 'the silent gaps' surrounding the signal in the continuously presented noise masker for tonal signal detection and for noise signal detection, respectively. The corresponding data for individual listeners are plotted in Figures 10 and 11.

Similarly, the values of the averaged slopes of the psychometric functions for different settings of 'noise-fringe duration' or 'gap-fringe duration' are plotted in Figures 12 and 13 for the tonal signal condition and the noise signal condition, respectively. Figures 14 and 15 show the corresponding results for individual subjects.

Table 4. Thresholds, in dB, of psychometric functions for detection of a tonal signal masked by a wideband noise (46.1 dB SPL) for variations in temporal settings.

		Fringe Duration (msec)								
	Ss	0	5	10	15	25	35	45	70	95
	PT	5.4	7.8	7.9	8.3	10.1	10.7	12.0	-	9.8
Noise-fringe	HT	2.4	6.2	7.5	8.3	10.6	10.0	9.0	9.8	10.1
Condition	SP	4.5	6.9	9.9	9.5	8.9	9.7	9.7	9.8	7.6
	MEAN	4.1	7.0	8.4	8.7	9.9	10.1	10.2	9.8	9.2
	PT	7.1	7.1	5.3	4.8	5.0	4.7	7.0	-	5.1
Gap-fringe	HT	6.2	7.0	4.5	4.5	5.5	5.4	4.7	5.1	6.5
Condition	SP	6.8	6.2	5.2	3.4	4.8	4.6	5.9	4.5	6.1
	MEAN	6.7	6.7	5.0	4.2	5.1	4.9	5.9	4.8	5.9

Table 5. Thresholds, in dB, of psychometric functions for detection of a noise signal masked by a wideband noise (46.1 dB SPL) for variations in temporal settings.

		Fringe Duration (msec)								
	Ss	0	5	10	15	25	35	45	70	95
	PT	-2.0	-2.5	0.0	-0.4	-0.4	1.2	-0.2	-	-0.7
Noise-fringe	HT	0.4	0.1	1.4	1.7	2.3	1.5	1.7	1.1	2.1
Condition	SP	-0.2	2.3	1.2	2.0	3.6	2.0	1.6	1.2	0.8
	MEAN	-0.6	0.0	0.9	1.1	1.8	1.6	1.0	1.2	0.7
	PT	-0.2	-1.4	1.1	-1.2	-0.8	-1.4	-0.5	-	-1.1
Gap-fringe	HT	-0.6	0.4	-1.9	-0.6	0.1	0.1	0.3	1.4	1.9
Condition	SP	-1.7	-3.0	-1.8	-1.0	-0.4	0.3	0.5	-1.2	2.5
	MEAN	-0.8	-1.3	-0.9	-0.9	-0.4	-0.3	0.1	0.1	1.1

Table 6. Slopes of psychometric functions for detection of a tonal signal masked by a wideband noise for variations in temporal settings.

		Fringe Duration (msec)								
	Ss	0	5	10	15	25	35	45	70	95
	PT	.77	.64	.61	.54	.87	.82	.70	-	1.15
Noise-fringe	HT	.60	.75	.90	.60	.59	.64	.87	1.21	1.06
Condition	SP	.74	.53	.68	.68	1.02	1.30	1.21	1.58	1.35
	MEAN	.70	.64	.73	.61	.83	.92	.93	1.40	1.19
	PT	1.35	1.26	1.11	.97	.83	.78	1.04	-	.96
Gap-fringe	HT	1.50	1.46	1.17	1.02	.89	1.15	1.13	1.16	1.03
Condition	SP	1.93	1.25	.98	.74	.95	.91	1.02	.84	.89
	MEAN	1.59	1.32	1.07	.91	.89	.95	1.06	1.00	.96

Table 7. Slopes of psychometric functions for detection of a noise signal masked by a wideband noise for variations in temporal settings.

		Fringe Duration (msec)								
	Ss	0	5	10	15	25	35	45	70	95
	PT	.93	.95	.82	.84	.98	1.27	1.20	-	1.10
Noise-fringe	HT	.98	.68	1.00	.95	1.26	1.09	1.11	1.18	1.33
Condition	SP	.64	.90	.76	.93	.88	1.19	1.35	1.36	1.17
	MEAN	.85	.84	.86	.91	1.04	1.18	1.22	1.27	1.20
	PT	2.38	.99	1.18	.91	1.05	.91	.95	-	.86
Gap-fringe	HT	1.47	1.39	.80	.91	.95	.62	.79	1.19	.92
Condition	SP	1.71	.82	.85	1.14	.75	.85	.76	.90	.93
	MEAN	1.85	1.07	.94	.99	.92	.79	.83	1.05	.90

Figure 8. Thresholds for d' = 1 as a function of the duration (one-sided) of either a "fringe of noise" or a "fringe of gap" surrounding the basic 11.5-msec signal interval. The signal is a 400-Hz tone burst. Data points are averages over three listeners.

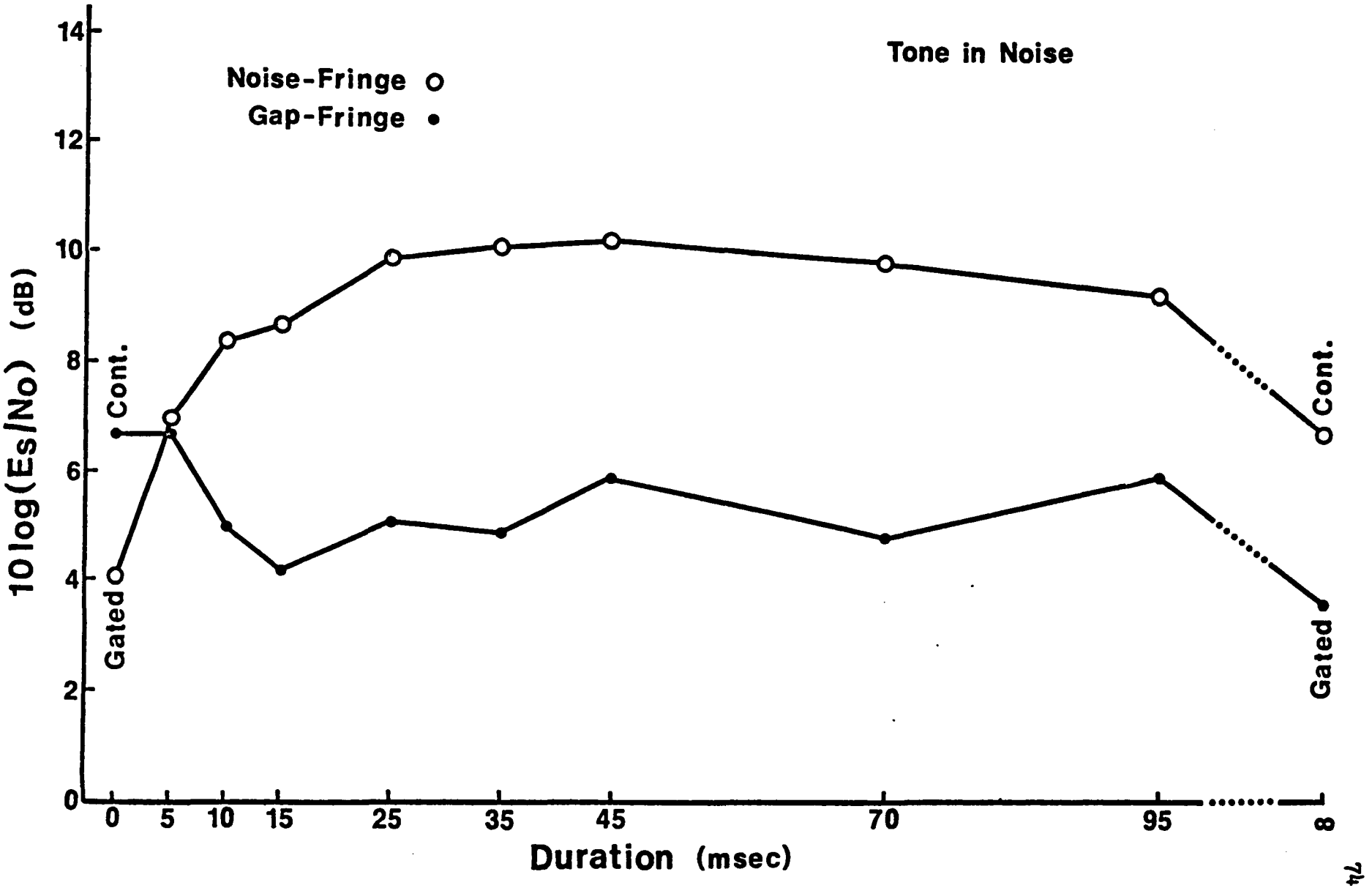
Tone in Noise
Noise-Fringe ○
Gap-Fringe ●
10 log (Es/No) (dB)
14
12
10
8
6
4
2
0
Cont.
Gated
Cont.
Gated
0
5
10
15
25
35
45
70
95
∞
Duration (msec)

Figure 9. Thresholds for d' = 1 as a function of the duration (one-sided) of either a "fringe of noise" or a "fringe of gap" surrounding the basic 11.5-msec signal interval. The signal is a broadband noise independent of the masker. Data points are averages over three listeners.

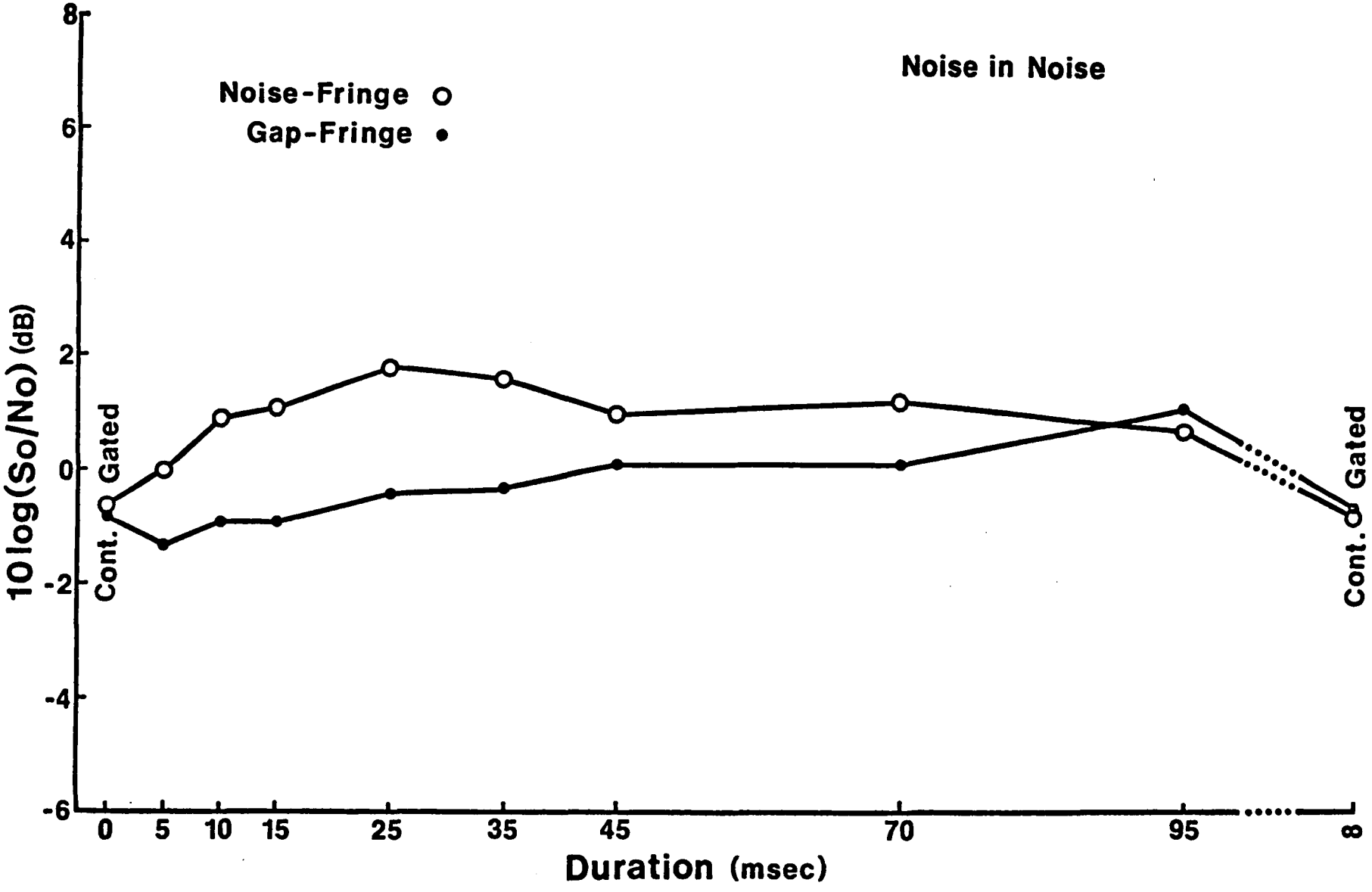
Noise in Noise
Noise-Fringe
Gap-Fringe
8
6
4
2
0
-2
-4
-6
10 log (So/No) (dB)
Cont.
Gated
Cont.
Gated
0
5
10
15
25
35
45
70
95
8
Duration (msec)

Figure 10. Thresholds for d' = 1 as a function of the duration (one-sided) of either a "fringe of noise" or a "fringe of gap" surrounding the basic 11.5-msec signal interval. The signal is a 400-Hz tone burst. Data points are for individual listeners.

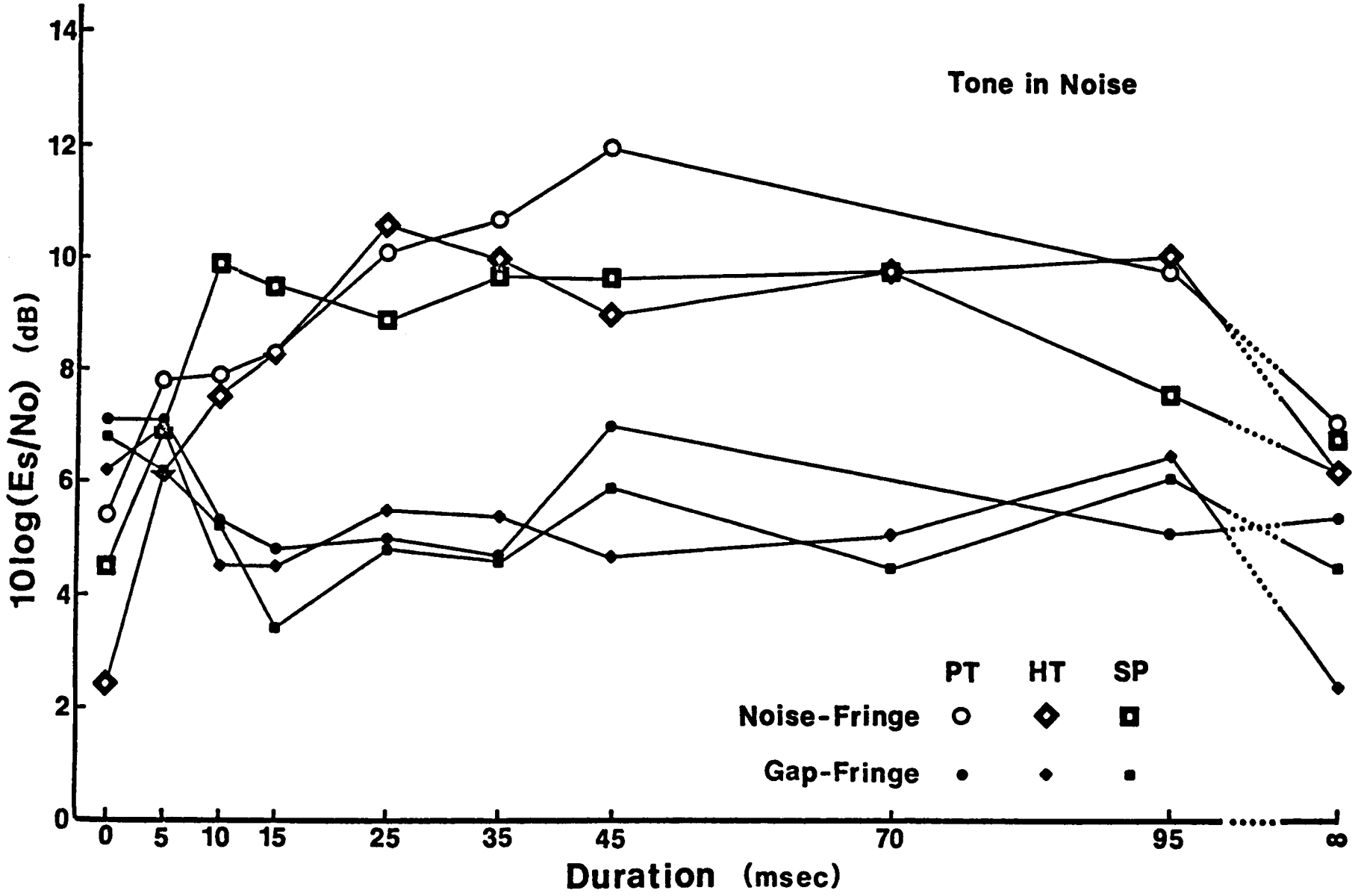
Tone in Noise
10log(Es/No) (dB)
14
12
10
8
6
4
2
0
0
5
10
15
25
35
45
70
95
∞
Duration (msec)
PT
HT
SP
Noise-Fringe
Gap-Fringe

Figure 11. Thresholds for d' = 1 as a function of the duration (one-sided) of either a "fringe of noise" or a "fringe of gap" surrounding the basic 11.5-msec signal interval. The signal is a broadband noise independent of the masker. Data points are for individual listeners.

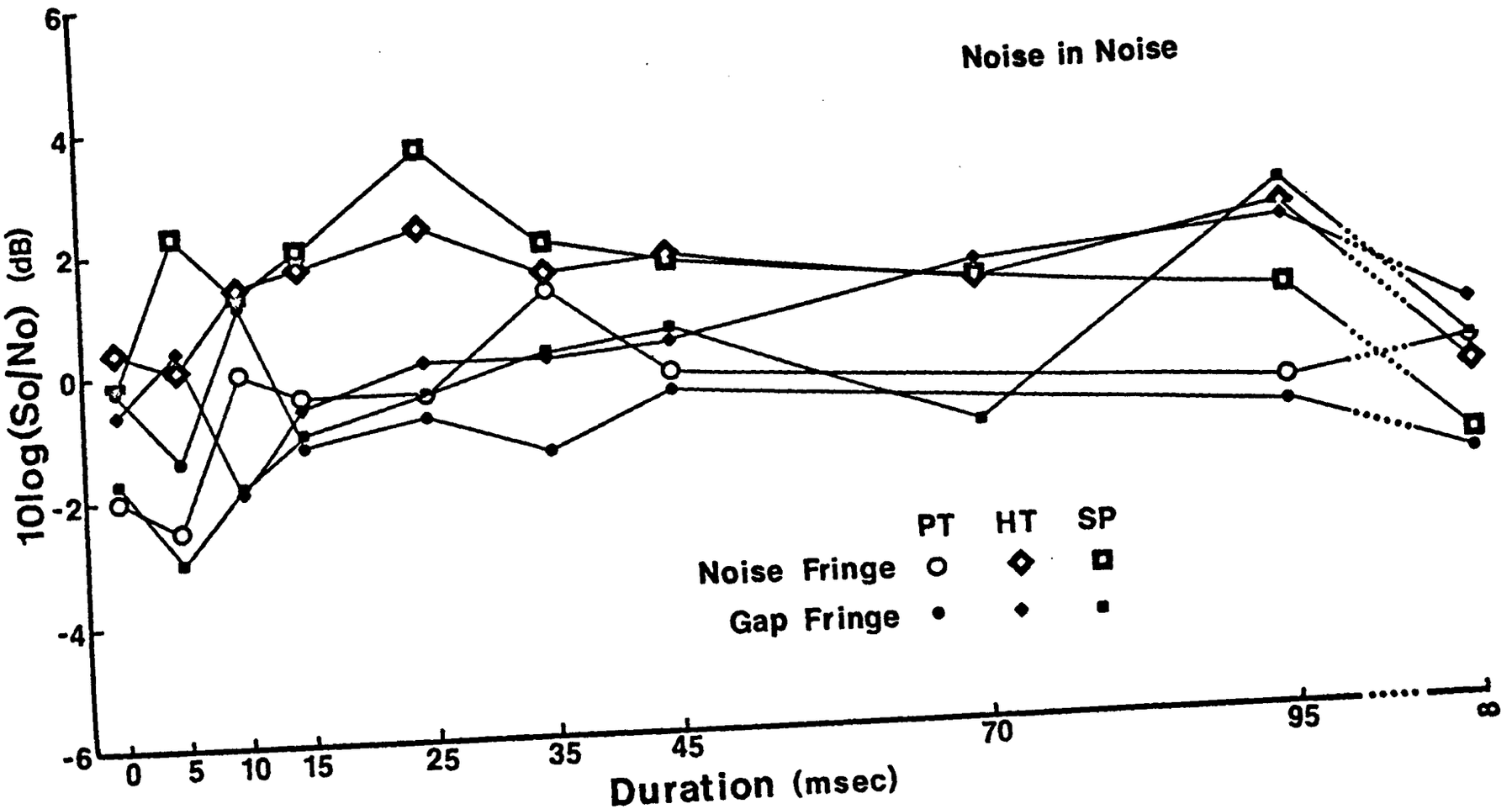
Noise in Noise
10log(So/No) (dB)
6
4
2
0
-2
-4
-6
0
5
10
15
25
35
45
70
95
∞
Duration (msec)
PT
HT
SP
Noise Fringe
Gap Fringe

Figure 12. Slopes of the psychometric functions as a function of the duration (one-sided) of either a "fringe of noise" or a "fringe of gap" surrounding the basic 11.5-msec signal interval. The signal is a 400-Hz tone burst. Data points are averages over three listeners.

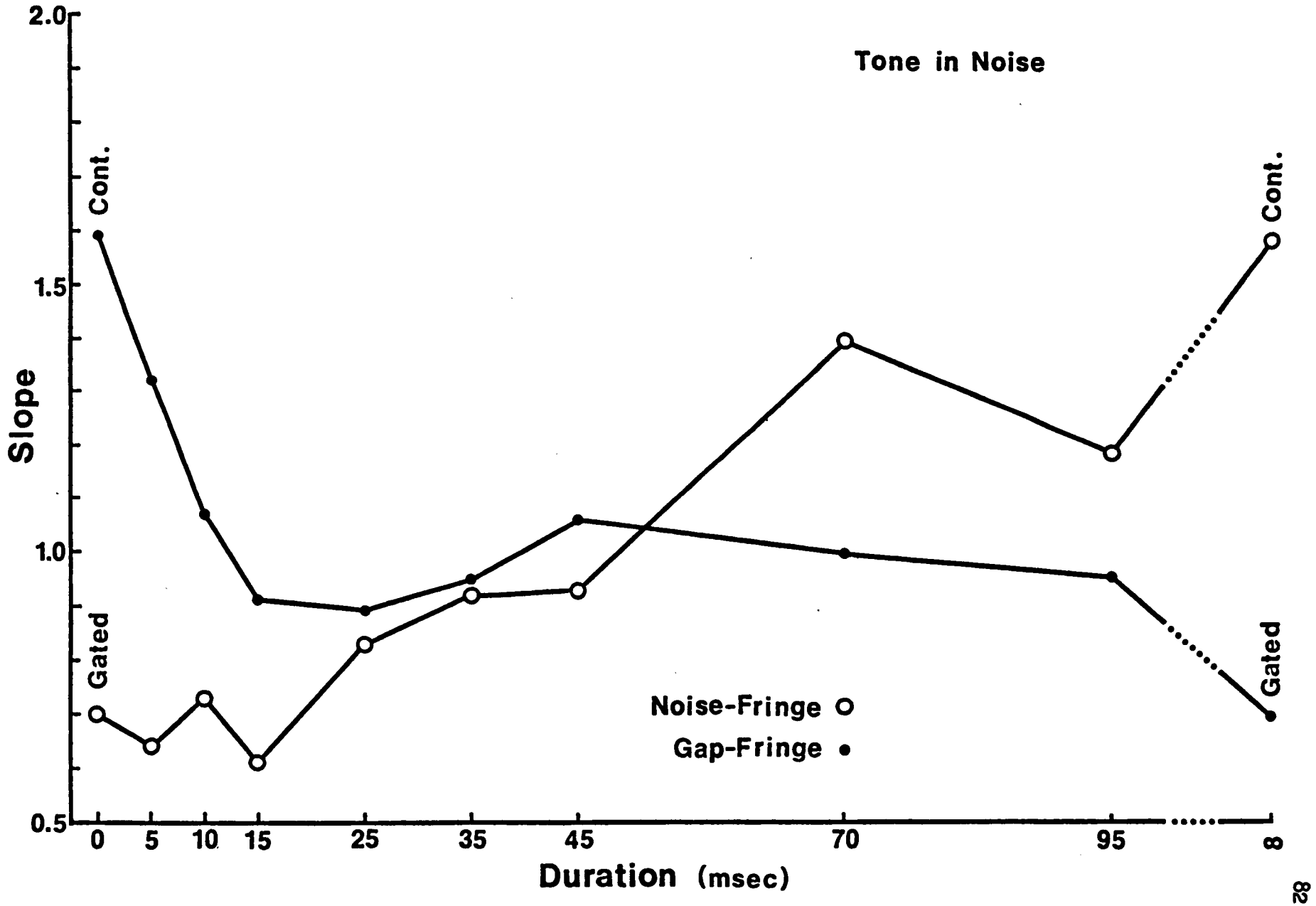
Tone in Noise
2.0
1.5
1.0
0.5
Slope
Cont.
Gated
Cont.
Gated
Noise-Fringe
Gap-Fringe
0
5
10
15
25
35
45
70
95
∞
Duration (msec)

Frigure 13. Slopes of the psychometric functions as a function of the duration (one-sided) of either a "fringe of noise" or a "fringe of gap" surrounding the basic 11.5-msec signal interval. The signal is a broad-band noise independent of the masker. Data points are averages over three listeners.

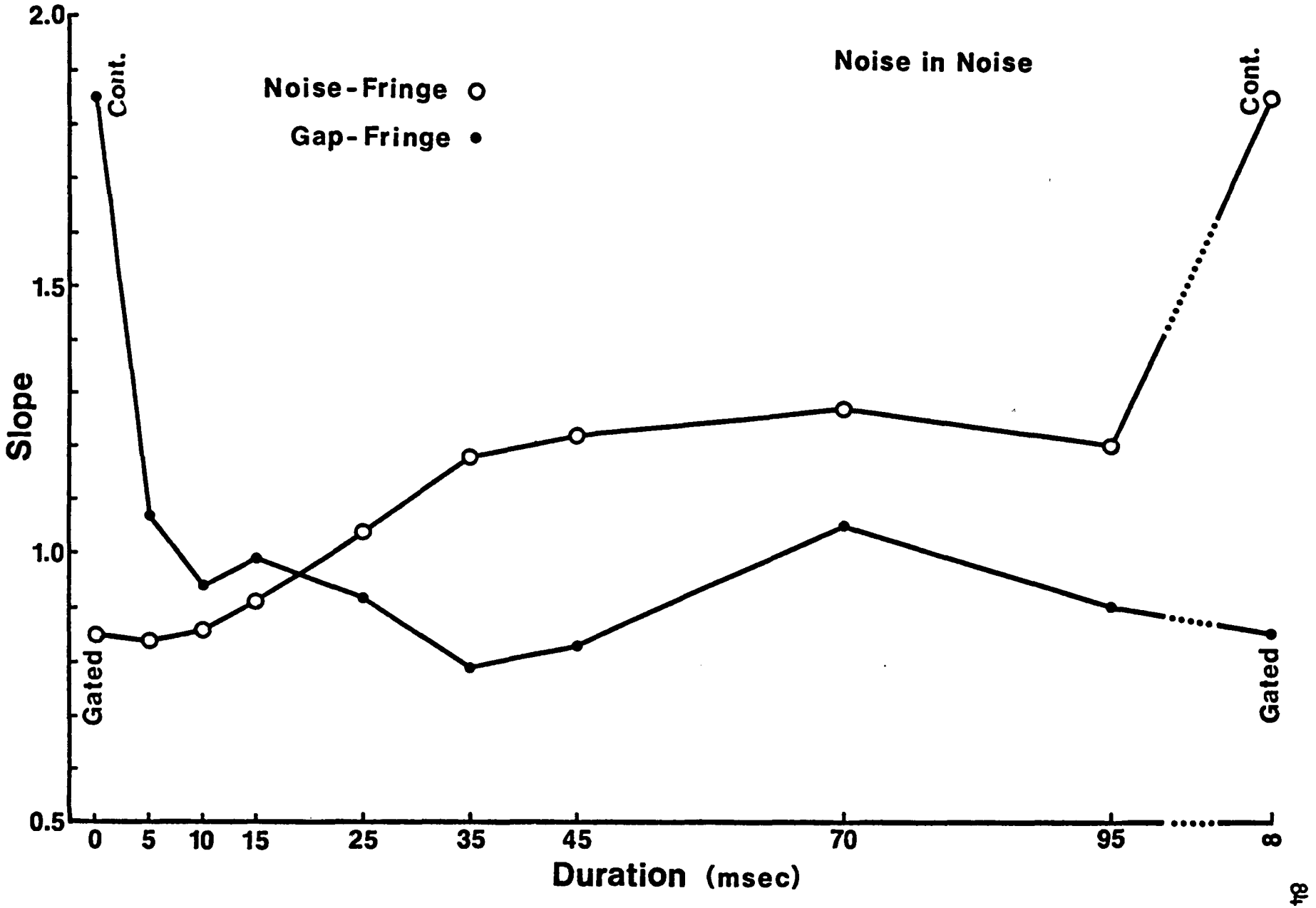
Noise in Noise
Noise-Fringe
Gap-Fringe
Cont.
Cont.
Gated
Gated
Slope
2.0
1.5
1.0
0.5
0
5
10
15
25
35
45
70
95
8
Duration (msec)

Figure 14. Slopes of the psychometric functions as a function of the duration (one-sided) of either a "fringe of noise" or a "fringe of gap" surrounding the basic 11.5-msec signal interval. The signal is a 400-Hz tone burst. Data points are for individual listeners.

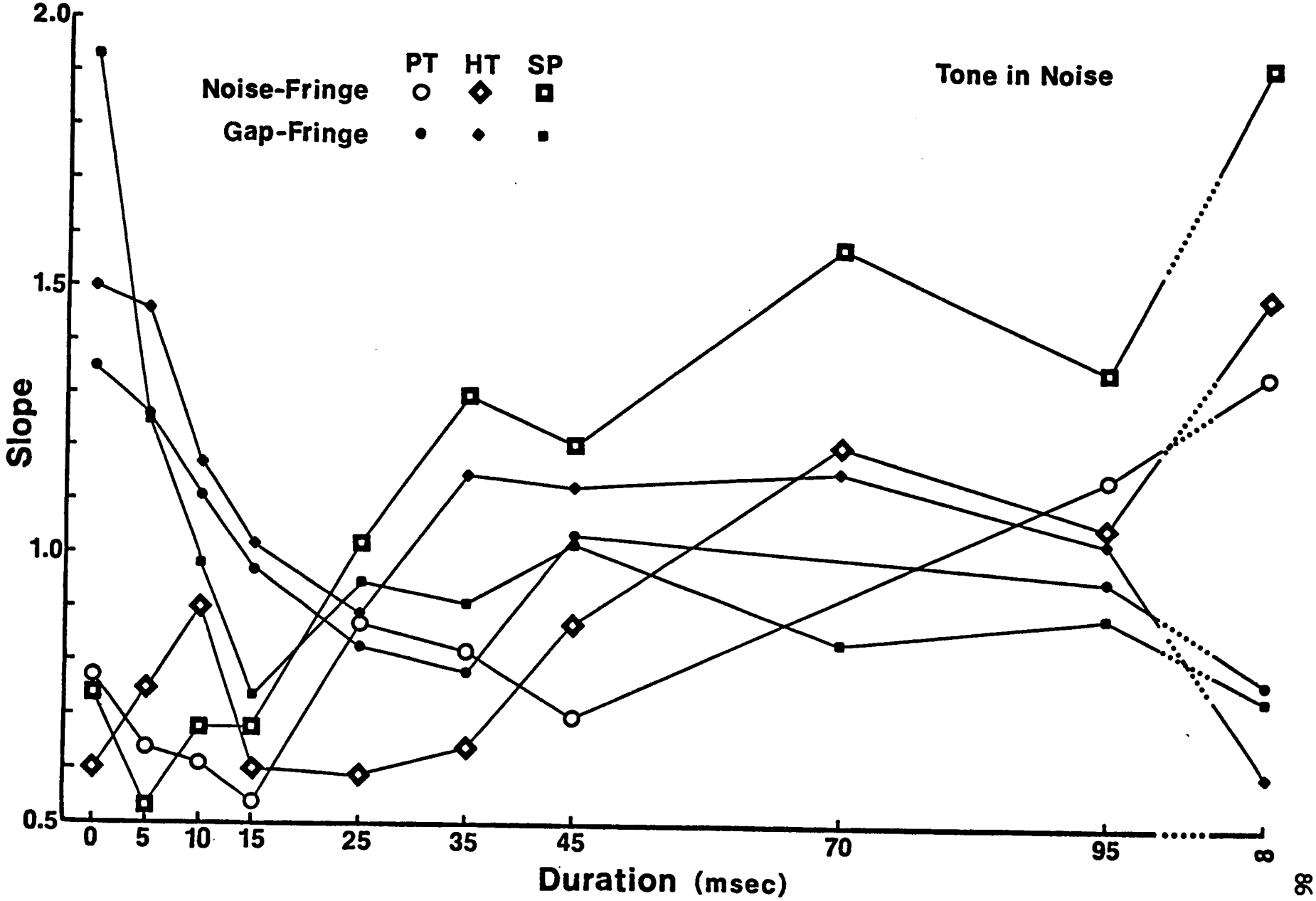
2.0
1.5
1.0
0.5
Slope
PT HT SP
Noise-Fringe
Gap-Fringe
Tone in Noise
0 5 10 15 25 35 45 70 95 ∞
Duration (msec)

Figure 15. Slopes of the psychometric functions as a function of the duration (one-sided) of either a "fringe of noise" or a "fringe of gap" surrounding the basic 11.5-msec signal interval. The signal is a broadband noise independent of the masker. Data points are for individual listeners.

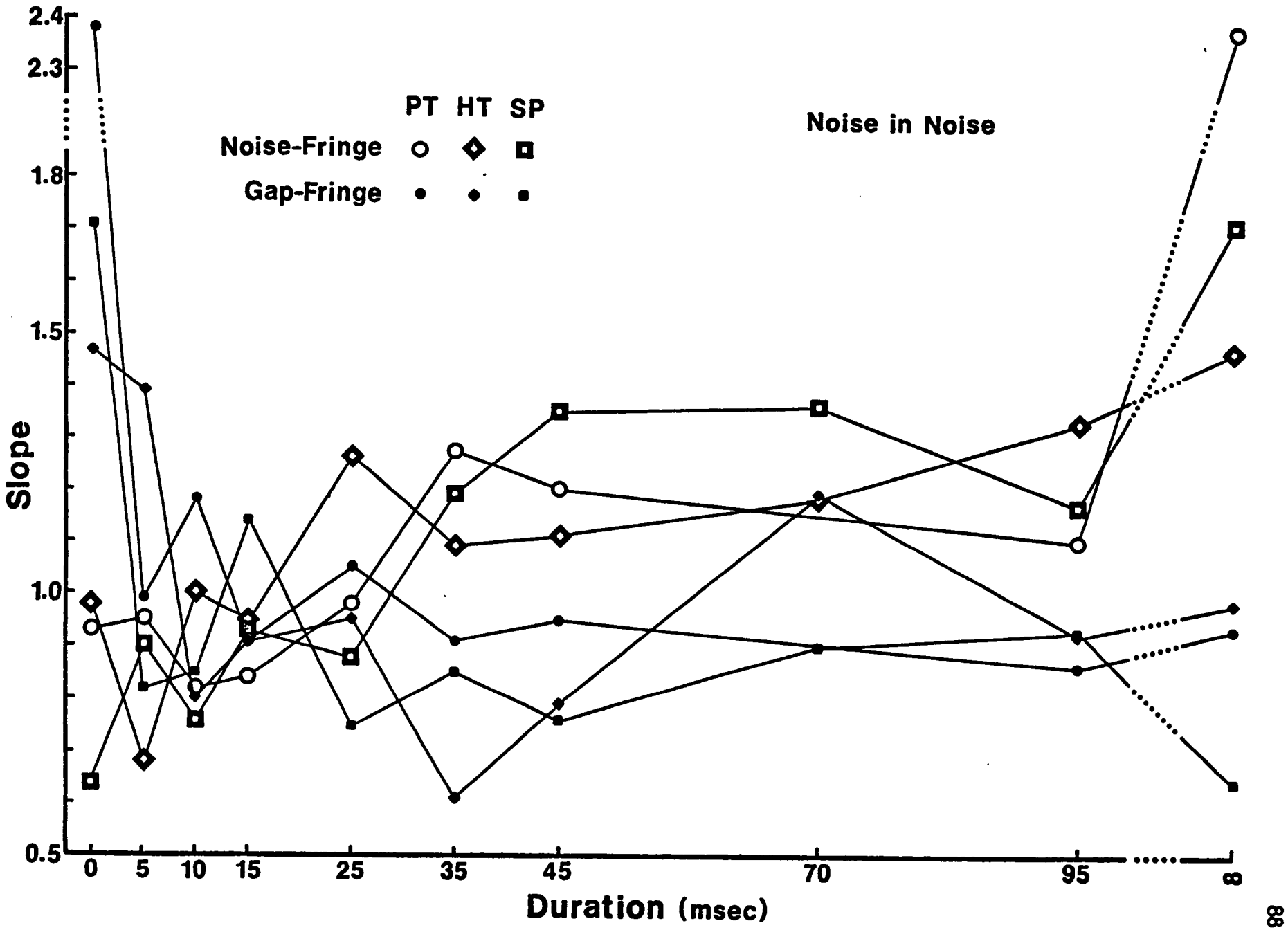
2.4
2.3
1.8
1.5
1.0
0.5
Slope
PT HT SP
Noise-Fringe
Gap-Fringe
Noise in Noise
0
5
10
15
25
35
45
70
95
∞
Duration (msec)

Tone in noise: thresholds

Beginning with the gated masking (0-msec noise-fringe) condition for tonal signals, note that the energy E_s/N_0 threshold value of 4.1 dB agrees well with other published values (e.g. Tucker et al., 1968). As the noise-fringe is extended the threshold is driven up along a negatively accelerated course to peak after a rise of 6.1 dB at a fringe duration of 45 msec. Beyond that point the threshold drops gradually out to 95 msec. The limiting value with increasing fringe may be taken as the threshold for the continuous masking (virtually infinite noise-fringe) condition, 6.7 dB, which also agrees with other research (e.g. Green, 1960b; 1966). As a gap-fringe is introduced, the threshold is stable for 5 msec and then drops to a minimum of 4.2 dB at 15 msec, after which it appears to rise slightly and hover around 5 to 6 dB out to 95 msec. The limiting gap-fringe threshold value is the gated masking threshold, which is reached by a subsequent drop.

The individual subjects' data agree extremely well with each other and with the average results for noise-fringe and gap-fringe thresholds out to 10 msec, where the only intersubject differences that stand out are the somewhat lower threshold of HT for gated masking and the somewhat higher threshold of SP for the 10-msec noise fringe. For fringe duration of 10 msec or greater the individual differences may be more important, and the trend of the average data must be qualified by the following points. The peak of the noise-fringe function varies from 10 to 25 to 45 msec across the three

subjects in the order SP, HT, PT, and the trend beyond the peak out to 95 msec is not a consistently gradual decline. However, the overshoot reflected in the final drops to the continuous masking threshold is clear for all three subjects. Although the individual differences are neglible for the gap-fringe data out to 35 msec, the small variations beyond that value may discredit the slight rise for the average data, and, except for subject HT, there is no large drop when the gap is maximized.

Tone in noise: slopes

For noise-fringe durations from 0 msec (gated masking) to 15 msec, the average slope of the psychometric function remains within the range from 0.60 to 0.75, and rises for further increases in fringe duration, crossing 1.0 between 45 and 70 msec. The slope remains above 1.0 for the longer noise-fringes, and is a maximum of about 1.6 for continuous noise. As a gap-fringe is then introduced and expanded the slope declines smoothly, crossing 1.0 between 10 and 15 msec. The slope is a minimum of about 0.9 at 15 and 25 msec, then increases and declines again by very small amounts, remaining in the region of 1.0 for further increases out to the 95-msec gap-fringe. Returning to the gated masker condition, which is the maximal gap-fringe, the slope has dropped back to 0.70.

Careful examination of the individual slope data reveals that the pattern of the average results described above is well-supported for each subject, except for qualifications regarding individual differences

in numerical values. In particular, note that the individual curves cross 1.0 at very different durations for noise-fringe.

Tone in noise: threshold/slope comparisons

Gated masking (0-msec noise-fringe) thresholds are lower than continuous masking (0-msec gap-fringe) thresholds for each subject. The average difference is 2.6 dB. The noise-fringe and gap-fringe thresholds are nearly equal for the 5 msec fringe, with differences for individual subjects of no more than 0.8 dB. For longer fringe durations thresholds are consistently greater for every subject for the noise-fringe than for the gap-fringe conditions. Slopes are consistently lower for every subject under noise-fringe conditions than under gap-fringe conditions out to 15 msec. Beyond 15 msec the individual differences are more prominent, but the average slopes for noise-fringe and gap-fringe are nearly the same from 25 to 45 msec, and are larger for noise-fringe than for gap-fringe beyond 45 msec.

Averages for thresholds and slopes are jointly non-decreasing or non-increasing functions of fringe duration for noise- or gap-fringe conditions. Note that the 15-msec fringe duration appears to be an important demarcation point. Noise-fringe thresholds rise and slopes are level from 0 to 15 msec, after which the slope rises rapidly while the threshold continues to rise slowly to its peak value. Both slopes and thresholds for gap-fringe drop between 0 and 15 msec, and both show the same pattern beyond 15 msec (including a minor peak at 45 msec). The slope-threshold covariation is excellent for gap-fringe conditions

from 5 msec out to and including the limiting gated-masking condition. Local peaks occur in both threshold functions and in the gap-fringe slope function at 45 msec. The 45 msec region is also the location beyond which the two slope functions diverge. The slope for noise-fringe crosses the 1.0 level just beyond 45 msec. The small peak slope for gap-fringe is also near 1.0 at 45 msec, although the gap-fringe slope first crosses 1.0 between 10 to 15 msec. Both slope functions are in very close agreement from 25 to 45 msec. Lastly, examination of the data for individual subjects reveals that the values of noise-fringe duration for which the slope functions first cross the 1.0 level and the values of noise-fringe duration for which the threshold functions peak yield exactly the same ordering for the three subjects (SP, HT, PT).

Noise in noise: thresholds

Gated masking (0-msec noise fringe) thresholds for S_o/N_o average -0.6 dB, in close agreement with other research (e.g. Wightman and Green, 1966). As the noise-fringe is increased the threshold rises smoothly to peak less than 2.5 dB higher at 25 msec, beyond which it drops very slightly, remaining in the region of 1.0 dB from 45 to 95 msec. Maximizing the noise-fringe yields a drop to the continuous masking threshold value of -0.8 dB, only 0.2 dB below the gated masking threshold, in agreement with other work (e.g. Green, 1960a). Then as a gap-fringe is introduced and extended, there is an initial 0.5 dB drop at 5 msec, followed by a gradual rise out to 1.1 dB at

95 msec. The limiting value for maximum gap-fringe (gated masking) shows a subsequent drop back to the starting point. The gated and continuous masking thresholds are virtually identical, and both lie below all threhsolds for non-zero values of noise-fringe and all values for gap-fringe beyond 15 msec.

The individual subject data show an appreciable degree of irregularity. However, they are still in good agreement with the average with the following qualifications. The noise-fringe threshold functions for subject HT and SP conform well to the description of the average results (except that the HT threshold first rises between 5 and 10 msec), and so would the data of subject PT if they were shifted upwards by a constant 2 dB for all noise-fringe values from 0 to 95 msec (except that the peak for PT occurs at 35 rather than 25 msec). Smoothing the individual gap-fringe data would also show the individual subject results to conform reasonably well to the description given for the average. The only remaining discrepancies would be that the minimum for subject HT appears at 10 rather than 5 msec, the thresholds of subject PT from 15 to 95 msec are again relatively too low, for subjects HT and SP the gap-fringe thresholds do not consistently exceed both gated and continuous masker thresholds for fringe durations beyond 15 msec, and for subjects HT and SP the gated masking threshold is 1.0 to 1.5 dB above the continuous masking threshold.

Noise in noise: slopes

The average slope remains level near 0.85 for noise-fringe

durations from 0 msec (gated masking) to 10 msec. It increases along a negatively accelerated course for further increases in noise-fringe, crossing 1.0 before 25 msec, and peaking at 70 msec, after which there is a negligible drop at 95 msec. Maximum noise-fringe (continuous noise) yields a huge jump in slope to 1.85. The introduction of a 5-msec gap-fringe reduces the slope markedly to 1.07, and the curve crosses 1.0 between 5 and 10 msec, after which it behaves cyclically, remaining in the region from about 0.8 to 1.0 (exceeding 1.0 marginally at 70 msec). The maximization of the gap beyond 95 msec (gated masking) yields no significant change in slope.

There is sufficient variability in the individual slope data to question some features of the average curves, particularly the precise locations where noise-fringe or gap-fringe slopes cross the 1.0 level and the existence and location of significant peaks. For subject SP alone the slope is at its lowest value for gated masking. Otherwise however, smoothing the data for each individual subject does yield good agreement with the average curves, and in particular, the very large jump in slope for continuous masking is unquestionable.

Noise in noise: threshold/slope comparisons

Average gated and continuous (0-msec fringe) thresholds are virtually identical, but so are the average thresholds for noise- and gap-fringe durations of 95 msec. For all other (intermediate) values of fringe duration, noise-fringe thresholds are greater than gap-fringe thresholds. The most flagrant violation of this in the

individual data is that for subject PT. The first 10 msec of fringe duration appear important since the gap-fringe slope goes through its rapid decline from the gated masking value in this range, and the noise-fringe slope first begin to rise for longer durations. The two slope functions cross in the vicinity of 15 msec and remain separated on opposite sides of 1.0 for longer fringe durations.

Again, the average threshold and slope functions can be roughly characterized as jointly non-increasing or non-decreasing function of fringe duration. This is violated for noise-fringe durations from 25 to 45 msec, and for the gap-fringe data the characterization is poor if not inaccurate. The 10 to 25 msec region is significant for both slope and thresholds. Within this region the noise-fringe slope begins to rise while the threshold approaches its maximum, and the gap-fringe slopes drops to its roughly level region while the threshold begins a slow rise. The noise-fringe and gap-fringe slopes are markedly different for the 0-msec fringe duration and still clearly different for 95 msec, while at both 0-msec and 95-msec noise-fringe and gap-fringe durations are nearly the same.

Comparisons between tonal signal and noise signal data:

The results for tonal and noise signal thresholds show reasonably similar functions of noise-fringe or gap-fringe duration. The following comparative features are noted. The separation of noise-fringe and gap-fringe functions is everywhere larger for this tonal signal, and the gated-continuous difference is clear only for tonal

signal. The noise-fringe and gap-fringe curves meet at 5 msec for the tonal signal, but at 0 msec for the noise signal. For noise-fringe, both signals show near maximum masking at 25 msec, and for both there is an overshoot or peak, the subsequent decline occurring earlier for the noise signal. The gap-fringe threshold decline reaches minimum later for the tonal signal, while a slow rise beyond minimum is clear only for the noise signal.

The results for slopes for tonal and noise signals are very similar in shape, for the noise-fringe and for the gap-fringe data. The most important difference may be seen as follows. If the time scale for the noise signal data were stretched by a factor of approximately two, the result would be very good match to the tonal signal data. The tonal signal and noise signal slopes for noise-fringe settle in a range of comparable values below the 1.0 level, while for gap-fringe results the slopes below 1.0 are less for the tonal signal than for the noise signal.

The above comments support an interesting observation. For all the data for thresholds and slopes, the tonal signal and noise signal results would be much more alike if, for the tonal signal slope and threshold data, the noise-fringe and gap-fringe data were moved together in the vertical dimensions, and the time scale was simultaneously compressed.

IV. DISCUSSION

In the introduction to this dissertation, it was stated that most auditory theories do not differentiate whether the masker is gated synchronously with the signal or is present continuously. However, the amount of masking has been found to be different for gated and continuous masker, and this interacts with signal duration (e.g. Wightman and Green, 1966; Viemeister, 1974; Tucker et al., 1968). Since the results of this study show tone thresholds to be 2- to 4-dB lower with gated as compared to continuous maskers, the sparse results reported by Tucker et al. (1968) for brief signals are confirmed. That virtually no gated-continuous threshold difference was found for noise signals in this study conforms to the report of Wightman and Green (1966), since the signal duration used here is close to the duration of intersection of their continuous-gated threshold-duration functions. Further support for an increasing continuous to gated masking difference with decreasing signal duration in the low millisecond range is supplied by Penner et al. (1972), where for a 100- sec click signal and a common spectrum noise masker, performance in the gated condition was about 13 dB better than in the continuous condition.

The continuous-gated difference in slope of the psychometric function is perfectly clear in the results of this study. All three listeners obtained slopes of greater than 1.00 in the continuous masking conditions for both tonal and noise signals (average slopes

are 1.59 and 1.85 respectively). All slopes are less than 1.00 (averages are 0.70 for the tonal signal and 0.85 for the noise signal) in the gated condition. These results are consistent with all previous research (e.g. Green, 1960a, 1966; Osman, 1975, Leshowitz, 1969; see introduction). The findings reported here on gated and continuous noise masking of tones were confirmed for HT and PT in a replication by Osman, Tzuo, and Tzuo (1980, unpublished), which also showed that individual differences were prominent only for gated masking thresholds, where experienced listeners perform best. Slope data for all five listeners of that study replicated the finding reported here.

The mystery of why the gated-continuous masking differences exist has prompted speculation by various authors. Consideration has been given to neural adaptation, imperfect memory, pitch ambiguity, and the notion of the drifting filter band to explain the greater masking effect of gated over continuous sinusoidal maskers, found even for signal durations of the order of 10 msec (Campbell, 1966; Green, 1969). To explain contrasting results such as those reported in this study, suggested mechanisms include energy splatter in the frequency domain (Tucker et al., 1968), offered solely in regard to threshold data, and signal uncertainty (Green, 1960a; Green and Sewall, 1962; Leshowitz and Raab, 1967), discussed primarily with reference to slope data.

It seems a priori simplest to presume that the detector is a simple energy detector for the gated masking condition. Nothing else seems possible for the broadband noise signal. The brief tone has a fairly broad spectrum and the duration may be too short to allow

any frequency related qualities such as pitch to be very useful for detection. However, this intuition may be incorrect and will be qualified later.

Intuitively, uncertainty regarding signal location in time should confound the detection process with continuous maskers, since there are no noise-burst end points to serve as time markers. If the detector can precisely localize the signal interval in time, so that the signal is specified except for phase, the general detection model for signal uncertainty with phase unknown may be applied with $M = 1$. The psychometric function in this case is identical to that of the simple energy detector for tone in noise with a bandwidth-duration product of unity. Increasing M will yield steeper slopes and somewhat higher thresholds. However, theoretical considerations cannot ignore the existence of other sources of system noise (of biological origin), the simplest consideration being that it is additive. Such an assumption tends to weaken the theoretical correlation of threshold and slope values, and that may leave too wide a range of possible interpretations for the gated-continuous data.

This study provides an opportunity to evaluate the gated-continuous masking controversy in the context of the noise-fringe and gap-fringe masking results, and thereby should imply restrictions on reasonable or possible underlying mechanisms. Using the extended energy detector as the working or baseline model, it is immediately apparent that the model fails to explain much of the data. Whereas

it is conceivable that assumptions concerning internal noise might easily render discrepant threshold values compatible with energy detection, the slope results preclude energy detection as the sole mechanism for masking results with noise-fringe duration exceeding about 45 msec for the tonal signal and 20 msec for the noise signal, and also for gap-fringe duration less than about 10 msec (which includes the continuous case) for both types of signal. This is so because the value of k (the slope of the psychometric function) cannot exceed unity for the energy detector per se.

To determine whether energy detection is a feasible scheme for any portion of the results (where $k < 1$), the mathematical model presented earlier was applied with the following supplementary assumptions and considerations.

First, the choice of the weighting function $w(t-\tau)$ or temporal filter shape should be reasonable in consideration of the results of other research which has been concerned with temporal filtering. In this regard an exponential form for $w(t-\tau)$ is a popular one (e.g. Penner, 1975, 1978; Zwislocki, 1969), and provides for the continual 'leak' of the integrator. Thus the choice was

$$w(t-\tau) = \exp\left[-(t-\tau)/\xi\right], \quad \tau \leq t, \tag{70}$$

$$= 0, \quad \tau > t \; ; \; \xi > 0 . \tag{71}$$

If we consider the noise-fringe data and allow $\xi = \infty$, then we have a rectangular filter whose shut off coincides with that of the masker. Otherwise the general rectangular filter is specified by choice of t' and t, the leading and trailing edges of the filter;

$$w(t-\tau) = 1 , \quad t' \leq \tau \leq t , \tag{72}$$

$$= 0 , \quad \text{otherwise.} \tag{73}$$

These filter shapes are illustrated in Figure 16.

Two other choices that were necessary were the values of equivalent rectangular band-width, W, and the readout point of the filter, t. Values of W should be selected to be sensible with respect to signal bandwidth and related literature. For the tonal signal case, a relatively small W would be acceptable, but a large value of W would be required for the noise signal case (Green and Swets, 1966; Green and McGill, 1970). The values of W are presumed symmetric about the center frequency of the signal. Further considerations of filter shape in the frequency domain are considered irrelevant for our purposes (e.g. Patterson and Henning, 1977). The readout point was first selected as a fixed value, $t \geq T$, for all conditions of the study or was presumed to be sliding, so that t coincides with noise-burst termination up to some maximum value of noise-fringe duration. This is a result of realizing that, for an exponential filter, the initial rapid rise of threshold seen in the noise-fringe data would be mostly a consequence of backward masking. Sliding t changes the model structure slightly, although the basic derivation remains unchanged in general, and the results are exactly the same if $w(t-\tau)$ is exponential (see Appendix B). If the filter were sliding and the shape of $w(t-\tau)$ arbitrary, then it must be realized that the signal to be detected is in effect located at different places within the time span of the integrator as noise-fringe duration is

Figure 16. Temporal filter shapes of the leaky power integrator. The temporal filter is assumed to be either an exponential function with a time constant, ξ, or a rectangular filter, with t' and t as the leading and trailing edges, respectively.

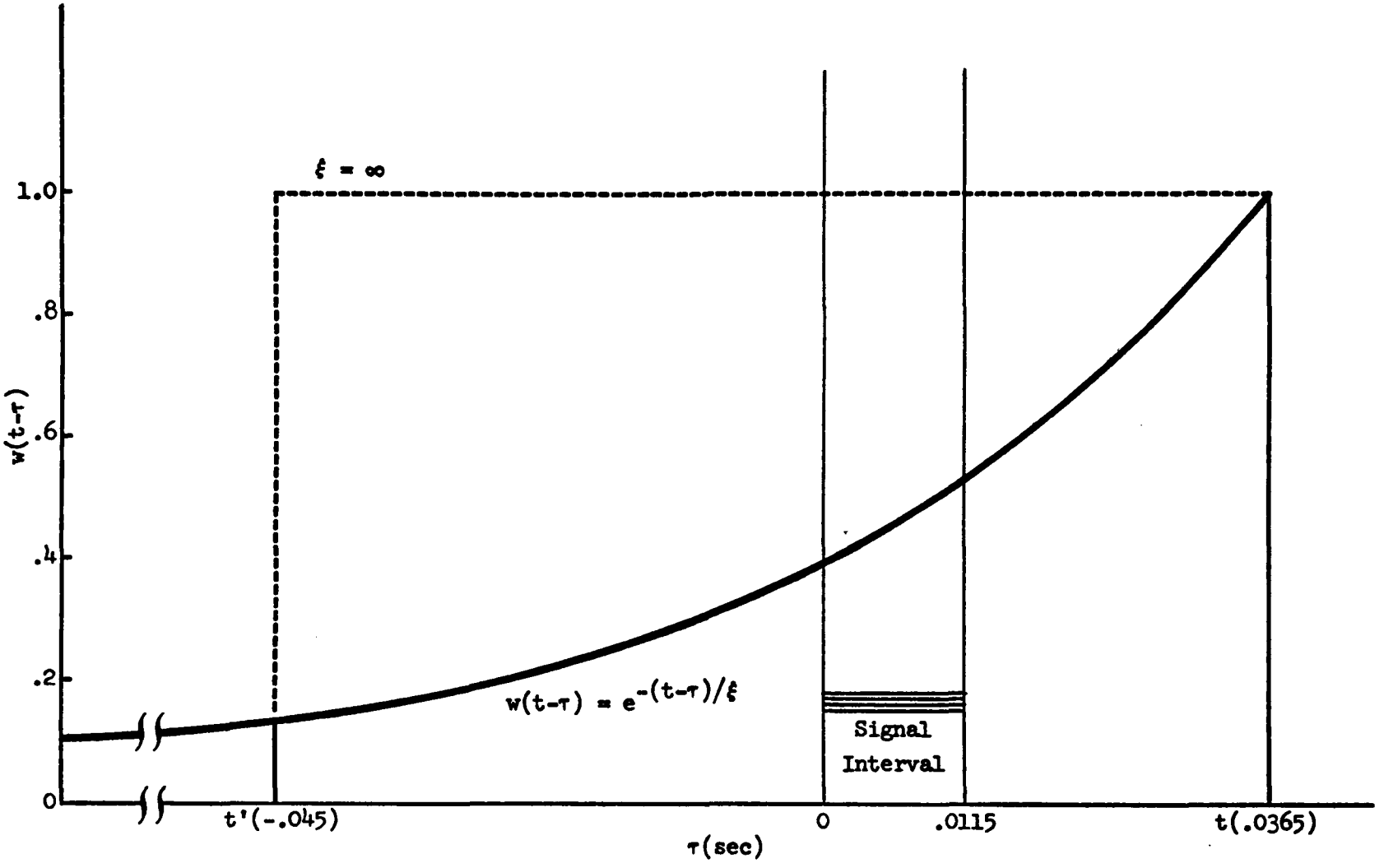
ξ = ∞
1.0
.8
.6
.4
.2
0
w(t-τ)
w(t-τ) = e^-(t-τ)/ξ
Signal
Interval
t'(-.045)
0
.0115
t(.0365)
τ(sec)

changed. Then threshold shifts may actually be due to loss of signal energy by leakage in the range of sliding t.

In order that the model used here makes sense, it is required that slope and threshold results are fit jointly using the same parameters. Here it is important to realize that psychoacoustic research has made clear the existence of internal or biological noise. It may be driven by or independent of input noise, and may exceed input noise in magnitude (e.g. De Boer, 1966; Green and Henning, 1969; McGill, 1967; Siebert, 1968; Osman, 1971). Then the value of N_o in our calculations might be inappropriate. Since noise level N_o is constant, any internal noise may be treated as if it were additive. This is because the resultant noise level, η_o, (after all noise sources have made their contribution to the masking process) could be treated as $\eta_o = N_o + (\eta_o - N_o)$, where $\eta_o - N_o$ is the "additive" internal noise. The problem could also be viewed by setting $\eta_o = N_o(1 + R)$, or $\eta_o - N_o = N_oR$, so that the dB shift attributable to the internal noise is given by $10 \log(1 + R)$, where $R = (\eta_o - N_o)/N_o$. The only requirement insisted on is that $1 + R$ is independent of noise-fringe or gap-fringe duration. Then theoretical results will be satisfactory if the function parallels the threshold data and the companion slopes are also compatible with the slope data.

Sample results of applying the leaky power integrator are illustrated in Figure 17 for the tonal signal case. It shows that the noise-fringe threshold data can be fit very satisfactorily for noise-fringe durations from 5 to 45 msec, while the corresponding

Figure 17. Theoretical noise-fringe threshold and slope functions for the leaky power integrator in the detection of a tonal signal masked by a broadband noise burst. The temporal filter shape is assumed to be either exponential with a time constant of 40 msec or rectangular. The frequency bandwidth is assumed to be in the range from 100 to 200 Hz. Theoretical noise-fringe thresholds shown in the figure are after an upward shift of 4.5 to 3.3 dB for the calculated thresholds. The shift is an adjustment for presumed internal noise and the difference between input signal energy and time filtered signal energy (about 0.5 dB). The maximum filter readout time, t, is assumed to be at 25 msec after signal termination.

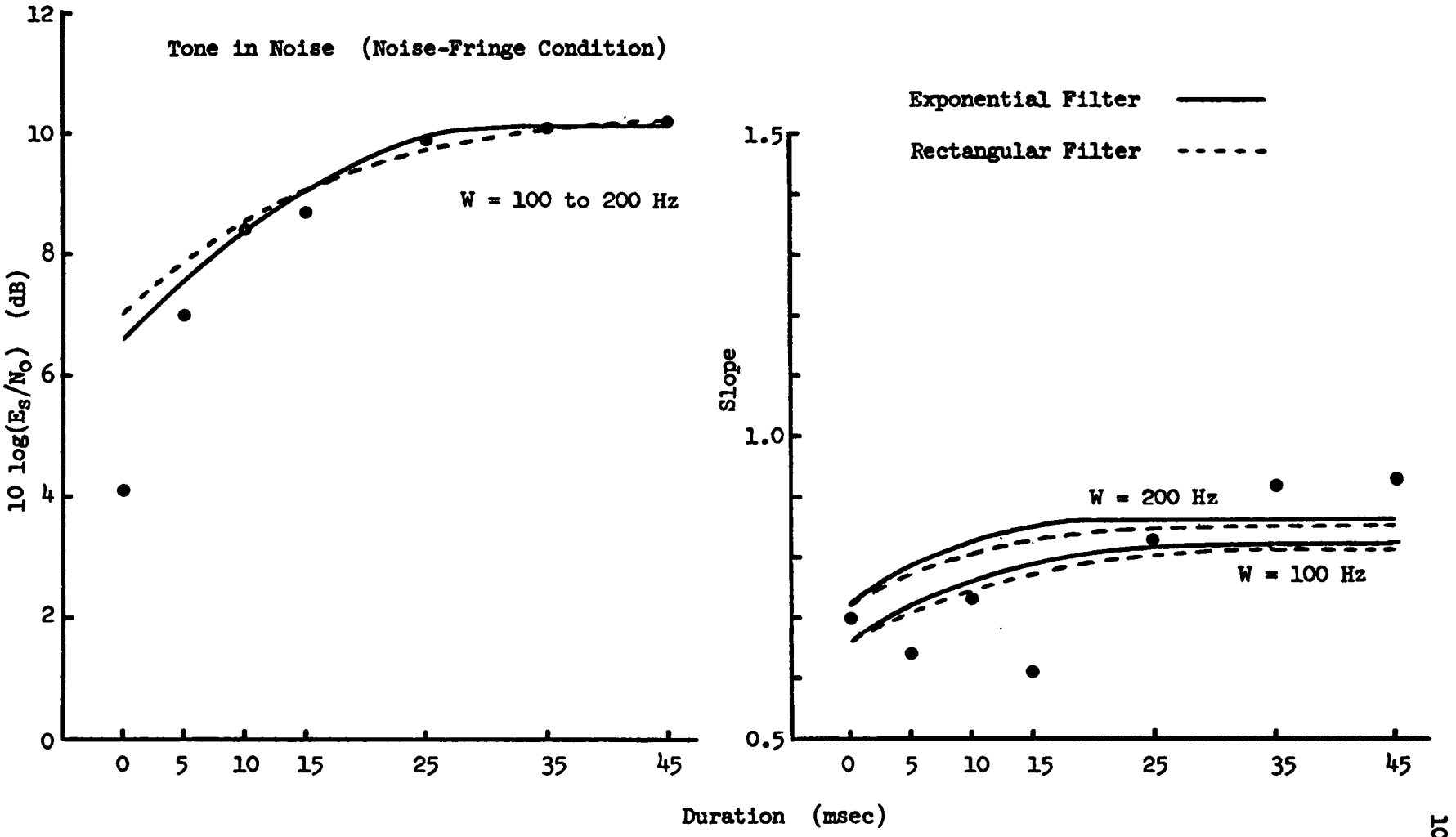
Tone in Noise (Noise-Fringe Condition)
Exponential Filter
Rectangular Filter
W = 100 to 200 Hz
W = 200 Hz
W = 100 Hz
10 log(Es/No) (dB)
Slope
Duration (msec)
12
10
8
6
4
2
0
1.5
1.0
0.5
0
5
10
15
25
35
45

slopes of the model lie in a range roughly compatible with the data. Most of the gradual increase in slope for the data as noise-fringe duration increases is attributed to growing 'uncertainty' and will be discussed further below. Choosing a limiting readout point $t = T + 25$ msec and a moderate bandwidth W of about 100 to 200 Hz led to similarly good fits whether the filter was rectangular or exponential with a time constant $\xi = 0.04$. Smaller time constants yield too steep a rise for the threshold function. One additional requirement was the assumption that internal noise coupled with the difference between input signal energy and time filtered signal energy yields a uniform upward shift of the theoretical curve of about 4.5 to 3.3 dB. About 0.5 dB of this is attributed to the effect of the exponential leak on calculated signal energy (see Appendix C). Curve fits for different sets of parameter values are shown in Appendix D.

Before considering the remainder of the data, some additional justification seems warranted for the choices of W and t. Critical bandwidth estimates for detection of tones in noise have been of the order of 50 to 100 Hz for signal frequencies from 250 to 500 Hz (Green and Swets, 1966). The brief gated signal used in this study should generate some spectral energy spread, suggesting the bandwidth to be used by the detector. A value of $W = 1/T$ is considered appropriate (Jeffress, 1968), and this does put W at about 100 Hz. A somewhat larger value, even 200 Hz, is not unreasonable. Selecting $t = T + 25$ msec implies that backward masking is much more important than forward masking up to 25 msec beyond signal termination, if the exponential filter has a sufficiently

rapid decay. For the choices in Figure 17, the decay was given by the time constant of 40 msec, so that most of the forward masking energy would have been lost by leakage. Note that the values for W and ξ are reasonably comparable to those used by Jeffress (1968) for his electrical analogue of a leaky integrator ($W \approx 50$ Hz, $\xi \approx 50$ msec).

Since this study can be thought to involve the joint effects of backward, forward and simultaneous masking segments, other work must be used to justify the choice of t. The most relevant studies are the temporal masking studies of Elliott (1962a, 1965). She demonstrated backward masking to be at least 6 dB more effective than forward masking over the first 5 msec beyond the signal interval, for a 10-msec, 1000-Hz signal and broadband noise of 50-msec duration. Her results also show that the combination of simultaneous and backward masking for those signal and masking noise parameters is more effective in raising signal threshold than the symmetrical combination of simultaneous and forward masking. This result was confirmed by Osman (1980, unpublished) for 400-Hz tones of 10-msec duration and a broadband masker of 125-msec duration. Simultaneous masking was also shown to be roughly equivalent to combined simultaneous and forward masking, while the thresholds were several dB higher for combined simultaneous and backward masking. Thus a dominant backward masking effect as dictated by the assumption of $t = T + 25$ msec is reasonable for the model as applied in this study.

Continuing to focus attention on the noise-fringe data of Figure 17, note that it is at about 25 msec of noise-fringe duration that

the slope begins to rise gradually, although it remains below 0.95 at 45 msec. The assumption of maximizing filter readout time t at T + 25 msec in the model is meant to imply that for the noise-fringe conditions the listener reads the output of the integrator at a point determined by noise-burst termination for noise-fringes not greater than 25 msec in duration. It is then reasonable to assume that some degree of uncertainty regarding where to locate t (and still effectively capture the signal interval in the process of integration) may develop for noise-fringe durations greater than 25 msec. This is compatible with the data as at least a reasonable assumption, considering that in the usual model of uncertainty with signal phase unknown, as M goes from 1 to 4, the slope shifts from 0.82 to 1.05 while the accompanying threshold rise is only 0.78 dB (see Table 1). (Note that for the leaky power integrator the slow continuing increase in threshold after the filter is presumed to have stopped sliding (i.e. the maximum upper limit of integration has been reached) is entirely attributable to forward masking.)

The remaining problem for Figure 17 is that the obtained gated (0-msec) masking threshold in particular (and possibly also the threshold at 5 msec) is too low and so may be the slope. One possible explanation for the rapid rise of threshold from the gated masking value with increasing noise-fringe is readily inferred from Duifhuis (1973). In considering backward masking for short silent intervals (of the order of a few milliseconds) between tone probe and noise masker, he argues that the relative time delays resulting from the phase

response of the peripheral filter would lead to the significant smearing of tone and noise in time at the output of the filter. By implication, the gated tone-in-noise threshold in this study may be especially low because the filter delay would effectively place the tone burst partially outside the noise in the gated condition. Actually, the delay is frequency dependent since it results from the phase-characteristic of the frequency domain filter. Note that the improvement could be thought of as due to discrimination of a difference in duration or a change in pitch quality.

A pictoral summary of this phase-delay argument appears in Figure 18. (The physiological mechanism underlying this phenomenon is not important for our purposes; however, it may be related to the well-known tuning curve characteristics of auditory neurons.) The conceptualization of the leaky power integrator model must include a band-pass peripheral filter which yields the input to the integrator. The resulting delay is then generally increased for filters with lower center-frequencies, or smaller bandwidths, or larger time constants for the integrator (Lakey, 1976).

Thus a satisfactory, if not unique explanation can be given for the entire set of tonal signal with noise-fringe data for noise-fringe durations from 0 to 45 msec.

Continuing to interpret the tonal signal data with increasing noise-fringe duration beyond 45 msec, the fact that the slopes increase significantly beyond unity suggests the operation of increasing uncertainty in the detection process. The formal mathematical model

Figure 18. A pictoral summary of the phase-delay argument. There is a relative frequency dependent time delay resulting from the phase-shift response of the peripheral (frequency domain) filter. Thus, lower frequency inputs to this filter yield correspondingly longer output response delays as sketched.

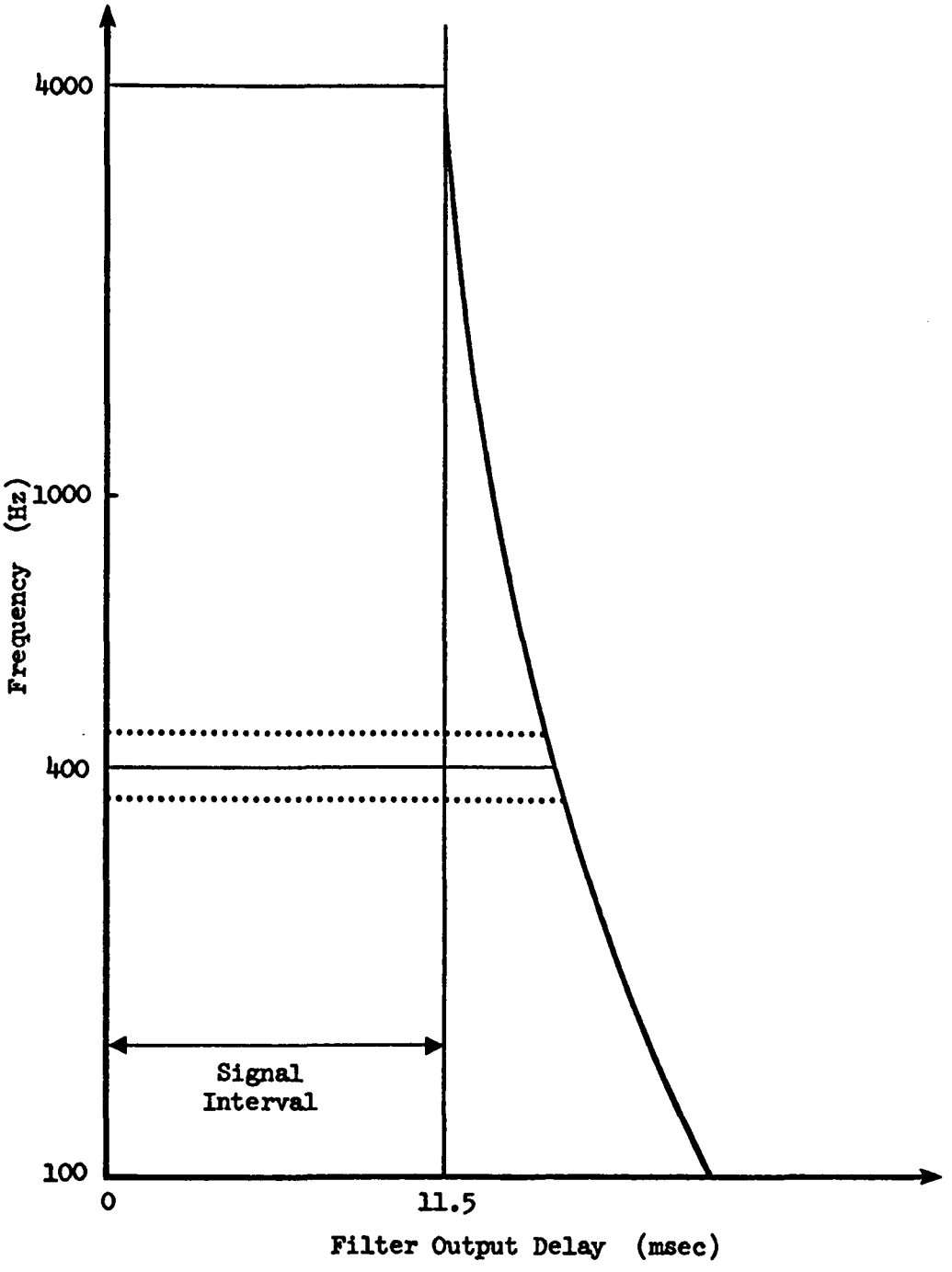
4000
1000
400
100
Frequency (Hz)
Signal
Interval
0
11.5
Filter Output Delay (msec)

of uncertainty discussed in the introduction however, is clearly inadequate. For the model, any increase in the index of uncertainty M forces joint increase in threshold and slope. For the noise-fringe data this may be applied below 45 msec but not above since the threshold slowly decreases with increasing noise-fringe duration (beyond 45 msec) as the slope increases well above one. At this point a closer examination of the slope-threshold relations is warranted.

Figure 19 shows sample psychometric functions with the threshold defined at 76 percent correct for each. (Psychometric functions for all 36 stimulus conditions are shown in Appendix E.) Notice that a joint increase in threshold and slope implies that the decrement in performance is relatively largest for weak signals (Green and McGill, 1970) as compared to strong signals, as is the case for the "M" uncertainty model as well as for the data to the left of 45 msec. A further increase in slope coupled with a small decrease in threshold suggests a relative enhancement of the detection of strong signals. To make sense of the data, the following argument is suggested. The key to the argument is temporal uncertainty, but the formal "M alternatives" model is not applied. Note that that model may be inapplicable for at least two reasons. First, identification of the "M" alternatives is difficult to imagine, unless they are temporal locations. If M alternatives somehow associated with positions in time were identifiable, it is not at all clear that they would be "orthogonal" as required by the model. Thus the discussion here must be qualitative and somewhat intuitive. Temporal uncertainty, that

Figure 19. Sample psychometric functions with threshold defined at 76 percent correct for the tonal signal/noise-fringe conditions. Roman numerals indicate the duration of the noise-fringes.

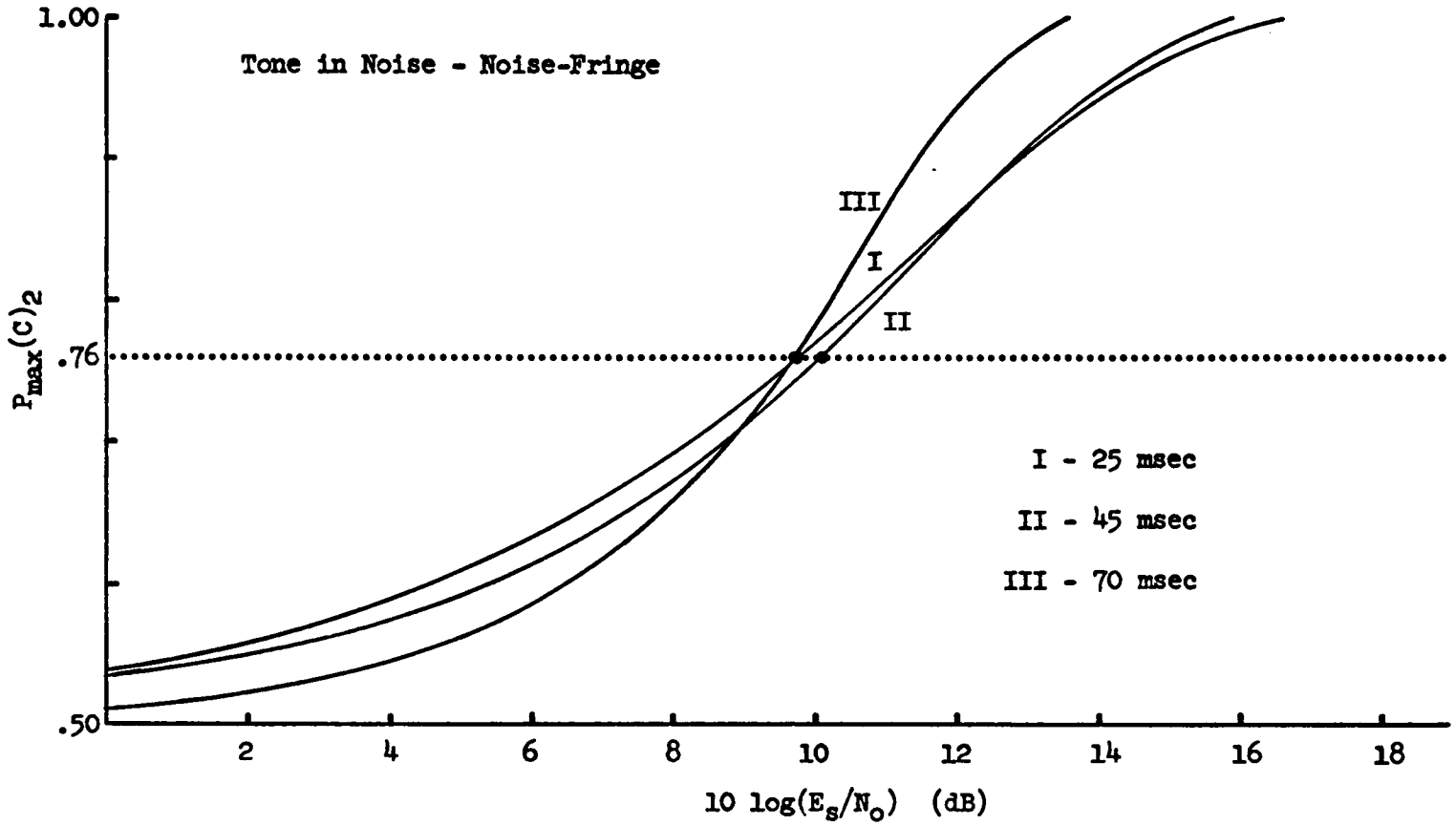
Tone in Noise - Noise-Fringe
1.00
.76
.50
$P_{max}(C)_2$
III
I
II
I - 25 msec
II - 45 msec
III - 70 msec
2
4
6
8
10
12
14
16
18
10 log(E_s/N_o) (dB)

is - not knowing when to read out a value from the integrator, should lead to a greater depression of performance for weak signals, since strong signals may "peak" the integrator sufficiently often to signal the detector about their temporal location. If this large signal peaking of the integrator is for some reason not often detected over the range in which small signals are very difficult to detect because of temporal uncertainty, and that range is then identified with noise-fringe duration less than 45 msec, then the resulting increase in both threshold and slope will be less than expected. Thus the threshold and slope increases from 25 to 45 msec of noise-fringe duration are viewed as less than might otherwise be the case if large signal peaking were not somehow masked. Now, what is responsible for temporal uncertainty and what is masking large signal peaks? Possibly the same variable - the transients of the masker. The 'onset' and 'offset' transients of the noise masker would serve as excellent time markers. They could be thought of as 'enable' and 'disable' signals for the integrator. Indeed, that function is exactly what is implied by assuming the integrator readout point to slide with noise-burst termination. The existence of noise transients close in time to the signal interval however, may mask the large signal peaks. Neural peak responses to transients - particularly "on" responses (e.g. Elliott, 1965; Green, 1969; Zwicker, 1965) may be responsible. This may be true even while those same transients are aids to detection in their service as precision time markers. Now temporal uncertainty regarding signal location would grow as the noise transients become

sufficiently distant from the signal, but while they are still the most precise time selection mechanism available to the detector. However, this temporal uncertainty should soon saturate as the transients move further from the signal interval. This would occur because the detector should have some other less precise time marking mechanism in the context of the experiment, which would ultimately be more dependable than the noise-burst transients. Suppose that that occurred when the noise-fringe duration grew somewhere beyond 45 msec. Now the data show that as noise-fringe duration grows beyond 45 msec, the signal threshold actually decreases. The inference is that temporal uncertainty is saturating, and also that the noise burst end-points are so far from the signal interval that they are rapidly becoming less effective as maskers of the strong signal peaks. Consequently, strong signals will be detected with increasing probability, while the probabiltiy of detecting weak signals remains fairly constant. Thus the signal detection threshold will be decreasing as the slope of the psychometric function increases. All this provides an excellent qualitative description of the pattern of changes in the psychometric functions derived from the data, as already shown in Figure 19. Note that those noise transients may never lose their power to suppress detection. The results of this study suggest that the gradual threshold drop may continue for some time as noise-fringe duration increases. Indeed, the 'infinite' fringe or continuous masking threshold is a consequence of a comparatively large drop in threshold from the values evident f

other long but 'finite' noise-fringe durations. This result must somehow be due to the fact that for the continuous masker only are there no noise-fringe transients at all.

Given the qualitative argument outlined above for tonal signal detection with varying noise-fringe duration, can the behavior of the tonal detection results with varying gap-fringe duration be satisfactorily explained? It is convenient to continue the argument from the continuous masker condition, which is the 0-msec gap-fringe case. Since both gap-fringe thresholds and gap-fringe slopes decrease to a local minimum as the gap increases from 0 to 15 msec, that region appears of special significance. The slope decline brings k to just below unity, where energy detection might again be considered a dominating factor. As the noise-gap is increased, the noise on/off transients - for the simultaneous gated segment - may serve as excellent time markers, particularly if they are embedded within a distinguishable gap of silence. The large drop in slope from 0 to 5 msec of gap-fringe indicates that a clearly distinguishable gap threshold should be of the order of less than 5 msec. To confirm this a supplementary experiment was conducted. The results are shown in Figure 20.

The noise-gap detection experiment was simply a 2AFC detection paradigm using the noise parameters of the main study, but where the listener's task was to detect the presence of a single silent gap in otherwise continuous noise. The gaps were produced with rapid (virtually 0-msec) 'off/on" times. The psychometric functions of

Figure 20. Psychometric functions for the noise-gap detection experiments for 3 subjects.

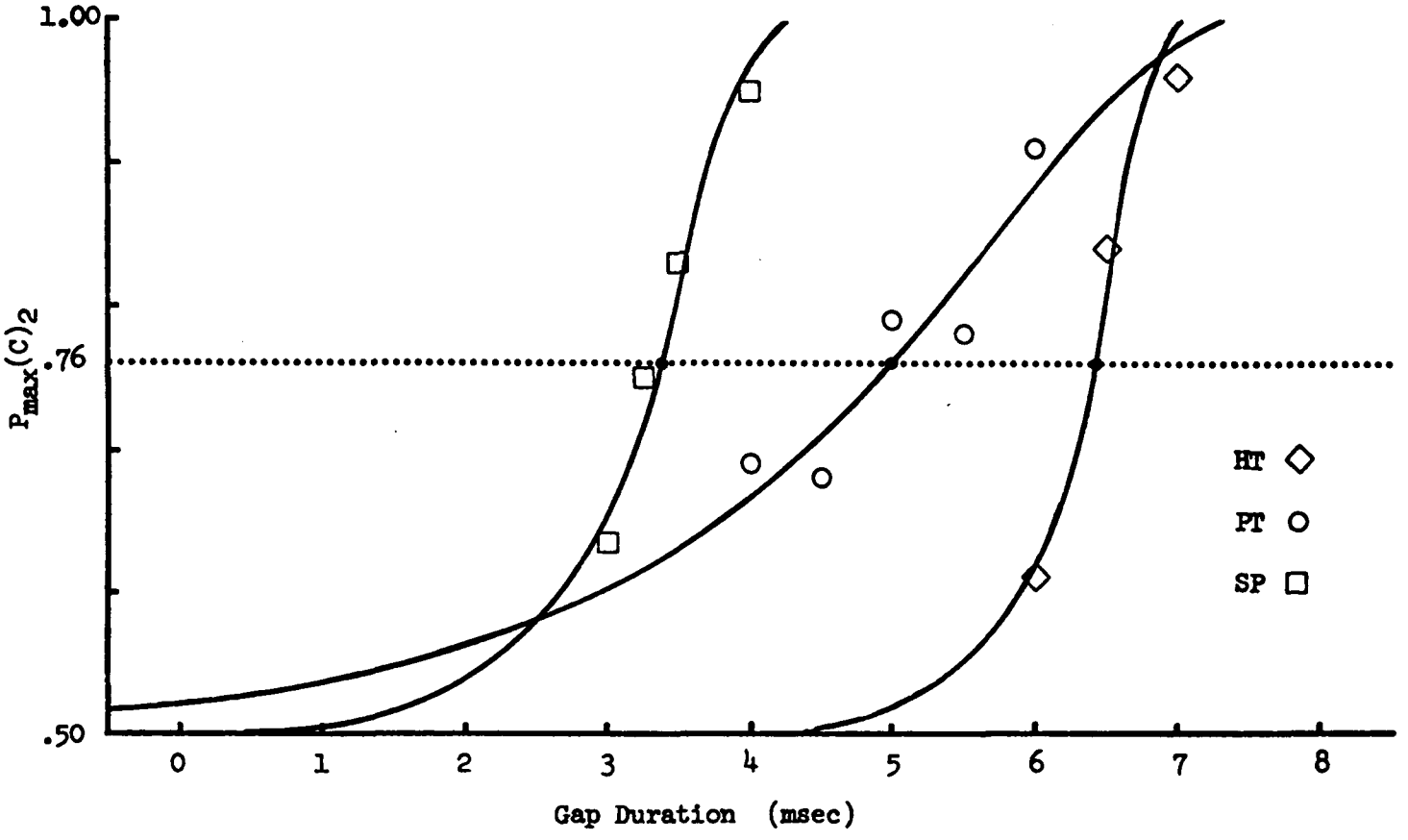
1.00
.76
.50
$P_{max}(C)_2$
0
1
2
3
4
5
6
7
8
Gap Duration (msec)
HT
PT
SP

Figure 20 show the 76 percent noise-gap threshold to be of the order of 3 msec, confirming Penner (1975). Most important for the present analysis is the fact that the individual differences of noise-gap detection match the individual differences of signal-in-noise detection for brief gap-fringe durations. Thus, for the three listeners the gap detection thresholds were in the order: SP - 3 msec, PT - 5 msec, and HT - 6 msec. This same ordering also appears for the rapid drop of the gap-fringe data, where the drop occurs earliest for SP and latest for HT (and is on the order of 5 msec in each case). As gap-fringe duration increases to some extent beyond 15 msec, there appears to be a very slow increase in the average signal threshold and possibly in the average slope as well, although neither (particularly the slope changes) could be considered significant in view of the individual differences. If these changes are meaningful, the argument presented for the noise-fringe duration results may help explain them. Over the gap-fringe range from 5 msec to 15 msec the silent gaps, determined by the sequence of 'off/on/off/on' transients of the masker, may be an increasingly significant aid in localizing the signal interval in time, and hence the readout point of the integrator. As the gap increases beyond 15 msec, the 'gap' per se may become less useful for temporal localization, and in fact the transients of the masking noise surrounding the gap may become a source of confusion for the detector. This is suggested by the fact that there appears to be a signifant decline in threshold and slope when those outside transients are entirely removed and the pure gated

masking condition is reestablished. (Note the implication that events occurring very far away in time, at least as far as an adjacent trial in the experiment, are irrelevant.) The function of the outside transients for the gap-fringe condition may have little to do with the masking of strong signal peaks, contrary to what is suspected for the noise-fringe results. This is an acceptable argument because any such transient masking of those peaks may be maximized by the transients of the simultaneously gated noise-burst segment. In support of this is the fact that changes in threshold and slope are generally unidirectional for the gap-fringe data.

Comparing noise-fringe and gap-fringe results in the context of the inferences so far presented, it is most reasonable to assume that the readout point of the integrator does indeed slide in time with noise offset up to a limit. This not only accounts for the noise-fringe results out to noise-fringe durations of 25 msec, but is also compatible with gap-fringe results since thresholds do not decline at all (let alone rapidly) as the gap-fringe exceeds 15 msec. Presumably the integrator is read at the termination of the signal interval as triggered by the offset transient of the simultaneously gated segment of masker. As a further noise-fringe/gap-fringe comparison, note that the argument regarding frequency dependent delay (Duifhuis, 1973) would also apply for all non-zero values of gap-fringe. For very short gaps in fact, signal detection might actually be accomplished by reversing the choice in 'gap detection'.

The tone-in-noise results have now been discussed in great

detail and a semi-quantitative, semi-qualitative argument was developed to explain them. Now, what about the noise-in-noise results? To begin with, the forms of dependency of slopes as well as thresholds on the noise-fringe or gap-fringe duration values are nearly the same for both the tone-burst and noise-burst signals. Note that the formal derivation of the simple energy detector (see introduction) leads to threshold and slope changes which must be positively correlated for tonal signals, but negatively correlated for noise signals - over the same range of values of masker bandwidth-duration product (or alternatively, degrees of freedom, ν). In this study, as it was made clear for the tone-in-noise conditions that slope changes dictated by the leaky power integrator model are small relative to those seen in the data, for the noise-in-noise conditions the model slope is constant (see Figure 21 and the discussion to follow). Again, the model cannot explain slopes exceeding unity, and the main explanation for slope changes and some threshold changes comes from consideration of mechanisms having to do with temporal uncertainty and the role of 'on/off' transients. Thus the noise-in-noise results may be explained as were the tone-in-noise results, and there is no need to repeat the argument. However, certain features of the noise-in-noise results do require further examination.

Unlike the tonal signal, the noise signal threshold for gated masking falls near threshold values derived by fitting noise-fringe results out to 25 msec with the leaky power integrator, as shown in Figure 21. This is a reasonable finding, given the explanation

Figure 21. Theoretical noise-fringe threshold and slope functions for the leaky power integrator in the detection of a noise signal masked by another independent broadband noise burst. The temporal filter shape is assumed to be either exponential with a time constant of 40 msec or rectanguler. The frequency bandwidth is assumed to be in the range from 600 to 900 Hz. Theoretical noise-fringe thresholds shown in the figure are after an upward shift of 3 to 2 dB for the calculated thresholds. The shift is an adjustment for presumed internal noise and the difference between input signal energy and time filtered signal energy (about 0.5 dB). The maximum filter readout time, t, is assumed to be at 25 msec after signal termination.

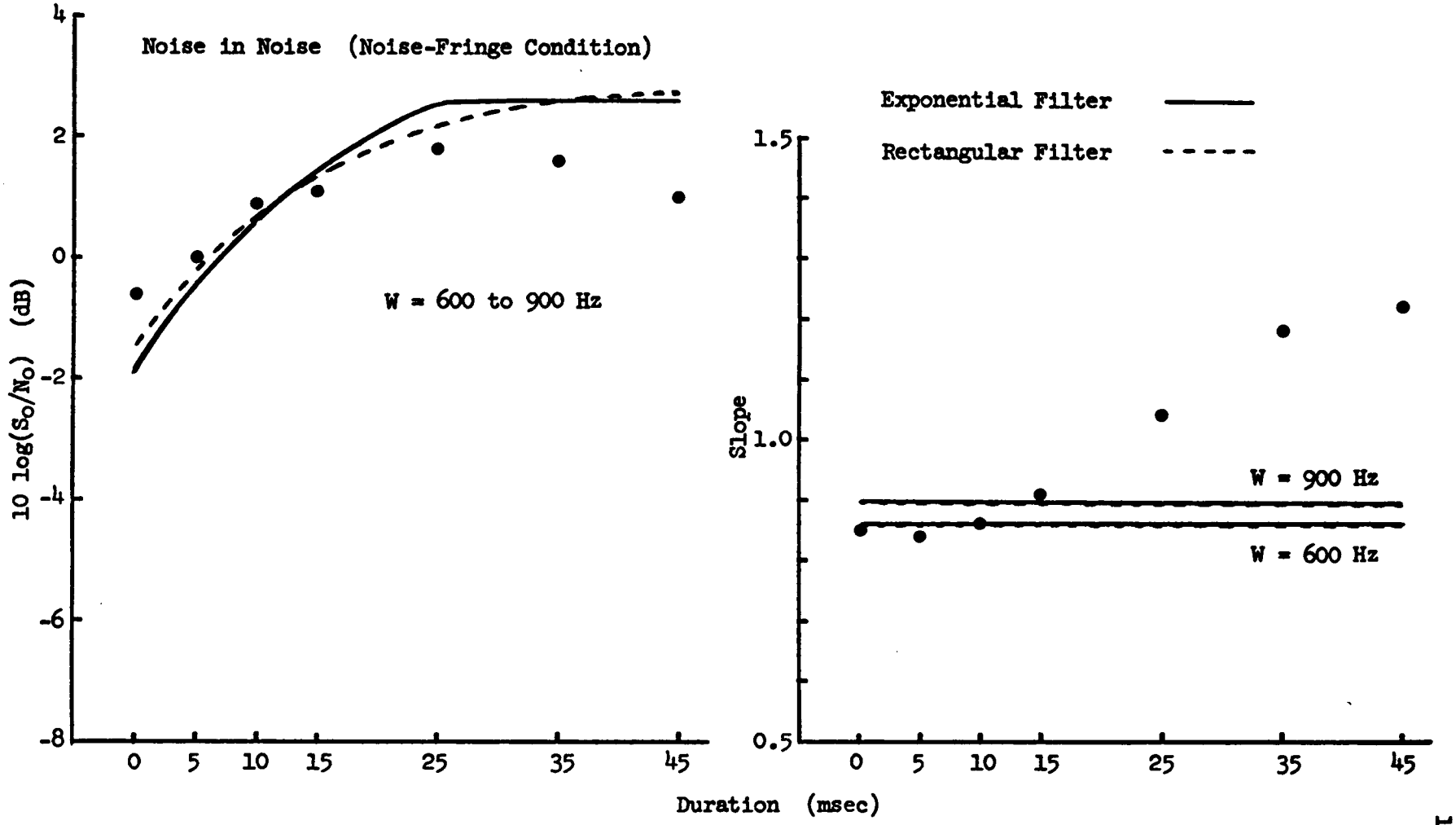
Noise in Noise (Noise-Fringe Condition)
Exponential Filter
Rectangular Filter
W = 600 to 900 Hz
W = 900 Hz
W = 600 Hz
10 log(So/No) (dB)
Slope
Duration (msec)
4
2
0
-2
-4
-6
-8
1.5
1.0
0.5
0
5
10
15
25
35
45

for the tonal gated masking threshold based on frequency dependent phase-delays of the peripheral (frequency domain) filter. Since the noise-signal has a power spectrum identical to that of the masker, no enhancement of detectability is expected in its gated masking condition except for that due to reducing the noise-fringe input to the leaky power integrator.

The noise-signal data, as pointed out in the results section, show a pattern very similar to those of the tonal-signal results, for both thresholds and slopes. Some adjustment of parameters is required to best fit the noise-signal data (to the extent that it can be fit) with the leaky power integrator. The bandwidth, W, must be large; this is a priori true. The limit of the sliding integrator readout point, t, may be about 25 msec, since the average noise threshold data peak at this value.

Choosing the exponential time constant at 40 msec and the readout limit at 25 msec beyond noise-signal termination essentially determines a match to the shape of the threshold function for the noise-fringe condition. Changing the value of W simply yields a vertical displacement of the threshold function. (The shift is approximately a lowering of the function by 10 $\log\sqrt{W}$.) Raising W would increase the noise-signal slope function (but without changing its slope from zero). If the calculations are now adjusted to account for the existence of internal noise by assuming that the N_o represented in the equations should have been denoted $\eta_o = N_o(1 + R)$, as discussed earlier, then the threshold function alone is affected by a shift of

scale of magnitude 10 log (1 + R). The square root of the bandwidth, $\sqrt{W}$, trades (approximately) with (1 + R). Thus a choice of W on the order of 600 to 1,000 Hz is required to generate a slope value for gated and near gated noise-fringe conditions near the approximate level of 0.85 evident in the noise-signal data, as shown in Figure 21. (It would be expected a priori however, that the value of W should be greater; it should be as large as possible to approximate the bandwidth of the input as determined by the earphones; see Figure 5). To fit the threshold data with a choice of W of 900 Hz, 10 log(1 + R) must be about 3.0 dB. That represents an internal-to-external noise ratio of R = 1. This is a very reasonable assumption, since such large (and sometimes larger) levels of internal noise have been unavoidable inferences drawn from many attempts at modeling in psychoacoustics (Green, 1964b; Osman, 1971; Siebert, 1968). Indeed, Siebert's (1968) neural pulse model virtually ignores the statistics of the input noise; masking noise is generated internally. (For comparison, with W at 600 Hz, the implied internal-to-external noise ratio would be 2 dB.)

It is parsimonious to assume that the internal noise level depends only on the level of input noise, so that the same levels operate for the tonal signal conditions as for the noise signal conditions. The predictions are only modestly close for this study. Thus, for an internal-to-external noise ratio of 4.0 dB, W for the tonal signal would be about 100 Hz, to place the predicted threshold and slope values as shown in Figure 17. For the tonal signal the value of $1/\sqrt{W}$ trades (approximately) with (1 + R) to determine the vertical location of

the threshold function. The only other determinant to consider was the value of 10 $\log(E_s/E_1)$, which contributes about 0.5 dB of an upward shift in the threshold equation (Eq. 51) as pointed out earlier. Of these last threshold parameters, only W affects the slope predictions; the slope increases with increasing W. Again, as shown in Figure 17, a choice of WT of approximately unity, so that W is about 100 Hz, yields satisfactory positioning of the theoretical functions, given the qualifications introduced earlier to explain the low gated threshold. (The fact that the slopes for the tonal signal condition dip at 15 msec for each listener, and are significantly variable on the average, compared to the smooth slope function for the noise-signal, might somehow be a consequence of the phase delay mechanism, and the confusion generated for the listeners due to the alternative choices of 'what to listen for'.)

The main theoretical finding of this study then, is that the leaky power integrator model fails. At very brief (near zero) noise-fringe durations for tones, the data may be a consequence of phase-delays and related detection strategies. Only the noise signal results are reasonably well explained by the leaky power integrator, although only for noise-fringe duration below about 25 msec, and the accompanying slopes require that W be only moderately large. The other major features of the pattern of changes in slope as well as location for the psychometric functions in this study are attributed to mechanisms of temporal uncertainty and the special contribution to the masking process of the transients of the masker. The problem

of temporal uncertainty is understandable with reference to the masker alone, in terms of the location of its on/off transients. However, those same transients are also of concern in terms of their possible interference with the detection of the signal (as discussed earlier in reference to large signal peaks). This role of the masker transients may be frequency dependent, and it is ultimately the neural transient response that must be understood to be responsible for the masking (e.g. Elliott, 1965; Zwicker and Fastl, 1972). No attempt to interpret the role of the transients in neural terms will be made here. Nevertheless, it is important to understand that that role clearly may be dependent on the frequency characteristics of the signal to be detected, as well as the masker. Thus the fact that the form of the noise-signal results of this study appears to differ from that of the tonal-signal results generally in terms of a compression of the time scale might be due to the time difference dependencies of the masker transients, with regard to their influence on signals with different power spectra. To further analyze the role of noise transients, it would probably be useful to pursue models with a more explicit physiological base such as those geared to neural pulse counting. Consideration of such models should include those of McGill (1967), McGill (1968a), Teich and Lachs (1979), Colburn (1973), Siebert (1968), and Duihfuis (1973). Such pursuits with respect to the present study are considered beyond the scope of this dissertation.

One last point will be made here with regard to the speculated role of the masker transients. Generally, the slopes, as well as

the thresholds, show large shifts in value as the condition of 95-msec noise-fringe durations or gap-fringe durations are replaced by continuous or gated masking. If it is reasonable to assume that the change in masker power increments that would contribute to a leaky power integrator are too far from the signal interval to be of great consequence, then the result must be due to the complete removal of those 'distant' masker transients. It is possible, of course, that those transients play a role in higher order processes that affect detection strategies. Further research to unravel the mystery is warranted.

The last item to be covered concerns the problem of estimating the "temporal critical masking interval". The present experimental results show that, in noise-fringe conditions for both tonal signal and noise signal detection, thresholds increase as the noise masker duration is increased and after reaching a maximum, they decrease gradually with much lower rates of change and then drop to the level of continuous masking. Penner (Penner et al., 1972; Penner et al., 1973; and Penner, 1975) also obtained similar functions by using a brief click signal. Penner determined the temporal critical masking interval as the noise masker duration at the intersection of two straight lines which relate the threshold in dB and the noise masker duration in log units. The line with about zero slope represented the longer masker duration conditions and the line with positive slope (less than one) fit the data for the shorter masker durations. Penner chose to ignore the condition with greatest threshold in this process of

estimation for the temporal critical masking interval. The so-called "overshoot" effect appears in her data and has been found by other investigators (e.g. Zwicker, 1965).

To rephrase the argument presented earlier, the overshoot may mean that masker onset or offset (probably acting because of the abrupt change in neural responses at these time periods) causes extra interference with the detection of the signal. If this happens within the range of the temporal critical masking interval (i.e. sufficiently near the signal interval) the masker should have a significantly larger detrimental effect on performance than would be otherwise predicted. Increasing the masker duration so that it extends beyond the critical masking interval (i.e. so that transients are sufficiently far from the signal interval) should considerably reduce the interference of the masker transients. In accordance with the argument, a temporal critical masking interval could then be estimated empirically by using the duration which yields the maximum threshold. In the present study, consulting both individual data and the averaged data, the maximum threshold occurs for noise-fringe masking durations of around 25 to 35 msec for both tonal signal and noise signal detection. The sliding leaky power integrator model discussed in this dissertation employed the limit of the slide (the extent of backward masking) as a parameter. The choice of 25 msec also reflected the fact that the threshold functions appear to reach their maxima at about that value of noise-fringe duration. Another choice of definition for the critical masking interval

is to use the time constant of the leaky integrator. This reflects the shape of the early portion of the threshold growth function rather than the location of the maximum. The time constant of 40 msec is in agreement with other research (Jeffress, 1968). Together, these two parameters suggest a minimum integration time span (or critical interval) for the auditory mechanism, which extend backwards via exponential decay from about 25 msec beyond signal interval termination.

In gap conditions for both tonal and noise signal detection, thresholds drop to the level of gated conditions from the continuous masking condition within about 15 msec as the gap is widened. This suggests another concept for a temporal critical masking interval. It reflects the involvement of masking transients and temporal uncertainty as previously discussed.

A temporal critical masking interval may also be defined through the slopes of the psychometric functions. Where these functions, one for noise-fringe conditions and the other for gap-fringe conditions, cross each other, it might be presumed that, at about that fringe duration, the listener may significantly change his decision strategies or his degree of uncertainty about the signal. For both tonal signal and noise signal, most functions for individual listeners did cross at about 25 msec, so that 25 msec is again an estimate for a temporal critical masking interval.

Thus, in general, however the results are examined, estimates for the range of the temporal critical masking "intervals" cover about 25 msec beyond the signal interval (one sided). The minimum

integration time for the detection process surrounding the 11.5 msec signal is at least about 40 msec. These conclusions apply for both signal bandwidths, that is, for tonal signal and noise signal. The content of this discussion in general implies not only that performance of the listener is determined by several underlying processes which interact with one another, but that the concept of a critical masking interval is useful only as a general characterization of the results, at least until those underlying mechanisms are sufficiently well represented in quantitative models. The work most similar to this dissertation is Penner's work on click masked by noise (Penner et al., 1972; Penner et al, 1973; and Penner, 1975). Her explanations of critical masking interval estimation and the overshoot effect are limited in that they do not incorporate any representation of statistical variance, as was explicitly done in the leaky power integration model presented and analyzed in this study. Note that, considering the motivating argument given in the introduction to this dissertation, the fact that the pairs of slope and threshold functions for noise-fringe and gap-fringe conditions do not cross at the same values of fringe duration is due to the inapplicability of the leaky power integrator model as the sole explanation for the results. Finally, it should now be clear that, at least for brief signals, the similarities and differences between the psychometric functions found for continuous and gated masking are probably to be best understood in terms of the shifting roles of different underlying processes, as implied by the noise-fringe/gap-

fringe effects studied here.

One major contribution of this dissertation is the demonstration that important restrictions on theoretical interpretations of the psychophysical results are implied by analysis of complete psychometric functions.

APPENDIX A: MEASUREMENT OF THE SPECTRUM LEVEL OF THE NOISE MASKER

To determine N_o, the spectrum level of the masking noise at the output of the earphone (Telephonics TDH-39), the rms voltage level was first measured at the input to the earphone and compared to the manufacturer's earphone calibration curve at 400 Hz (see Figure 5). Thus, the 10-mV rms input to the earphone which was set for the experiment would yield an overall level of 88 dB SPL if the power was concentrated at 400 Hz. Two procedures were employed to reduce that overall level to spectrum level at 400 Hz.

(A) A Krohn-Hite filter (Model 3202R) was employed with norminal high-pass and low-pass settings of 300 Hz and 500 Hz, respectively. An oscillator (General-Radio, Model 1309-A) and an oscilloscope were employed to carefully determine the relative attenuation produced by the filter as a function of frequency. This was done in steps of 10 Hz from 150 Hz to 900 Hz. The result is shown in Figure AA1. With the ordinate scaled in units proportional to power (rather than voltage), the total area (power) under the curve was calculated. The equivalent rectangular bandwidth was then defined as the total power divided by the (peak) power at 400 Hz. This bandwidth value turned to be about 265 Hz. Relative to a band one cycle wide, this represents a ratio of 24.2 dB. Inserting the filter into the circuit of Figure 4 just before electronic switch reduced the rms reading at the input to the earphone

Figure AA1. Relative attenuation produced by Krohn-Hite filter (Model 3202R) as a function of frequency.

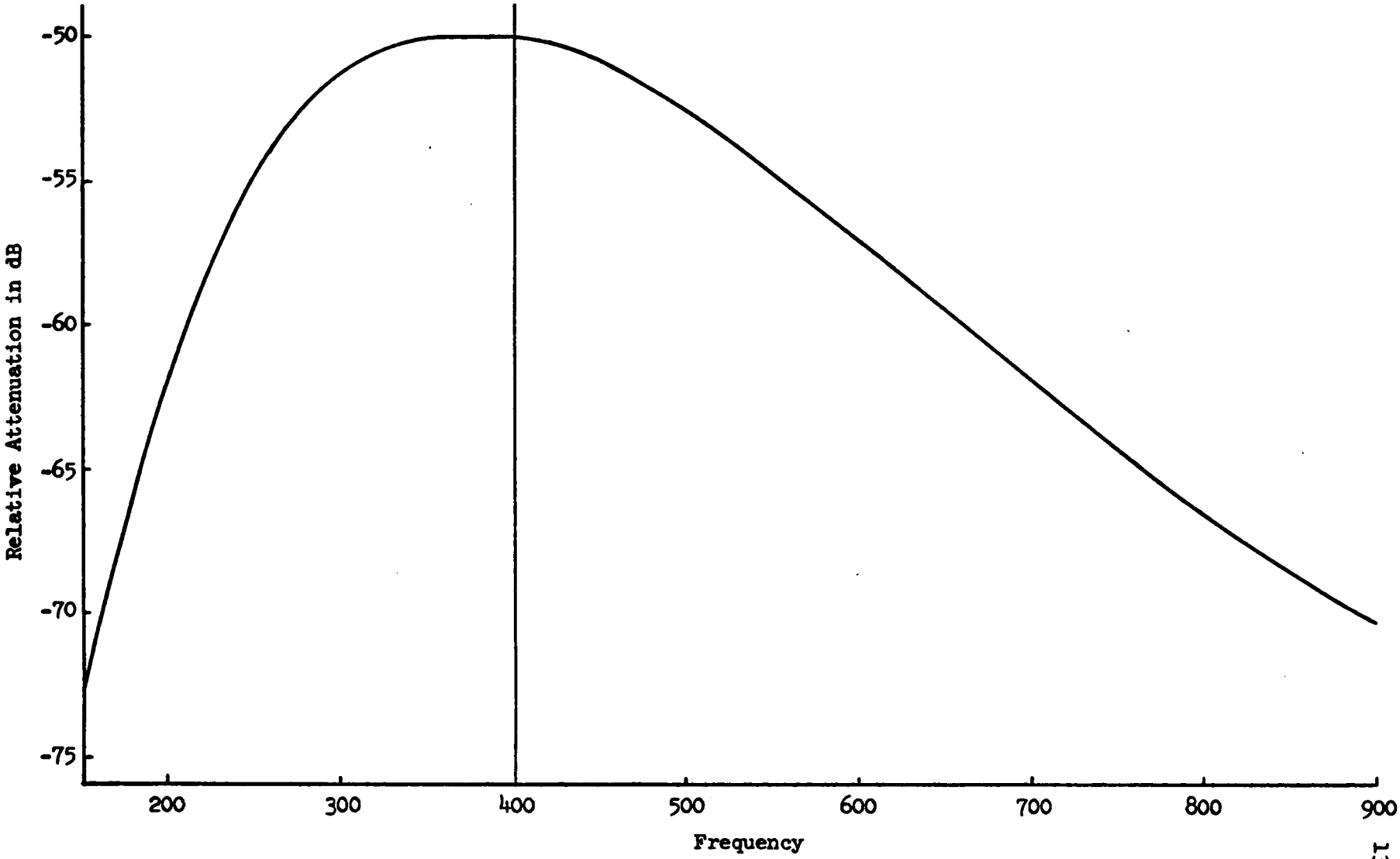
-50
-55
-60
-65
-70
-75
Relative Attenuation in dB
200
300
400
500
600
700
800
900
Frequency

by 18 dB. Thus, the correction for spectrum level (88 - 24.2 - 18) yields N_o = 45.8 dB SPL.

(B) A General-Radio Wave Analyzer (1% bandwidth, Model 1568-A, with a 2000 μF capacitative modification) (belonging to Prof. David H. Raab) was used to measure the noise level at the output of the Grason-Stadler electronic switch (Model 829E). The reading of the wave analyzer (which has a 400 x 0.13 = 5.2 Hz equivalent rectangular bandwidth at 400 Hz) gave a value of N_o re overall level of -46.858 dB. Since the UTC impedance matching transformer (Grason-Stadler, Model E10589A) used in the earphone circuit introduces low pass filtering as well as a voltage drop, a correction was determined for the filtering effect of the transformer. Comparing the transformer output to input ratios for circuits with and without additional low pass filtering indicated that the overall level would be reduced by the low pass characteristics of the transformer by 4.946 dB, so that the corrected value of N_o re overall level would be -41.9 (4.946 - 46.858) dB. Thus, the final correction for spectrum level (88 - 41.9) yields N_o = 46.1 dB SPL. (Profs. David H. Raab and Brian Moore assisted with these measurements.)

The resulting values of procedure (A) and (B) are clearly in satisfactory agreement.

APPENDIX B: COMPARISON OF THE SLIDING AND FIXED EXPONENTIAL LEAKY POWER INTEGRATORS

Equation (50) in the text shows that the quantity h for tone-in-noise/noise-fringe conditions is

$$h = \frac{(E_1/T)\int_0^T w(t-\tau)d\tau}{\sqrt{2N_o^2 W\left[\int_{-\infty}^{0} w^2(t-\tau)d\tau + \int_0^T w^2(t-\tau)d\tau + \int_T^t w^2(t-\tau)d\tau\right] + \left[(2cE_1N_o)/T\right]\int_0^T w^2(t-\tau)d\tau}} .$$

It was argued that the temporal filter may be either a fixed exponential integrator with the readout time restricted to some particular value of t ($t=t_f$), or a sliding exponential integrator with the readout time coinciding with noise termination, so that $t = t_2$, up to some maximum value of t_2 ($t_2=t_s$). (Both possibilities are illustrated in Figure AB1.) Generally, the equation simplifies by restricting the limits of integration to those values that yield nonzero integrals. Then, for the fixed exponential leaky power integrator with a noise duration of from t_1 to t_2 and time-filtered signal energy, E_{1_f},

Figure AB1. Temporal filters for the sliding and fixed exponential leaky power integrators. Upper rectangle represents the signal. Lower rectangle represents the noise. Δt represents the onset asynchrony of signal and noise, that is, the noise-fringe duration.

Fixed Exponential Filter

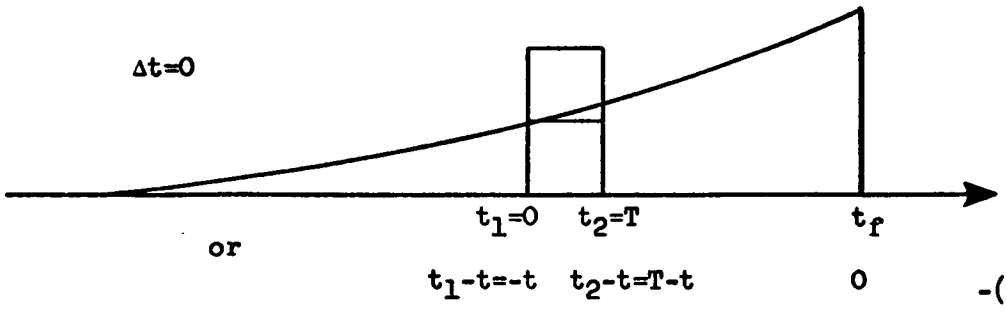

or

$t_1-t=-t$ $t_2-t=T-t$ 0 $-(t-\tau_f)$

where $t=t_f$

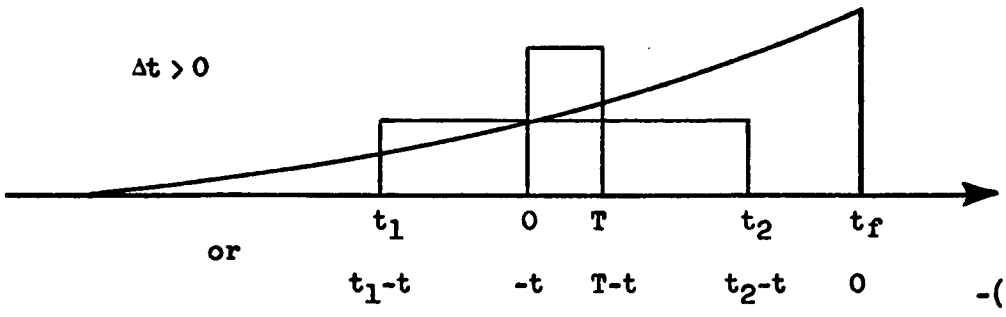

or

t_1-t $-t$ $T-t$ t_2-t 0 $-(t-\tau_f)$

where $t=t_f$

Sliding Exponential Filter

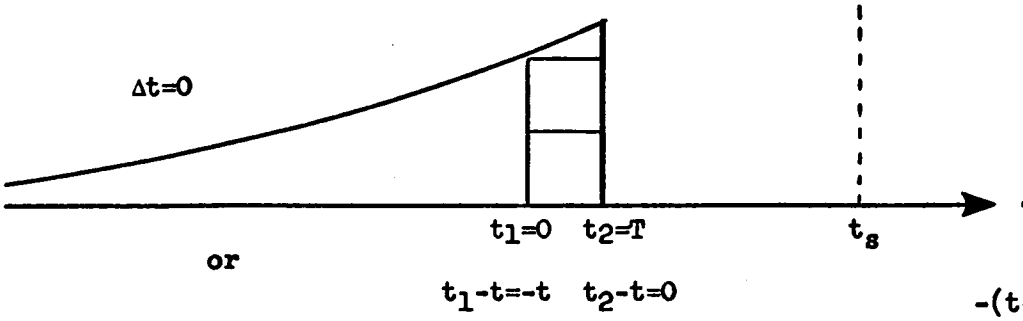

or

$t_1-t=-t$ $t_2-t=0$ $-(t-\tau_s)$

where $t=t_2$

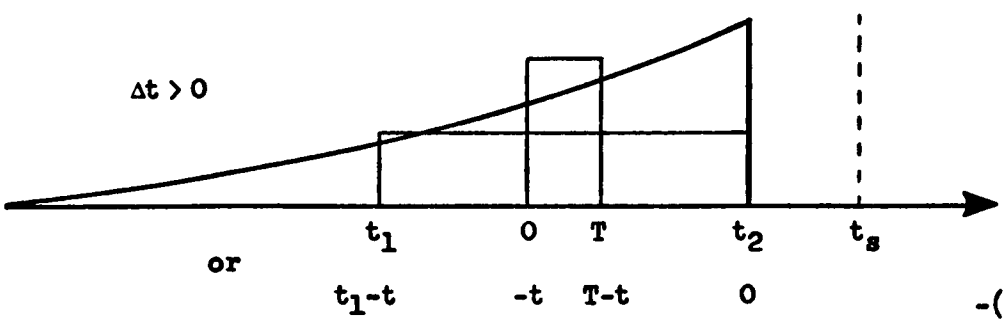

or

t_1-t $-t$ $T-t$ 0 $-(t-\tau_s)$

where $t=t_2$

Note: $\tau_f = \tau_s + (t - t_2)$

$$h_f = \frac{(E_{l_f}/T)\int_0^T \exp\left[-(t-\tau_f)/\xi\right] d\tau_f}{\sqrt{2N_o^2 W\left\{\int_{t_1}^{t_m} \exp\left[-2(t-\tau_f)/\xi\right] d\tau_f\right\} + \left[(2c_f E_{l_f} N_o)/T\right]\left\{\int_0^T \exp\left[-2(t-\tau_f)/\xi\right] d\tau_f\right\}}}$$

$$= \frac{(E_{l_f}/T)\left[\xi\exp(-t/\xi)\right]\left[\exp(T/\xi) - 1\right]}{\sqrt{2N_o^2 W\left[\xi\exp(-2t/\xi)\right]\left[\exp(2t_m/\xi) - \exp(2t_1/\xi)\right] + \left[(2c_f E_{l_f} N_o)/T\right]\left[\xi\exp(-2t/\xi)\right]\left[\exp(2T/\xi) - 1\right]}}$$

$$= \frac{\exp(-t/\xi)(\xi)^{\frac{1}{2}}(E_{l_f}/T)\left[\exp(T/\xi) - 1\right]}{\exp(-t/\xi)\sqrt{2N_o^2 W\left[\exp(2t_m/\xi) - \exp(2t_1/\xi)\right] + \left[(2c_f E_{l_f} N_o)/T\right]\left[\exp(2T/\xi) - 1\right]}}$$

$$= \frac{(\xi)^{\frac{1}{2}}(E_{l_f}/T)\left[\exp(T/\xi) - 1\right]}{\sqrt{2N_o^2 W\left[\exp(2t_m/\xi) - \exp(2t_1/\xi)\right] + \left[(2c_f E_{l_f} N_o)/T\right]\left[\exp(2T/\xi) - 1\right]}}$$

Where $t_m = t_2$ or t_f, whichever is smaller.

Similarly, for the sliding exponential leaky power integrator for the same conditions and time-filtered signal energy E_{l_s},

$$h_s = \frac{(E_{1_s}/T) \int_0^T \exp\left[-(t-\tau_s)/\xi\right] d\tau_s}{\sqrt{2N_o^2 W \left\{ \int_{t_1}^{t_m} \exp\left[-2(t-\tau_s)/\xi\right] d\tau_s \right\} + \left[(2c_s E_{1_s} N_o)/T\right] \left\{ \int_0^T \exp\left[-2(t-\tau_s)/\xi\right] d\tau_s \right\}}}$$

$$= \frac{\left[(E_{1_s}/T)\ \xi \exp(-t/\xi)\right]\left[\exp(T/\xi) - 1\right]}{\sqrt{2N_o^2 W \left[\xi \exp(-2t/\xi)\right]\left[\exp(2t_m/\xi) - \exp(2t_1/\xi)\right] + \left[(2c_s E_{1_s} N_o)/T\right]\ \left[\xi \exp(-2t/\xi)\right]\left[\exp(2T/\xi) - 1\right]}}$$

$$= \frac{\exp(-t/\xi)(\xi)^{\frac{1}{2}}(E_{1_s}/T)\left[\exp(T/\xi) - 1\right]}{\exp(-t/\xi)\sqrt{2N_o^2 W \left[\exp(2t_m/\xi) - \exp(2t_1/\xi)\right] + \left[(2c_s E_{1_s} N_o)/T\right]\left[\exp(2T/\xi) - 1\right]}}$$

$$= \frac{(\xi)^{\frac{1}{2}}(E_{1_s}/T)\left[\exp(T/\xi) - 1\right]}{\sqrt{2N_o^2 W \left[\exp(2t_m/\xi) - \exp(2t_1/\xi)\right] + \left[(2c_s E_{1_s} N_o)/T\right]\left[\exp(2T/\xi) - 1\right]}} \quad .$$

Where $t_m = t_2$ or t_s, whichever is smaller.

After crossing out the common factor for numerator and denominator for both h_f and h_s, h_f would equal h_s if it were true that both $E_{1_f} = E_{1_s}$ and $c_f = c_s$. To prove that $E_{1_f} = E_{1_s}$ and $c_f = c_s$, and consequently that the "sliding" and "fixed" exponential filter models yield identical

predictions, let us go back to Equations (42) to (47) in the text. For the numerator, s_n^2 has been shown to be

$$s_n^2 = (\sum_i w_i s_i^2)/(\sum_i w_i) \ .$$

If the leaky power integrator is of exponential form

$$w(t-\tau) = \exp\ [-(t-\tau)/\xi],$$

or

$$w_i = w_i(t-\tau_i) = \exp\ [-(t-\tau_i)/\xi].$$

Then

$$\begin{aligned} s_n^2 &= (\sum_i w_i s_i^2)/(\sum_i w_i) \\ &= \left\{\sum_i \exp\ [-(t-\tau_i)/\xi](s_i^2)\right\} / \left\{\sum_i \exp\ [-(t-\tau_i)/\xi]\right\} \\ &= [\sum_i s_i^2 \exp\ (-t/\xi) \exp(\tau_i/\xi)]/[\sum_i \exp\ (-t/\xi) \exp(\tau_i/\xi)] \ . \end{aligned}$$

Crossing out the common factor for numerator and denominator for s_n^2 yields

$$s_n^2 = [\sum_i s_i^2 \exp(\tau_i/\xi)] \ / \ [\sum_i \exp(\tau_i/\xi)] \ .$$

Thus, for the fixed exponential integrator

$$s_{n_f}^2 = [\sum_i s_i^2 \exp(\tau_{i_f}/\xi)] \ / \ [\sum_i \exp(\tau_{i_f}/\xi)] \ ,$$

and for the sliding exponential integrator

$$s_{n_s}^2 = [\sum_i s_i^2 \exp(\tau_{i_s}/\xi)] \ / \ [\sum_i \exp(\tau_{i_s}/\xi)] \ .$$

Since

$$\tau_f = \tau_s + (t-t_2) \ ,$$

multiplying both numerator and denominator of $s_{n_f}^2$ by a common factor, $\exp\left[-(t-t_2)/\xi\right]$, yields

$$s_{n_f}^2 = s_{n_s}^2 .$$

Following a similar argument, it can be readily shown that the same equality holds for the denominator of h. Thus, it is proven that for $w(t-\tau) = \exp\left[-(t-\tau)/\xi\right]$, $E_{1f} = E_{1s} = E_1$, and $c_f = c_s = c$, so that $h_f = h_s = h$. Thus the "fixed" and "sliding" exponential filter models under consideration are mathematically identical.

APPENDIX C: CALCULATION OF 10 $\log(E_s/E_1) \approx 0.5$ dB

The tonal signal used in this dissertation is a 400-Hz tone with 2.5-msec rise/fall times. Since its total duration is 11.5 msec, its equivalent rectangular duration is 9 msec (taking into consideration the envelope shape). The input signal energy is defined as

$$E_s = \int_{t_1}^{t_2} s^2(t)dt \ ,$$

where $t_2 - t_1 = T$ (signal duration).

For simplicity, we assume that the input signal is a 9-msec segment of a continuous sine wave of 400 Hz.

Thus,

$$E_s = \int_{t_1}^{t_2} \sin^2\left[2\pi(400)\tau\right] d\tau$$

$$= \int_{t_1}^{t_2} \tfrac{1}{2}\left[1 - \cos(1600\pi\tau)\right] d\tau$$

$$= \left[\tfrac{1}{2}\tau - (1/3200\pi)\sin(1600\pi\tau)\right]\Bigg|_{t_1}^{t_2} \ .$$

The second term is small enough to be neglected.

Therefore,

$$E_s \approx 0.5\ (t_2 - t_1)$$

If the temporal filter is of exponential form with a time constant of 0.04 sec, the time-filtered energy would be

$$E_1 = \int_{t_1}^{t_2} \sin\left[2\pi(400)\tau\right] \exp(\tau/0.04)\, d\tau \ .$$

It is known that

$$\int \exp(ax)\,\sin^2(bx)\,dx = 1/(a^2+4b^2)\left\{\left[(a)\sin(bx) - (2b)\cos(bx)\right]\exp(ax)\,\sin(bx) + (2b^2/a)\,\exp(ax)\right]\right\} .$$

Now for a = 25 and b = 800π, E_1 becomes

$$E_1 = 1/\left[625+4(800\pi)^2\right]\left\{\left[25\,\sin(800\pi\tau) - 2(800\pi)\,\cos(800\pi\tau)\right]\left[\exp(25\tau)\,\sin(800\pi\tau)\right] + \left[2(800\pi)^2/25\right]\exp(25\tau)\right\}\Bigg|_{t_1}^{t_2} .$$

The first term inside the braces yields zero (vanishes), so that

$$E_1 \approx \left\{1/\left[625+4(800\pi)^2\right]\,2(800\pi)^2/25\,\exp(25\tau)\right\}\Bigg|_{t_1}^{t_2}$$

$$\approx \left\{(0.02)\,\exp(25\tau)\right\}\Bigg|_{t_1}^{t_2} = (0.02)\left[\exp(25t_2) - \exp(25t_1)\right] .$$

Then the ratio of E_s/E_1 in dB would be

$$10\,\log(E_s/E_1) \approx 10\,\log\left\{\left[0.5(t_2-t_1)\right] / \left\{0.02\,\left[\exp(25t_2) - \exp(25t_1)\right]\right\}\right\} .$$

Then, for a 9-msec signal ($t_2 = 0$, $t_1 = -0.009$ sec),

$$10\,\log(E_s/E_1) \approx 10\,\log(0.4500/0.0040) \approx 0.5\ \text{dB} .$$

APPENDIX D: THEORETICAL NOISE-FRINGE THRESHOLD AND SLOPE FUNCTIONS FOR THE EXPONENTIAL LEAKY POWER INTEGRATOR IN THE DETECTION OF A TONAL SIGNAL MASKED BY A BROADBAND NOISE BURST

For several values of bandwidth from 100 to 200 Hz, the theoretical noise-fringe threshold and slope functions for the exponential leaky power integrator were calculated for the detection of a tonal signal masked by a broadband noise burst. These are shown in Figure AD1 along with the amount of upward shift needed to reach the data points for each value of bandwidth. Similar functions are also presented in Figure AD2 for varying values of the time constant of the exponential leaky power integrator. Figure AD2 shows that the time constant of 40 msec yields a relatively good it.

Figure AD1. Theoretical noise-fringe threshold and slope functions for the exponential leaky power integrator in the detection of a tonal signal masked by a broadband noise burst for several values of bandwidth from 100 to 200 Hz. The number in the parenthesis indicates the amount of upward shift needed to reach the data points for each bandwidth.

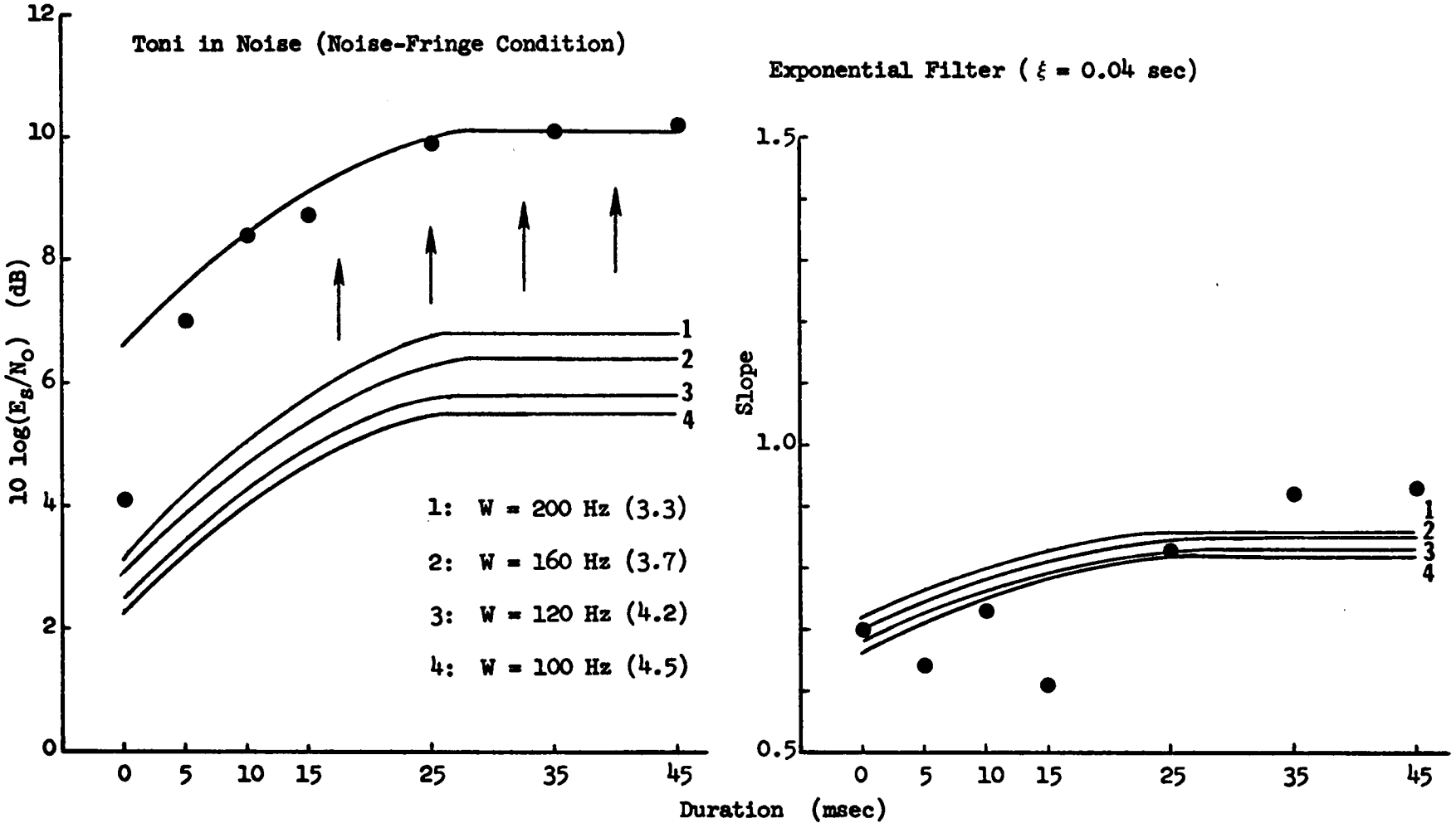
Toni in Noise (Noise-Fringe Condition)
Exponential Filter (ξ = 0.04 sec)
10 log(Es/No) (dB)
Slope
Duration (msec)
1: W = 200 Hz (3.3)
2: W = 160 Hz (3.7)
3: W = 120 Hz (4.2)
4: W = 100 Hz (4.5)

Figure AD2. Theoretical noise-fringe threshold and slope functions for the exponential leaky power integrator in the detection of a tonal signal masked by a broadband noise burst when varying values of the time constant of the exponential leaky power integrator. The number in the parenthesis indicates the amount of upward shift needed to reach the data points for each value of the time constant.

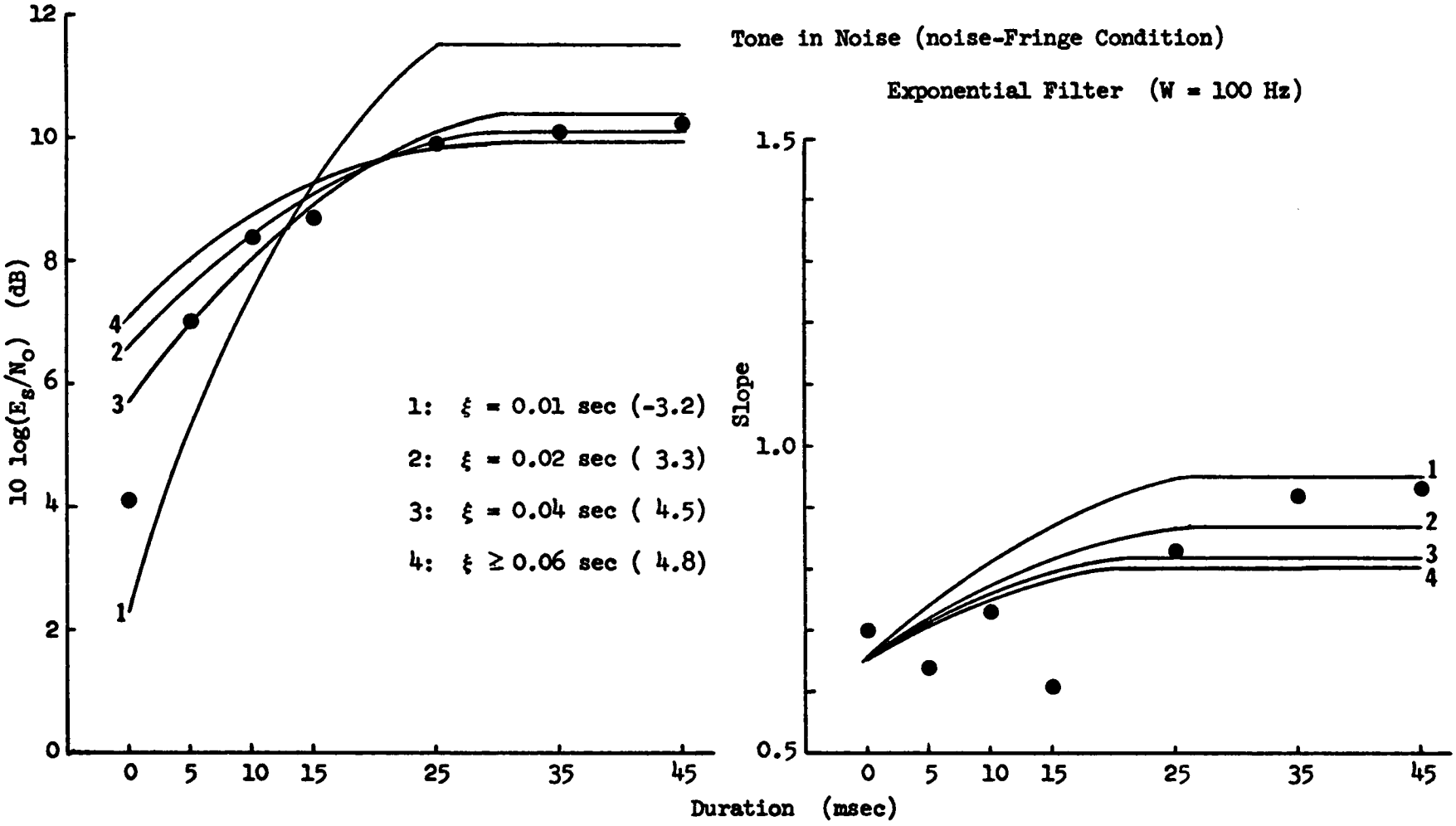
Tone in Noise (noise-Fringe Condition)
Exponential Filter (W = 100 Hz)
10 log(Es/No) (dB)
Slope
1: ξ = 0.01 sec (-3.2)
2: ξ = 0.02 sec (3.3)
3: ξ = 0.04 sec (4.5)
4: ξ ≥ 0.06 sec (4.8)
Duration (msec)

APPENDIX E: PSYCHOMETRIC FUNCTIONS FOR THE 36 STIMULUS CONDITIONS OF THIS STUDY

The following 36 figures, Figures AE1 - AE36, show the complete set of data points for each individual subject's psychometric functions, along with the functions fit with Egan's d' equation for all 36 stimulus conditions. The data points are also listed in Tables AE1 - AE12 (where duration refers to the one-sided noise-fringe or gap-fringe duration). The thresholds and slopes for the smooth fitted curves are the values presented in Table 4 to 7 of the text.

Figures AE1 - AE36. Data points for each individual subject's psychometric functions, along with the functions fit with Egan's d' equation for all 36 stimulus conditions: ☆ for PT, ○ for HT, and □ for SP.

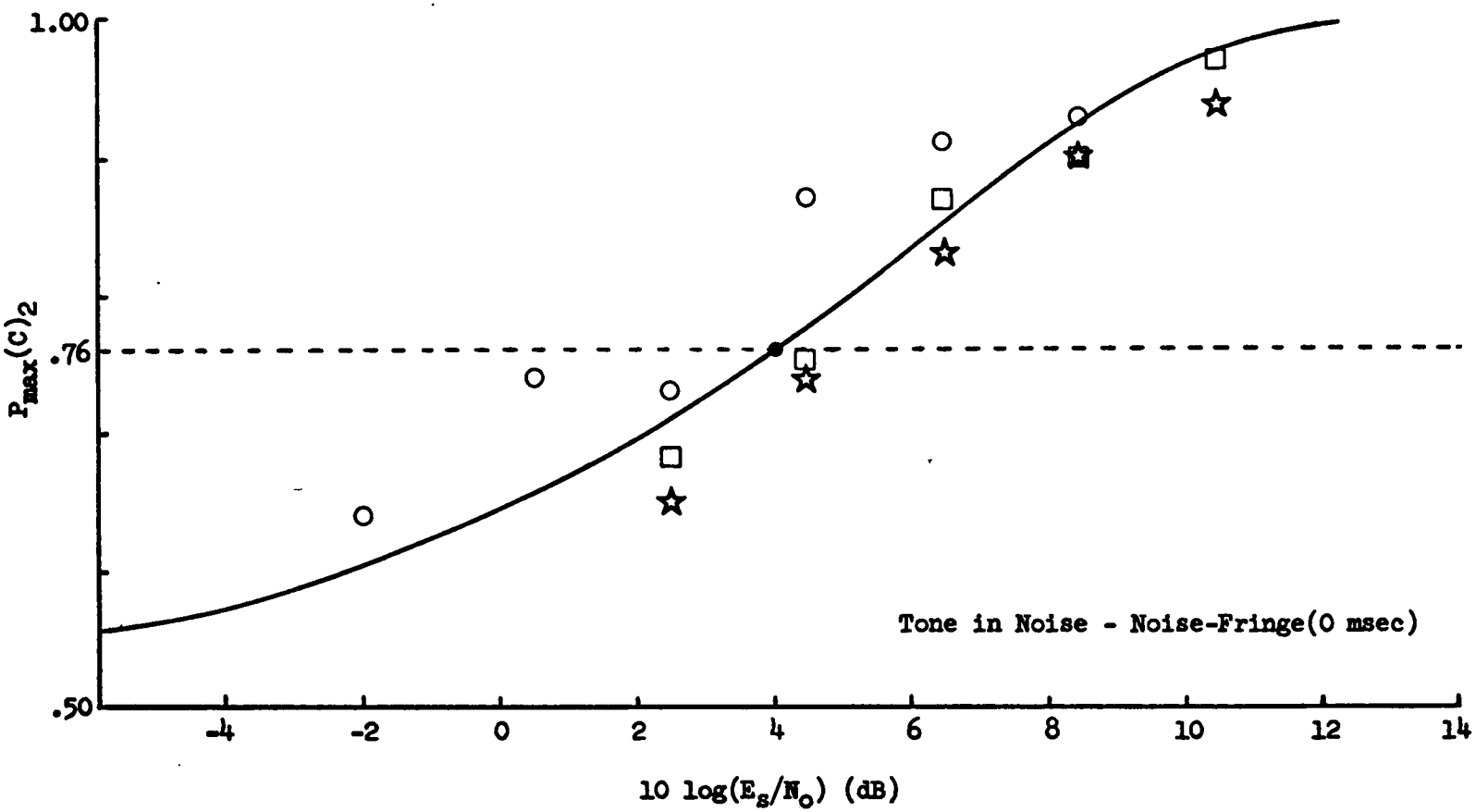
1.00
.76
.50
$P_{max}(C)_2$
-4
-2
0
2
4
6
8
10
12
14
10 log(E_s/N_o) (dB)
Tone in Noise - Noise-Fringe(0 msec)

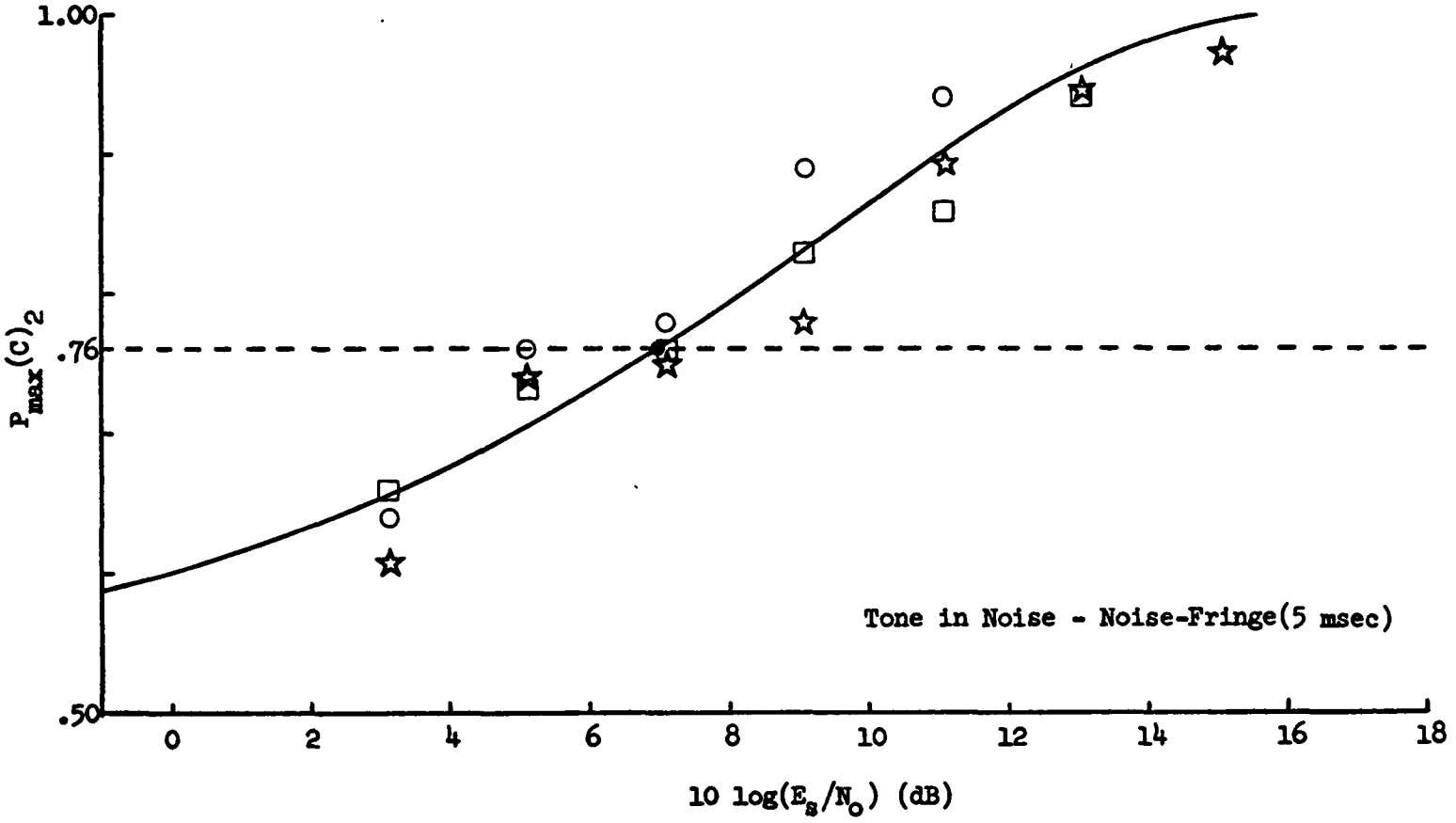
1.00
.76
.50
$P_{max}(C)_2$
0
2
4
6
8
10
12
14
16
18
10 log(E_s/N_o) (dB)
Tone in Noise - Noise-Fringe(5 msec)

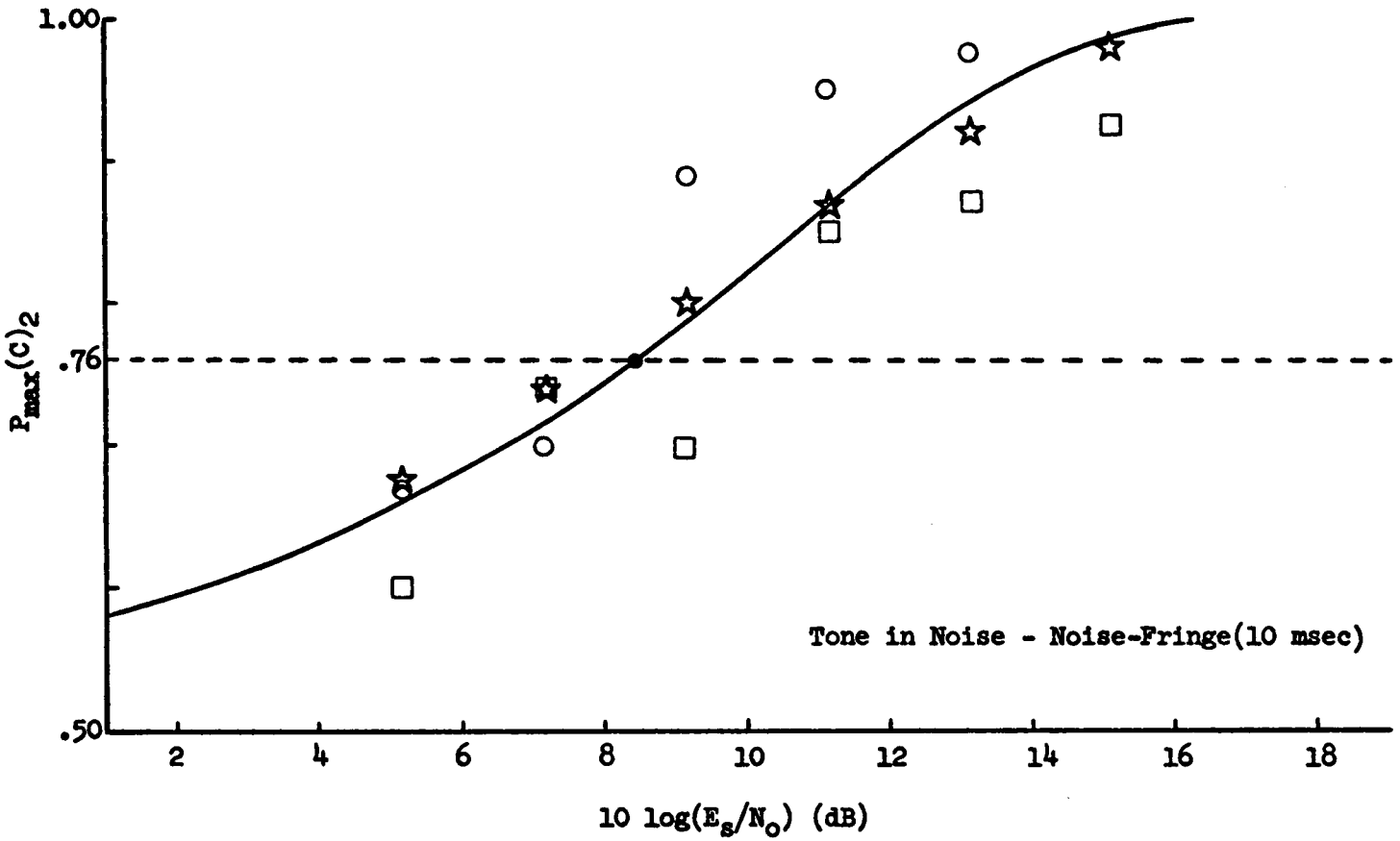
1.00
.76
.50
$P_{max}(C)_2$
2
4
6
8
10
12
14
16
18
10 log(E_s/N_o) (dB)
Tone in Noise - Noise-Fringe(10 msec)

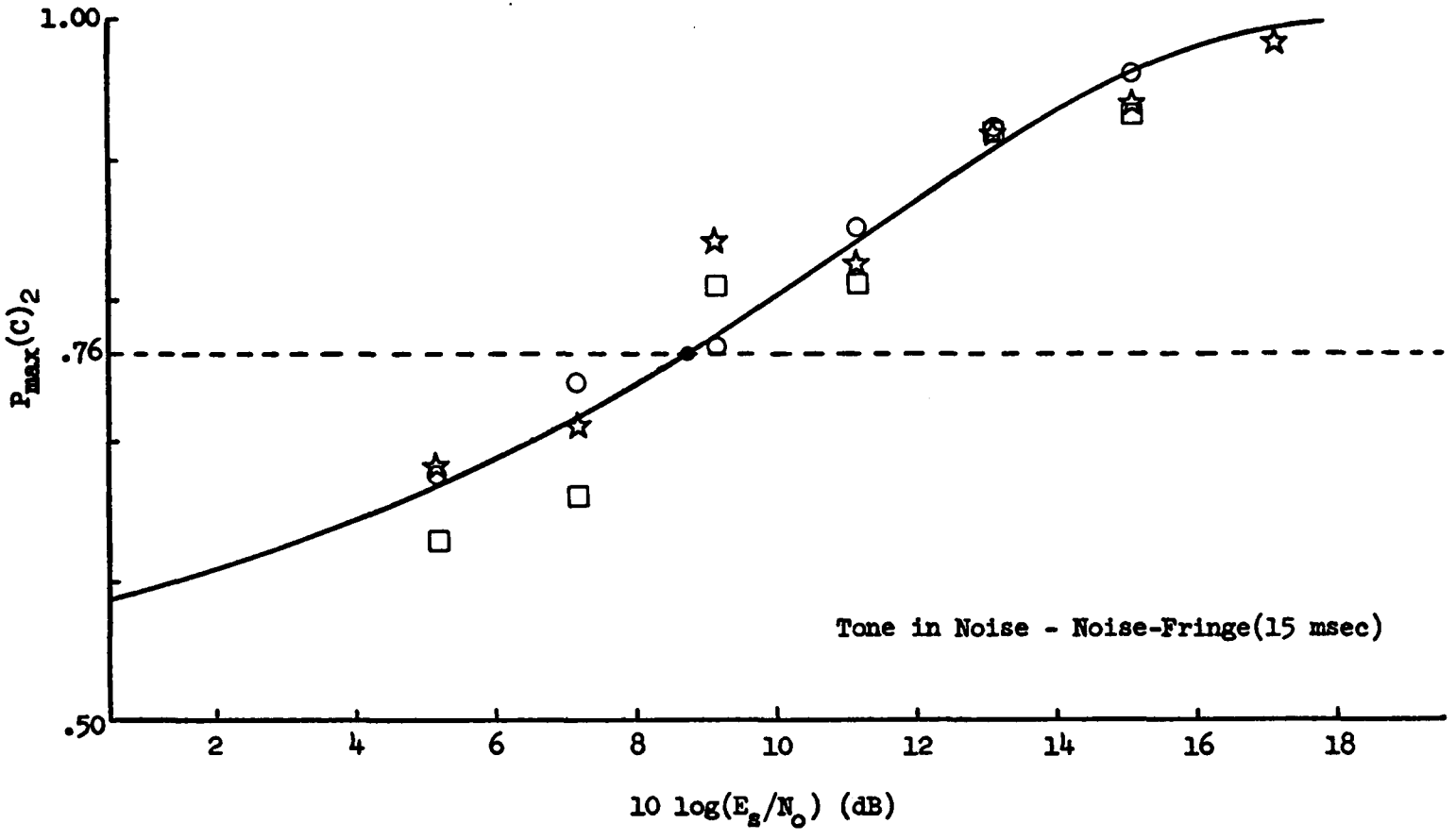
1.00
.76
.50
$P_{max}(C)_2$
2
4
6
8
10
12
14
16
18
10 log(E_s/N_o) (dB)
Tone in Noise - Noise-Fringe(15 msec)

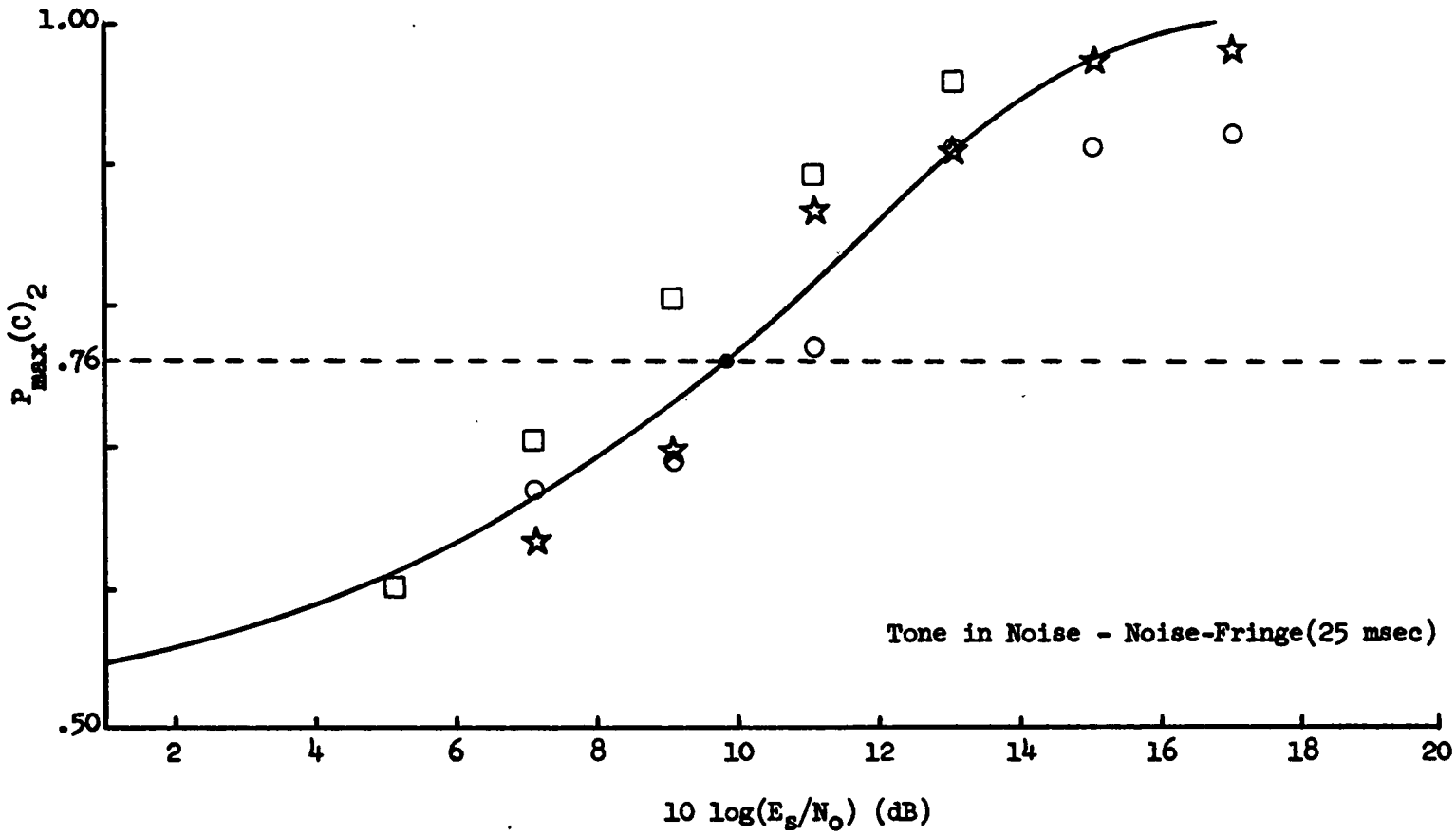
1.00
.76
.50
$P_{max}(c)_2$
2
4
6
8
10
12
14
16
18
20
10 log(E_s/N_o) (dB)
Tone in Noise - Noise-Fringe(25 msec)

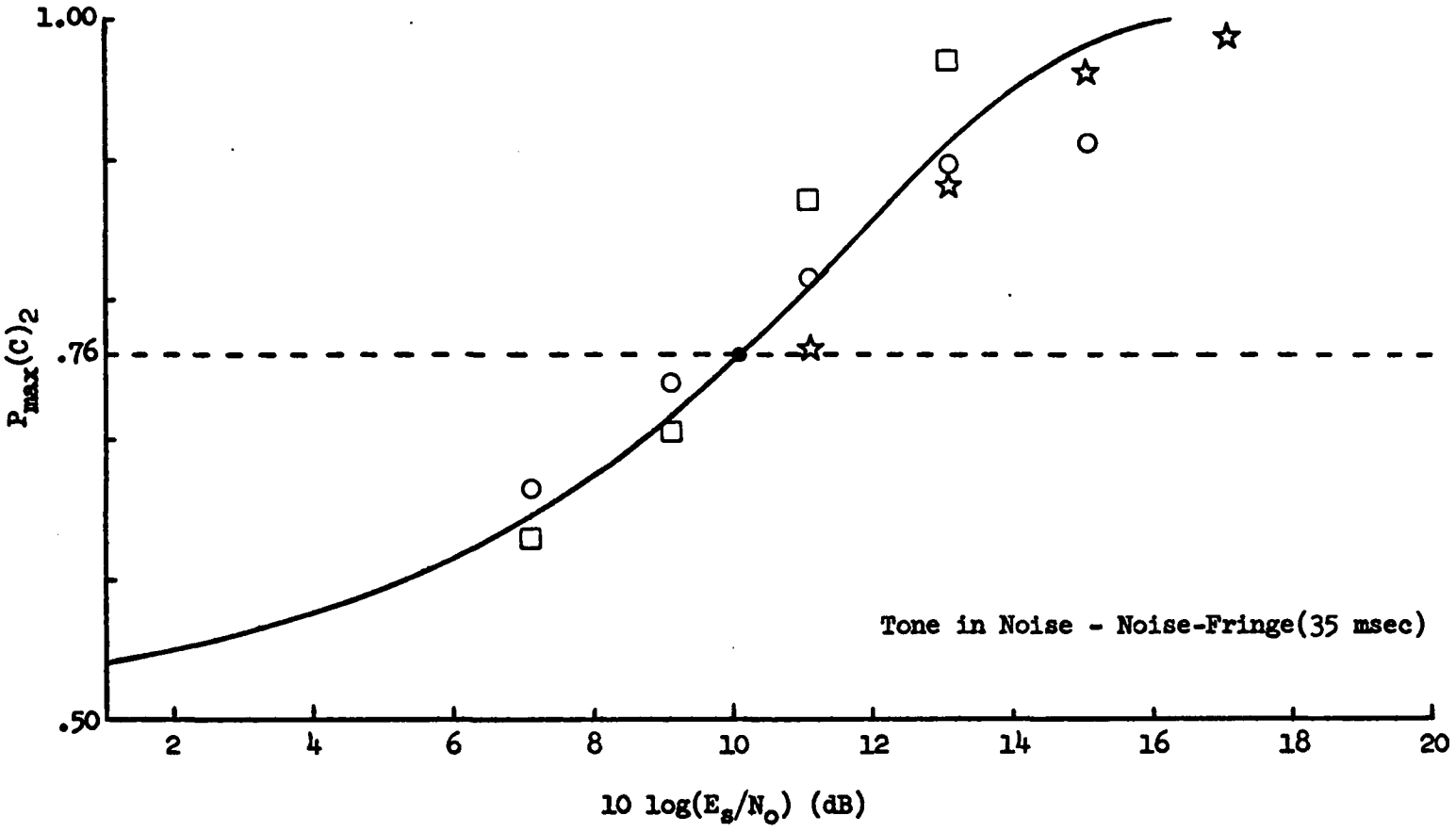
1.00
.76
.50
$P_{max}(C)_2$
2
4
6
8
10
12
14
16
18
20
10 log(E_s/N_o) (dB)
Tone in Noise - Noise-Fringe(35 msec)

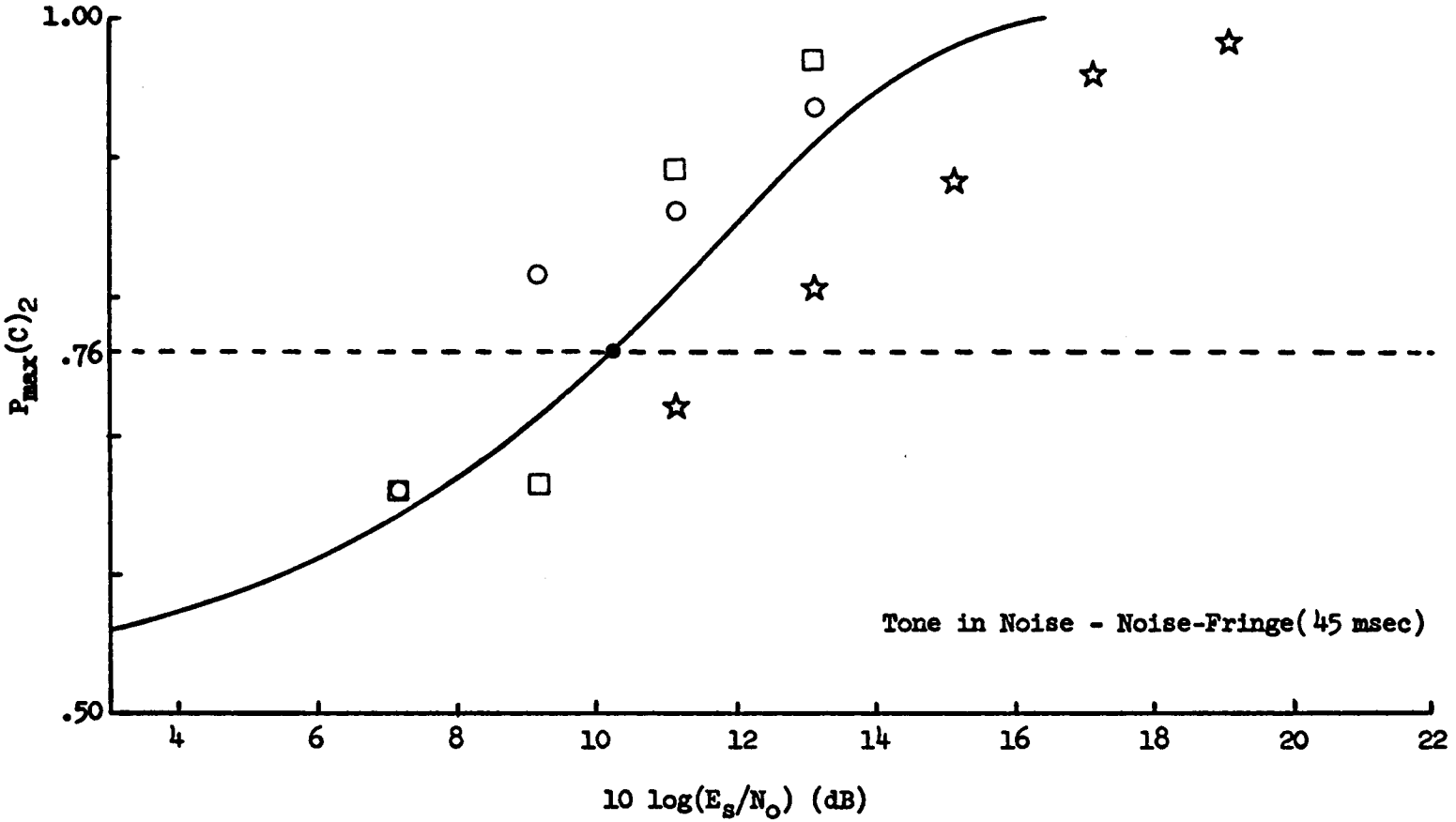
1.00
.76
.50
$P_{max}(C)_2$
4
6
8
10
12
14
16
18
20
22
10 log(E_s/N_o) (dB)
Tone in Noise - Noise-Fringe(45 msec)

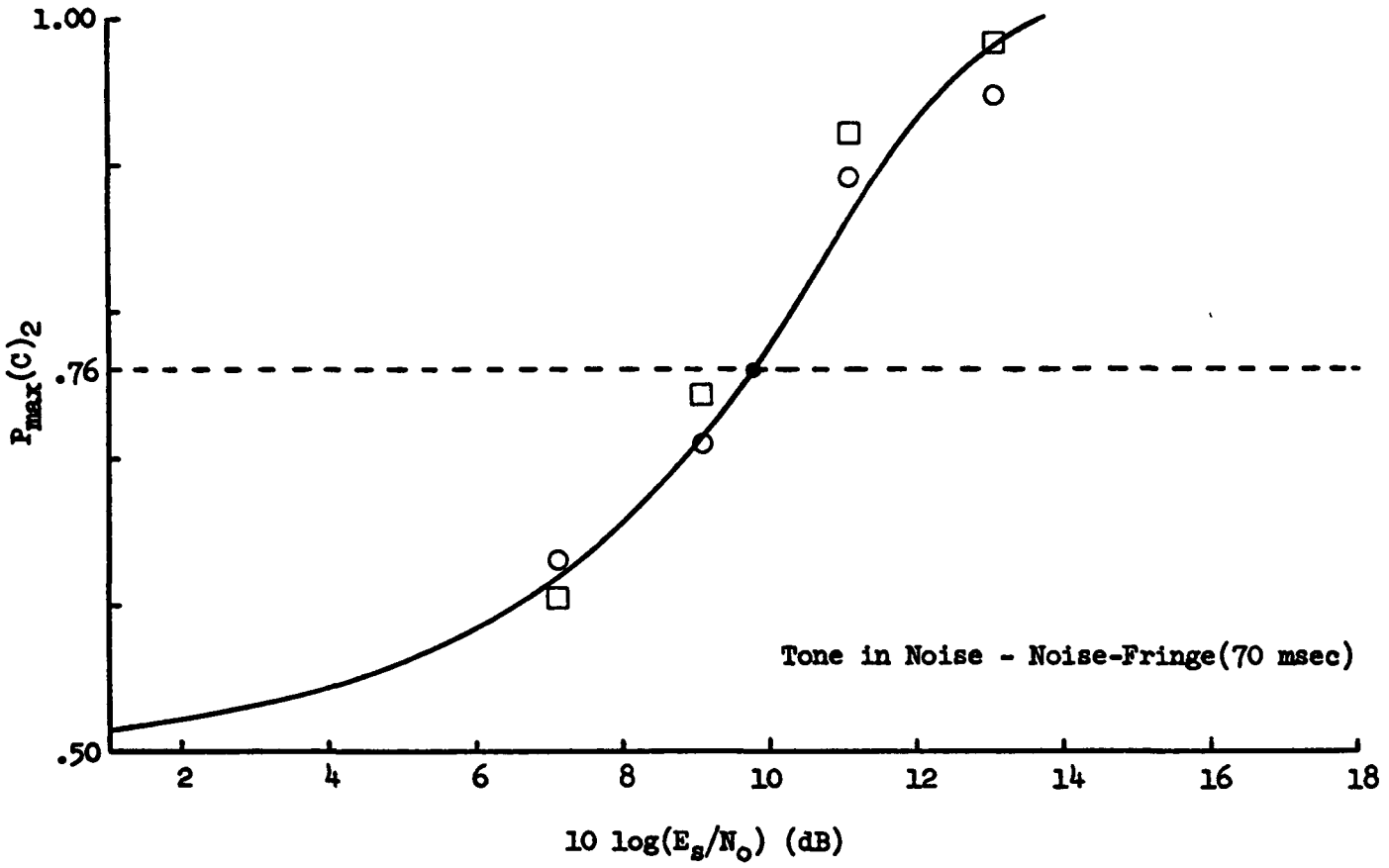
1.00
.76
.50
$P_{max}(C)_2$
2
4
6
8
10
12
14
16
18
10 log(E_s/N_o) (dB)
Tone in Noise - Noise-Fringe(70 msec)

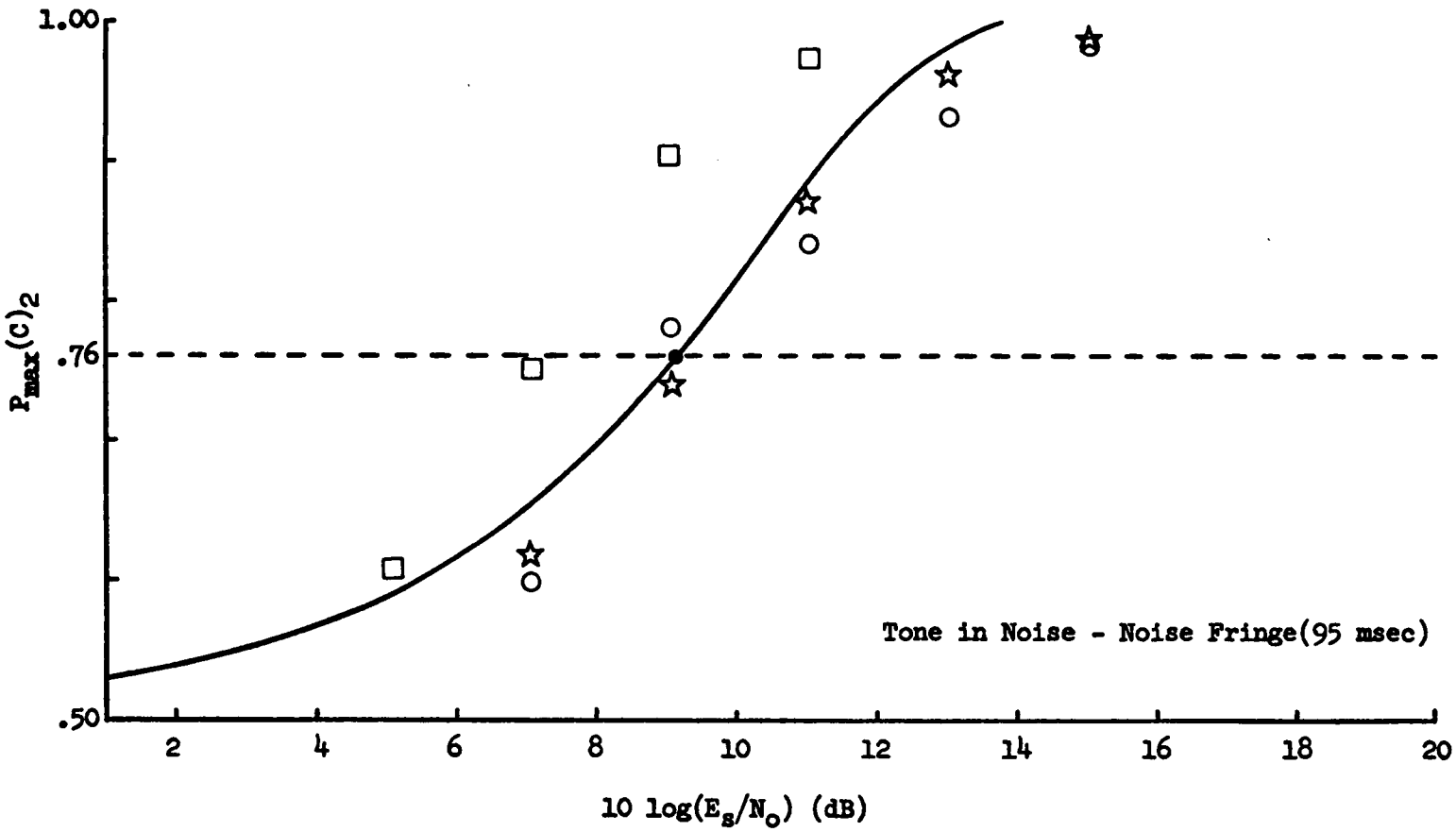
1.00
.76
.50
$P_{max}(C)_2$
2
4
6
8
10
12
14
16
18
20
10 log(E_s/N_o) (dB)
Tone in Noise - Noise Fringe(95 msec)

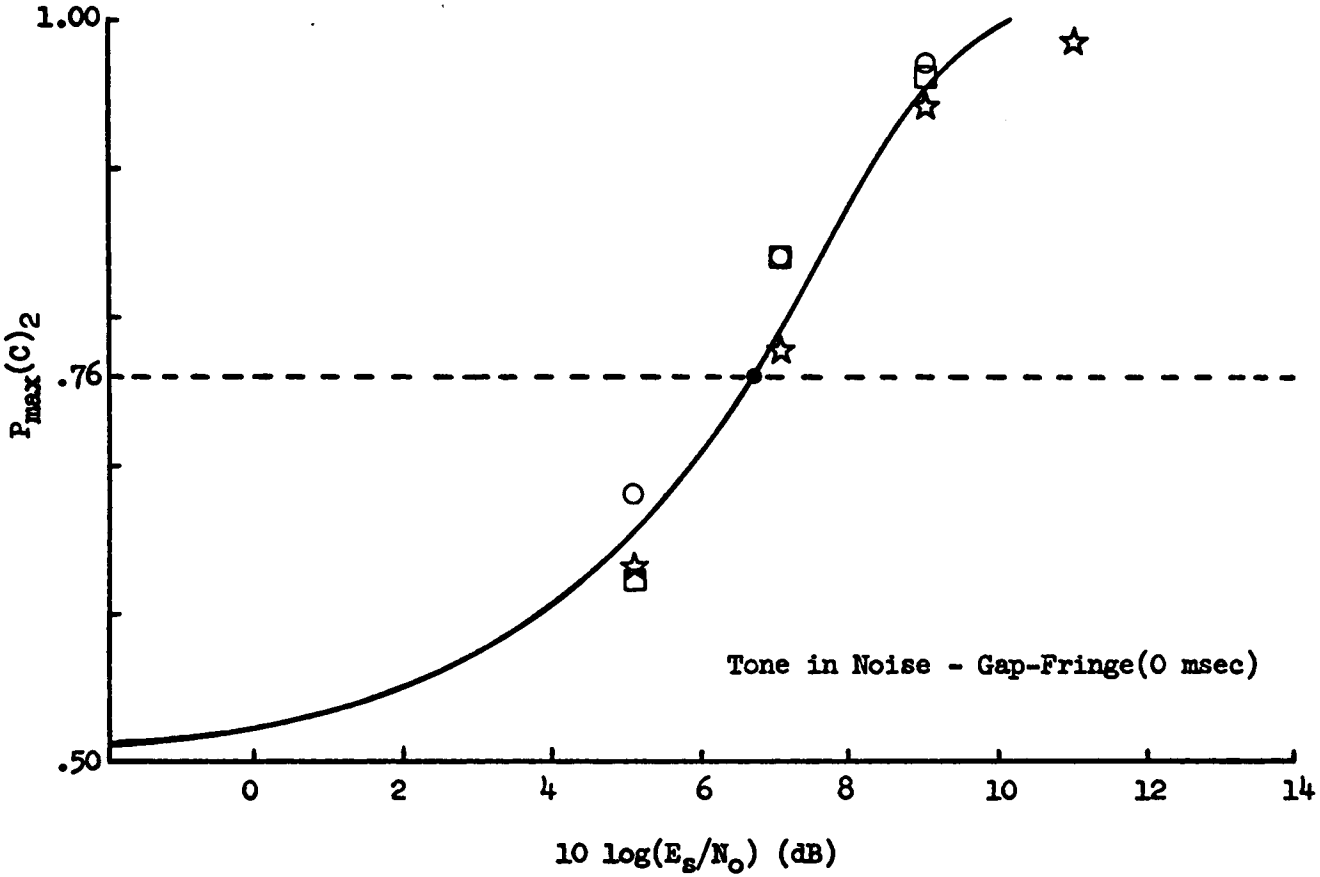
1.00
.76
.50
$P_{max}(C)_2$
0
2
4
6
8
10
12
14
10 log(E_s/N_o) (dB)
Tone in Noise - Gap-Fringe(0 msec)

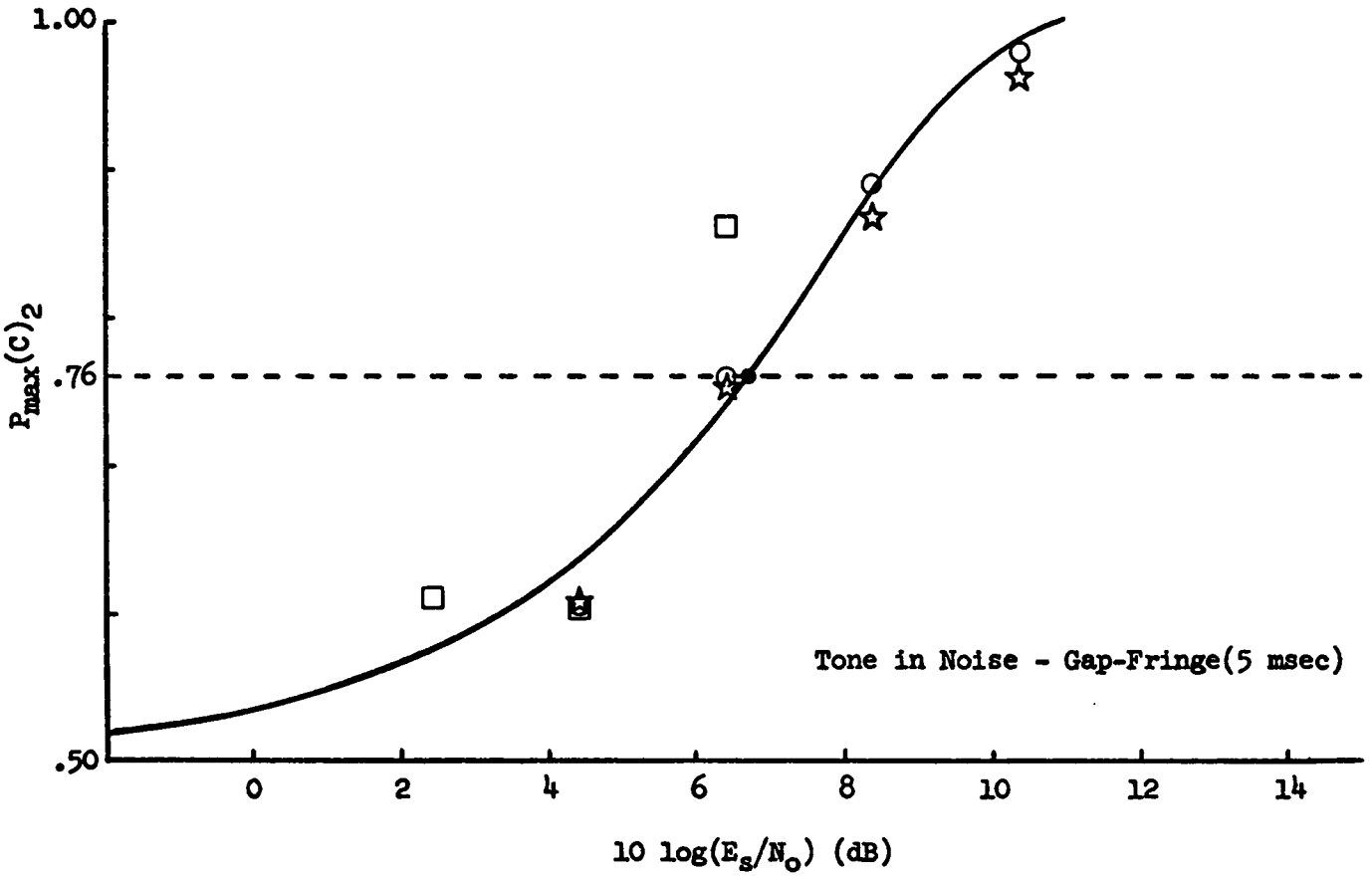
1.00
.76
.50
$P_{max}(C)_2$
0
2
4
6
8
10
12
14
10 log(E_s/N_o) (dB)
Tone in Noise - Gap-Fringe(5 msec)

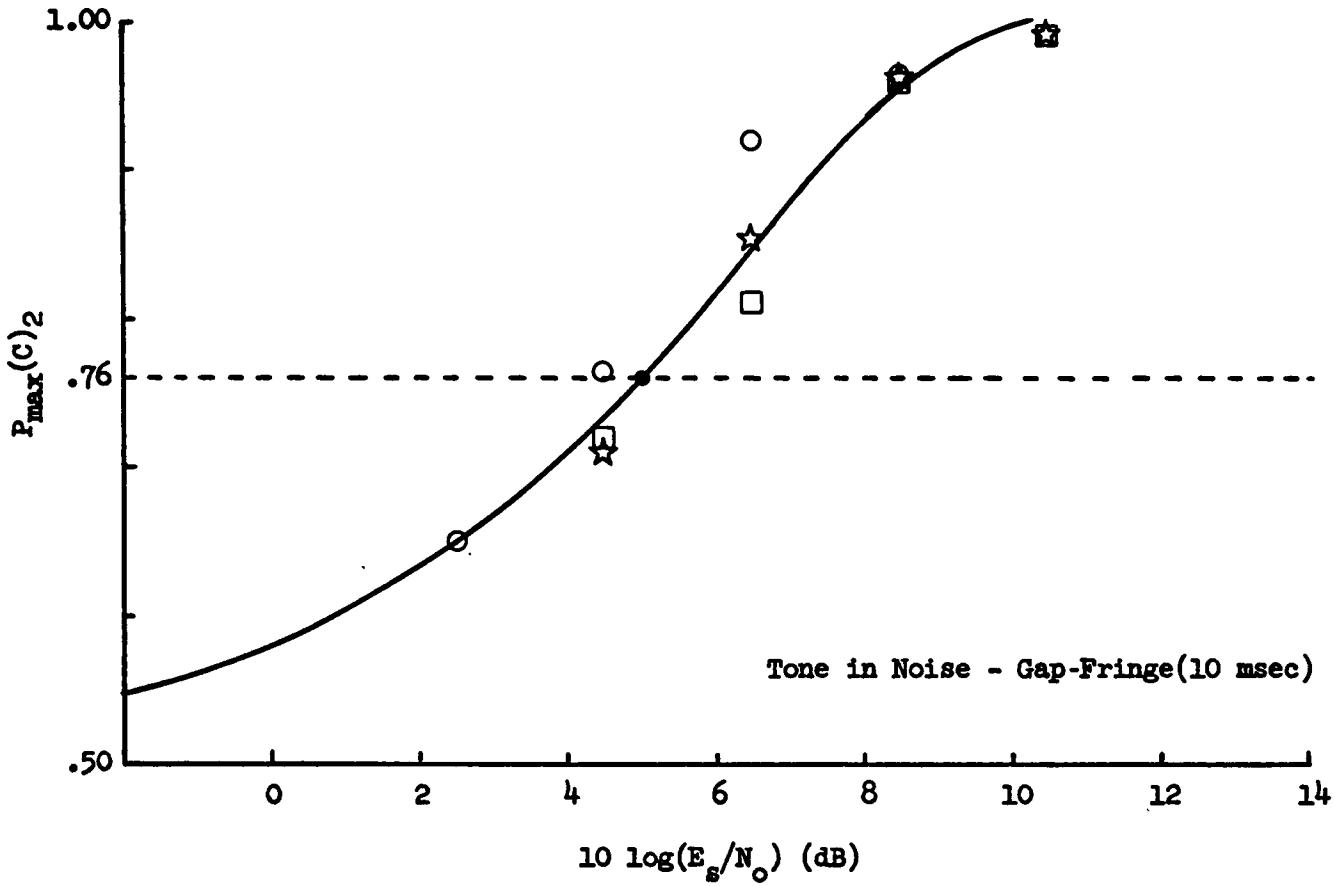
1.00
.76
.50
$P_{max}(C)_2$
0
2
4
6
8
10
12
14
10 log(E_s/N_o) (dB)
Tone in Noise - Gap-Fringe(10 msec)

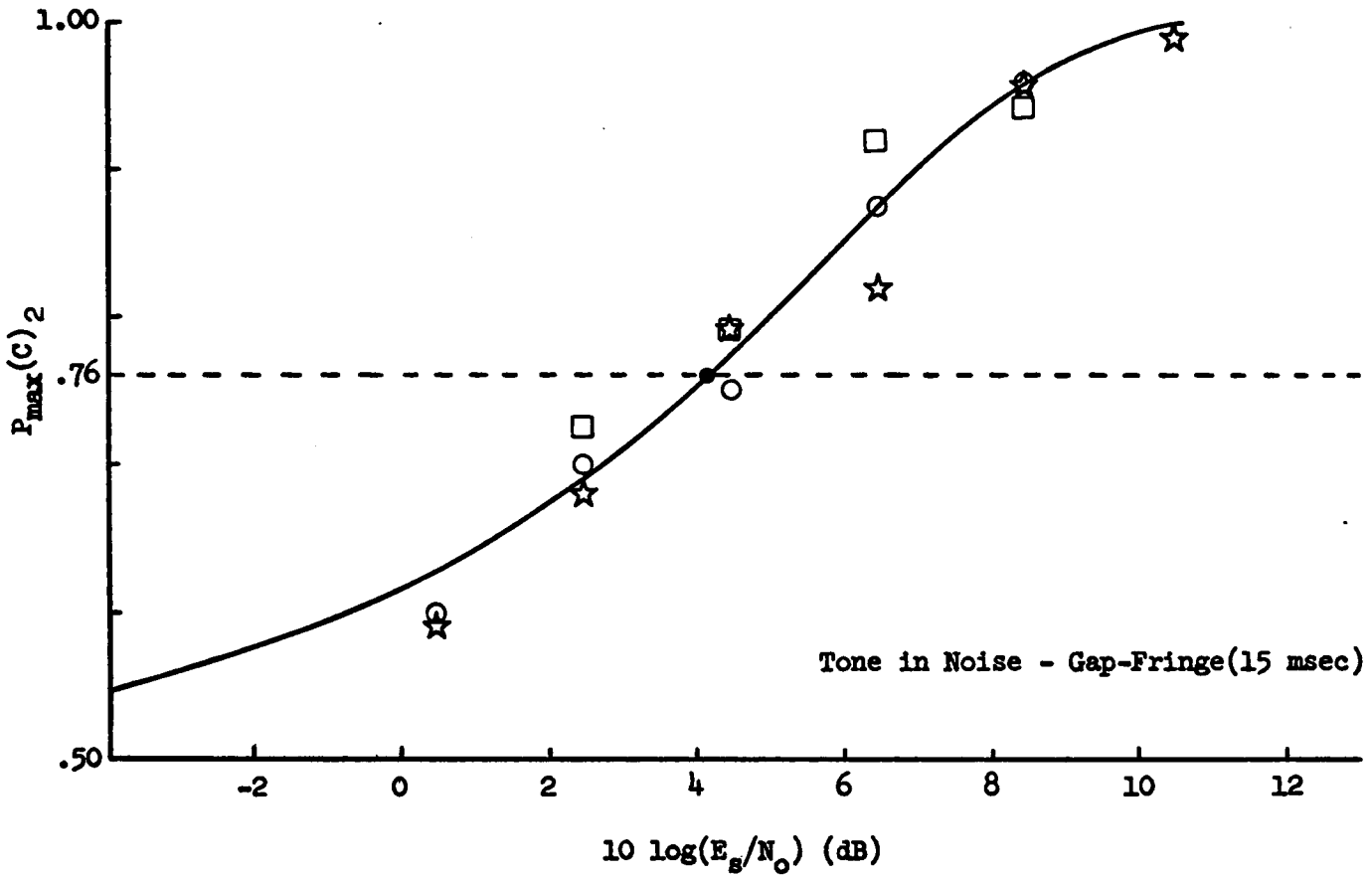
1.00
.76
.50
$P_{max}(C)_2$
-2
0
2
4
6
8
10
12
10 log(E_s/N_o) (dB)
Tone in Noise - Gap-Fringe(15 msec)

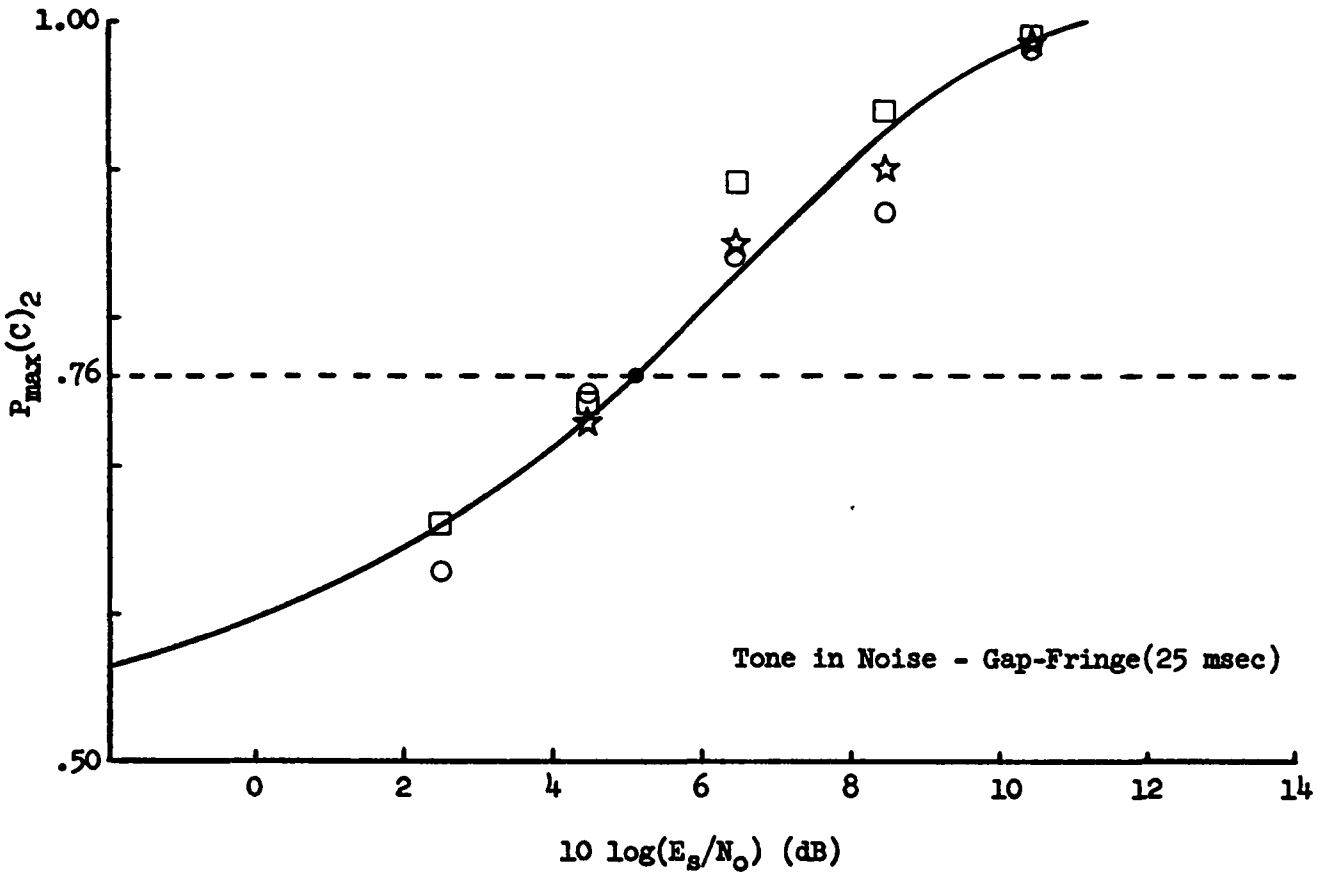
1.00
.76
.50
$P_{max}(C)_2$
0
2
4
6
8
10
12
14
10 log(E_s/N_o) (dB)
Tone in Noise - Gap-Fringe(25 msec)

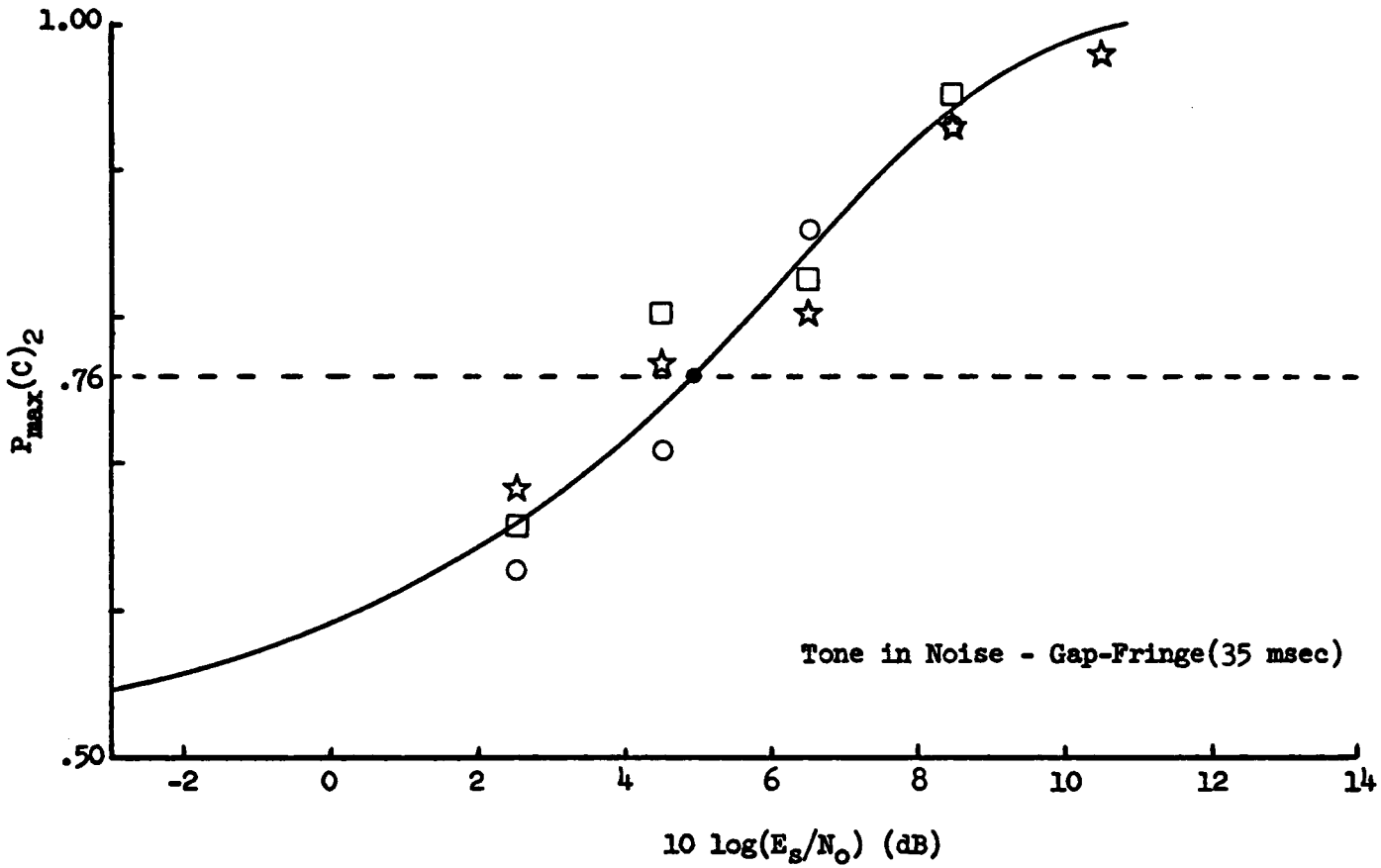
1.00
.76
.50
$P_{max}(C)_2$
-2
0
2
4
6
8
10
12
14
10 log(E_s/N_o) (dB)
Tone in Noise - Gap-Fringe(35 msec)

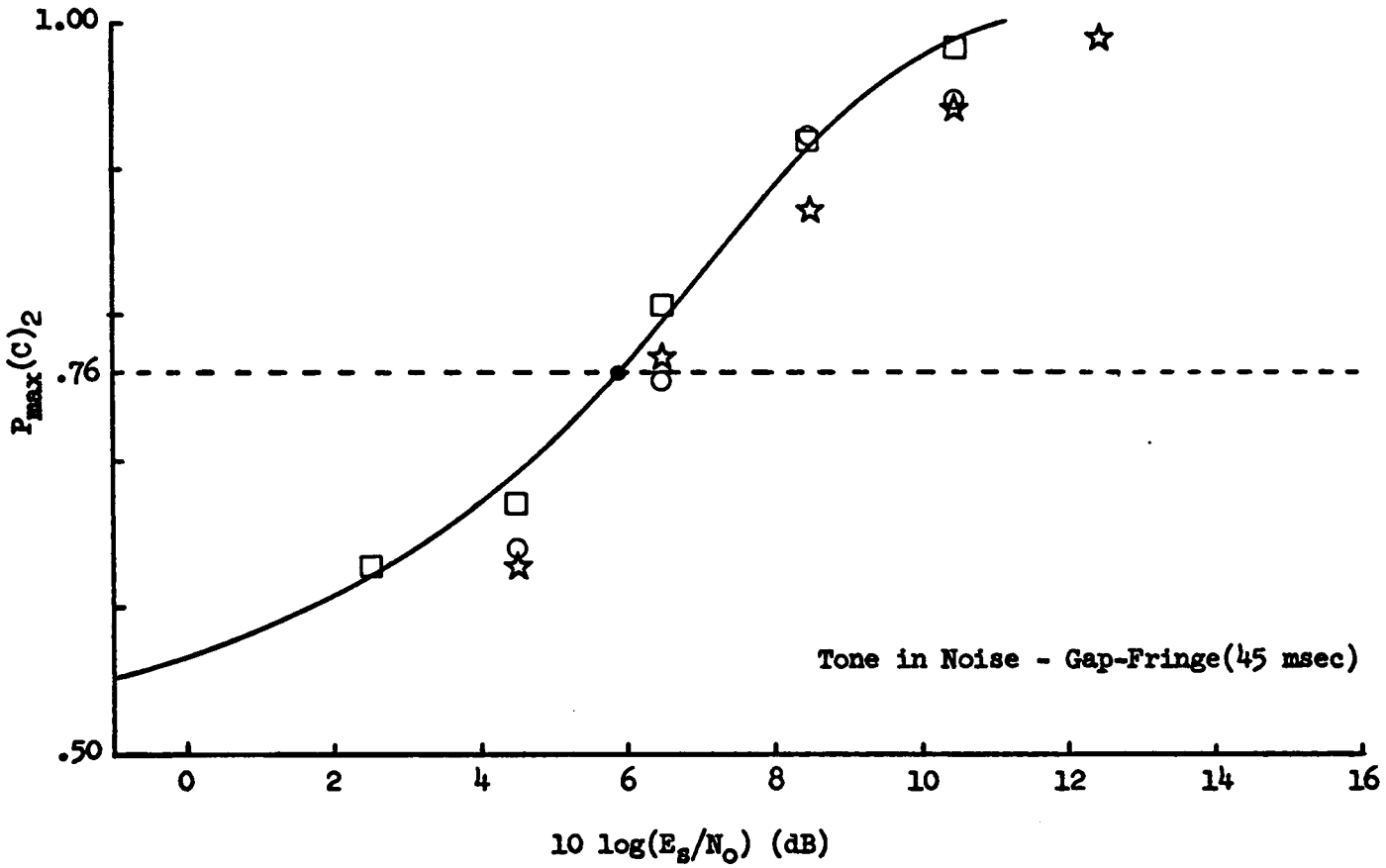
1.00
.76
.50
$P_{max}(C)_2$
0
2
4
6
8
10
12
14
16
10 log(E_s/N_o) (dB)
Tone in Noise - Gap-Fringe(45 msec)

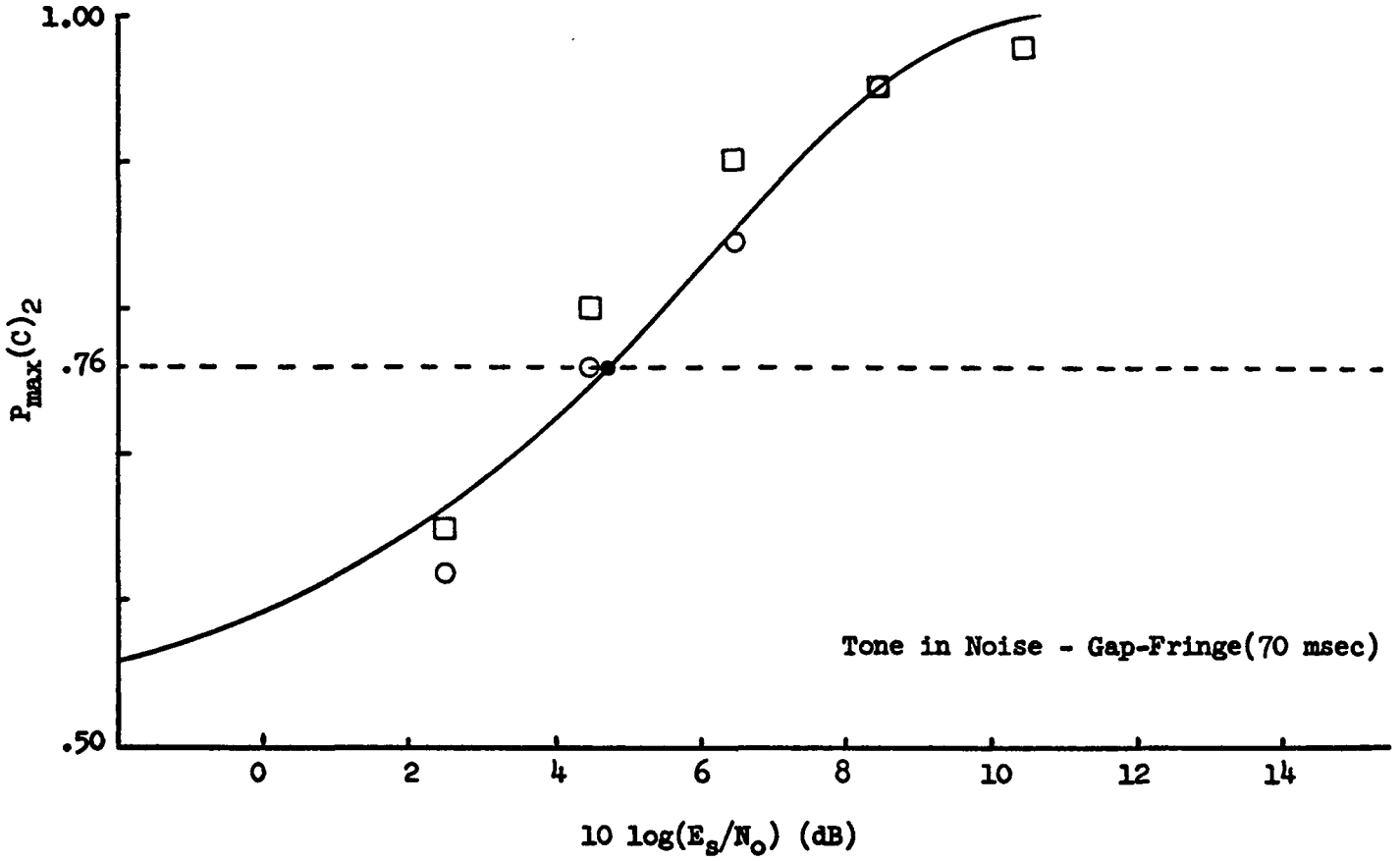
1.00
.76
.50
$P_{max}(C)_2$
0
2
4
6
8
10
12
14
10 log(E_s/N_o) (dB)
Tone in Noise - Gap-Fringe(70 msec)

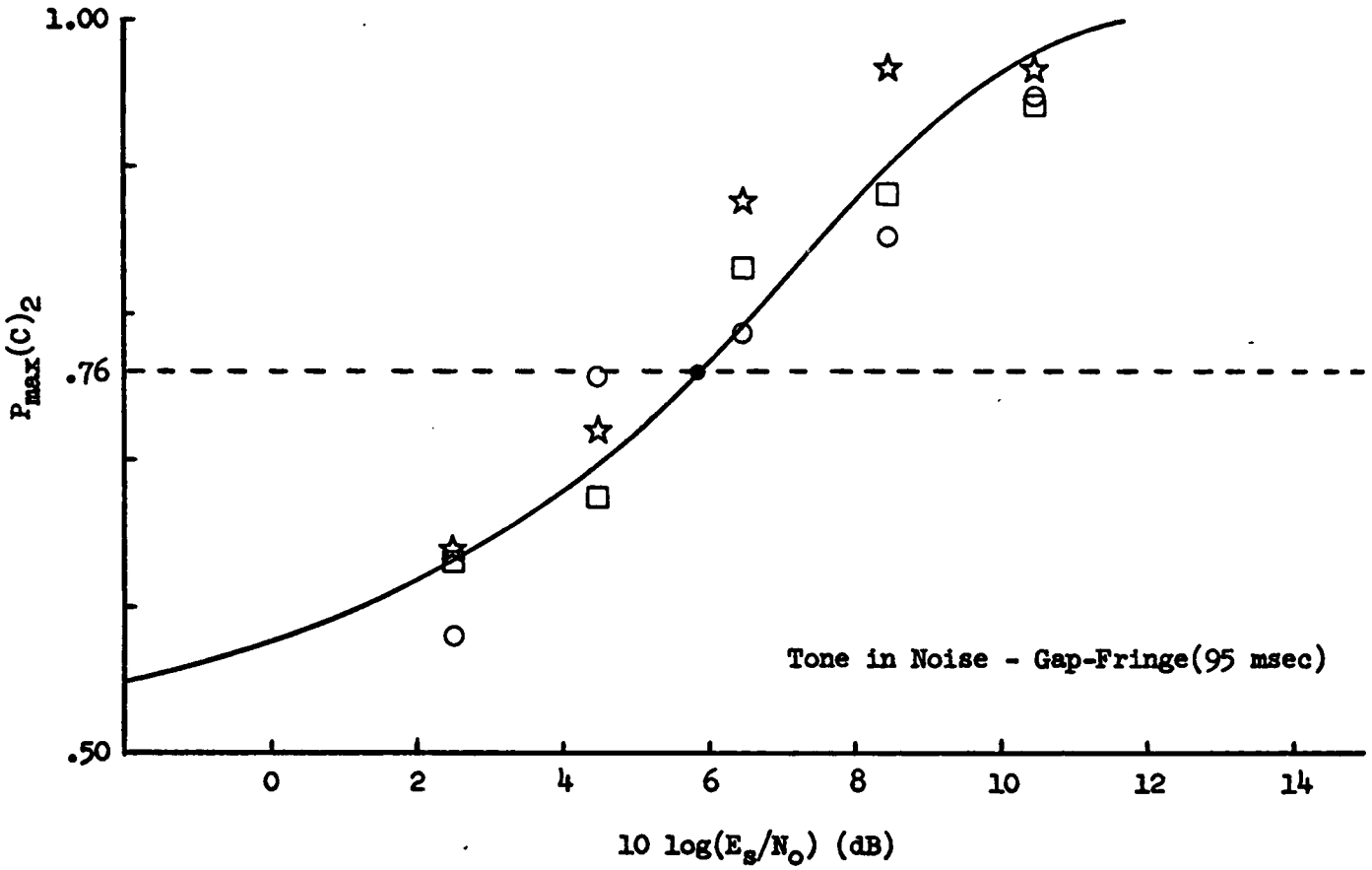
1.00
.76
.50
$P_{max}(c)_2$
0
2
4
6
8
10
12
14
10 log(E_s/N_o) (dB)
Tone in Noise - Gap-Fringe(95 msec)

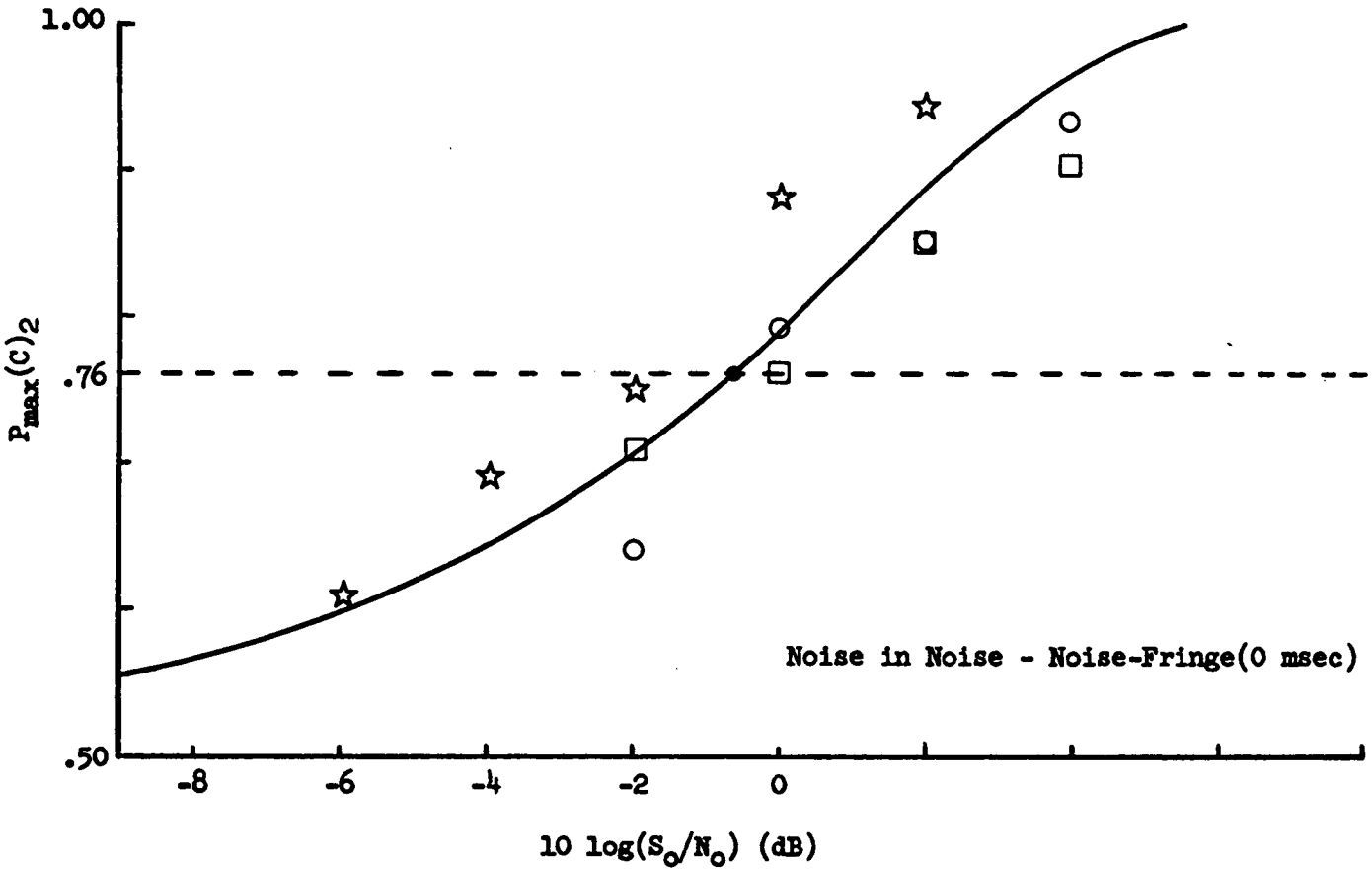
1.00
.76
.50
$P_{max}(C)_2$
-8
-6
-4
-2
0
10 log(S_o/N_o) (dB)
Noise in Noise - Noise-Fringe(0 msec)

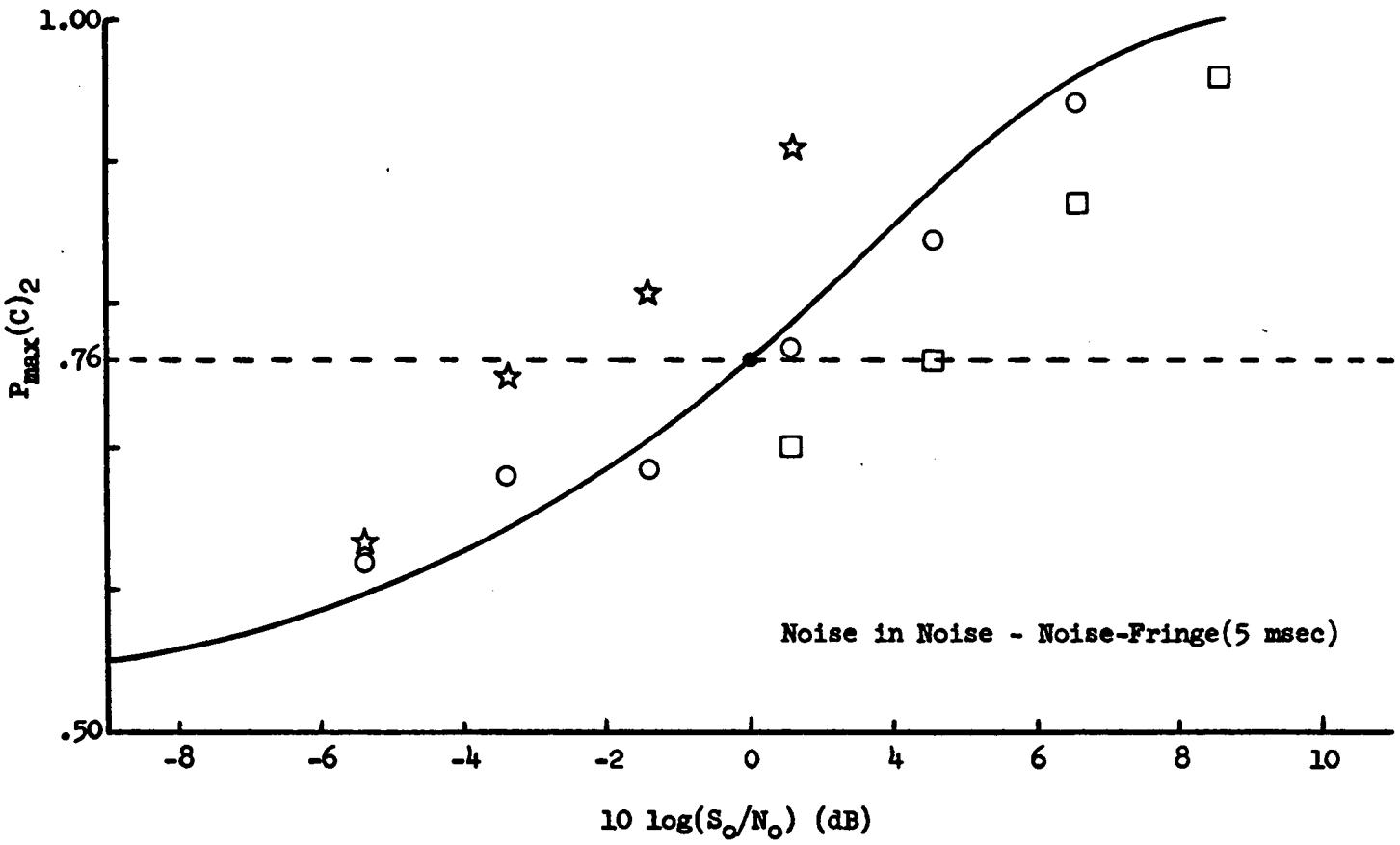
1.00
.76
.50
$P_{max}(C)_2$
-8
-6
-4
-2
0
4
6
8
10
10 log(S_o/N_o) (dB)
Noise in Noise - Noise-Fringe(5 msec)

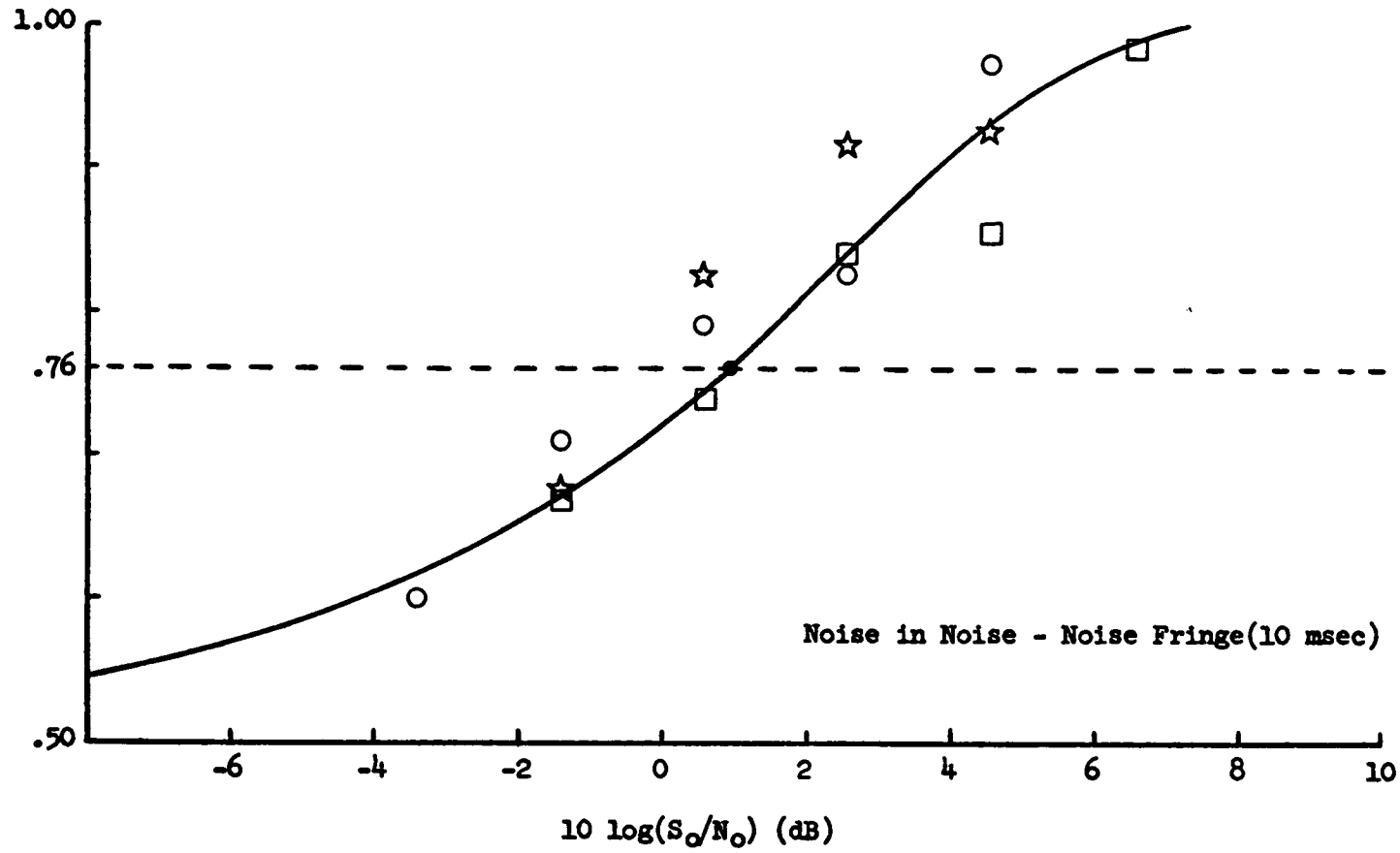
1.00
.76
.50
-6
-4
-2
0
2
4
6
8
10
Noise in Noise - Noise Fringe(10 msec)
10 log(S_o/N_o) (dB)

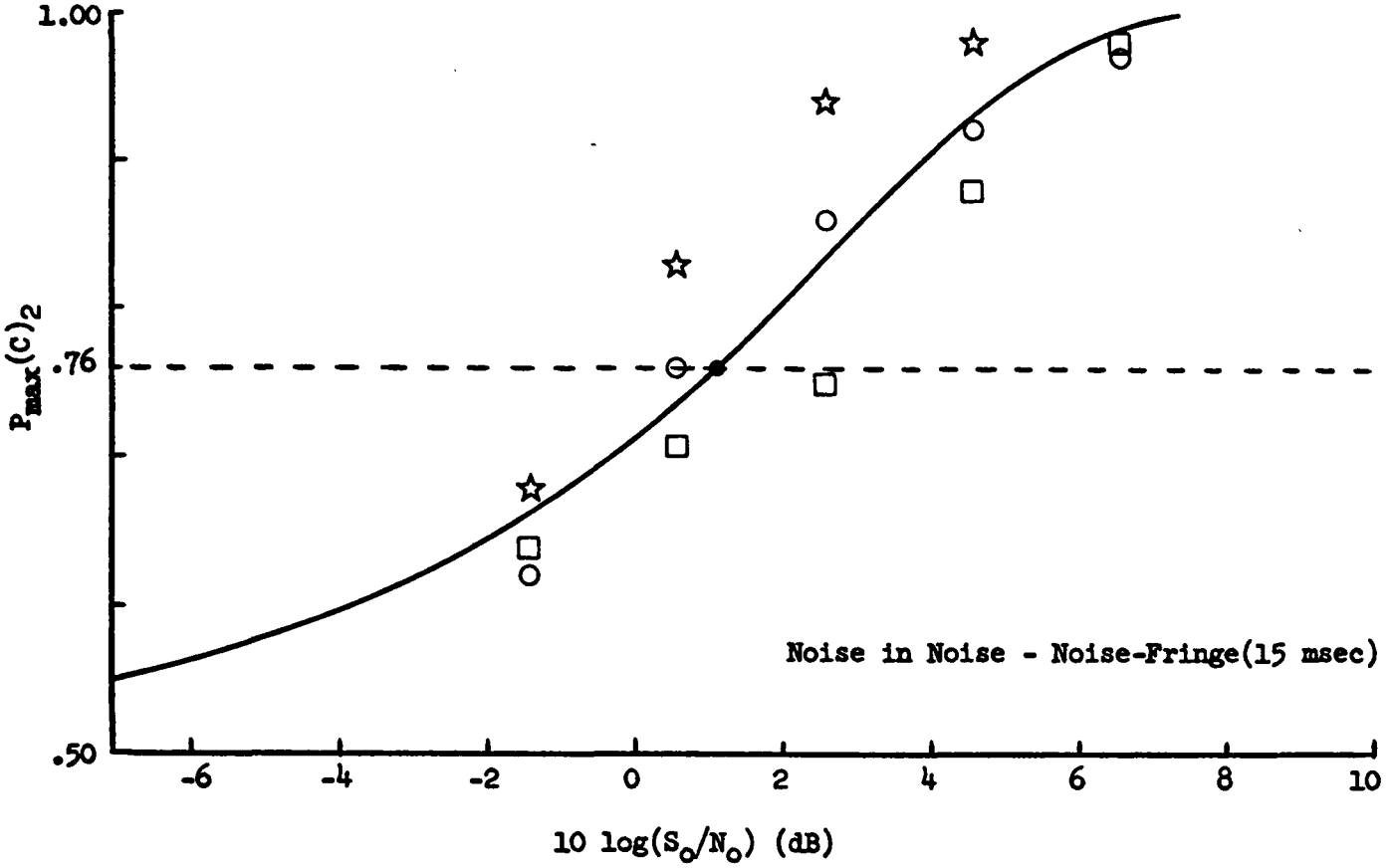
1.00
.76
.50
$P_{max}(C)_2$
-6
-4
-2
0
2
4
6
8
10
10 log(S_o/N_o) (dB)
Noise in Noise - Noise-Fringe(15 msec)

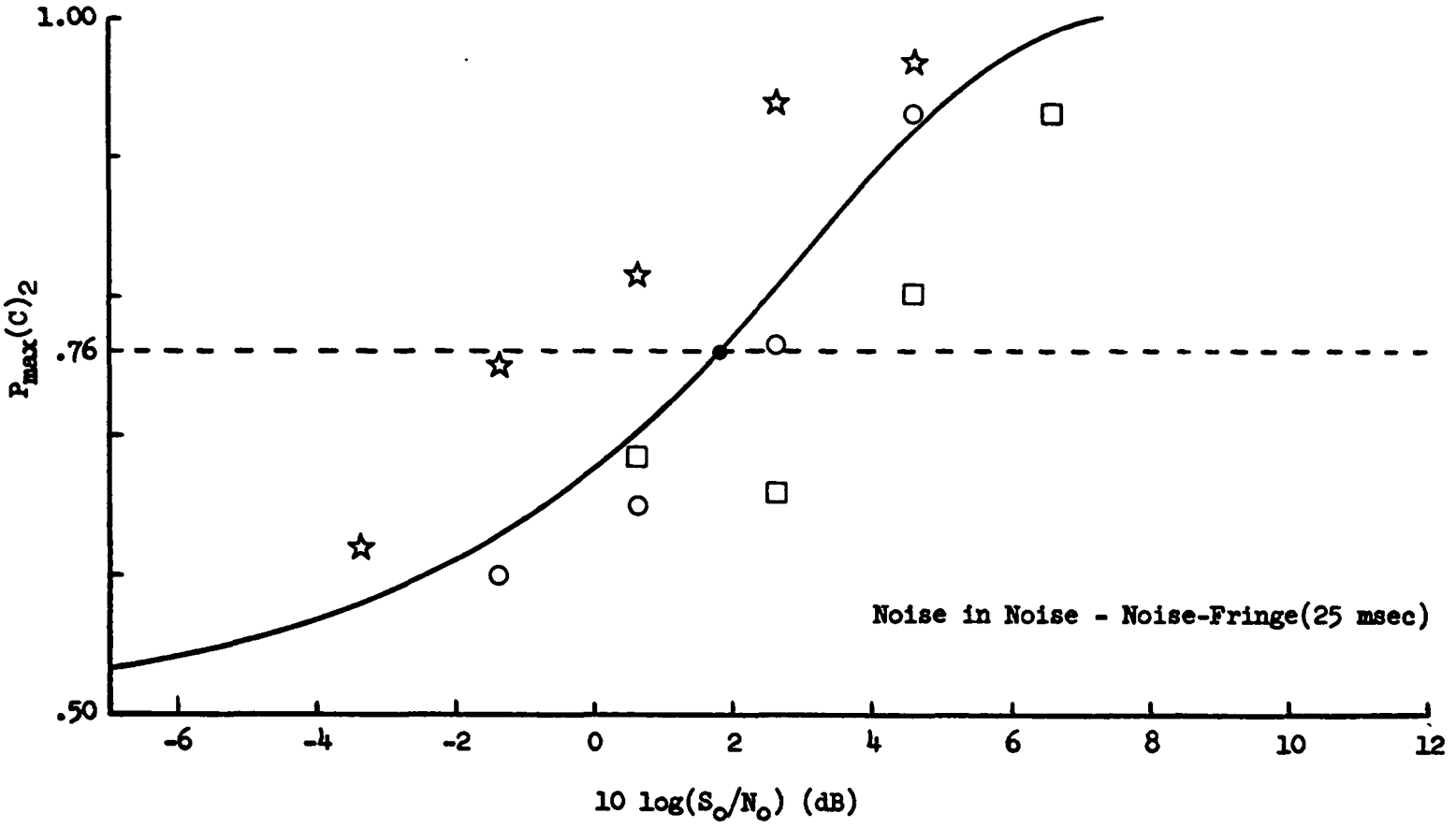
1.00
.76
.50
$P_{max}(C)_2$
-6
-4
-2
0
2
4
6
8
10
12
10 log(S_o/N_o) (dB)
Noise in Noise - Noise-Fringe(25 msec)

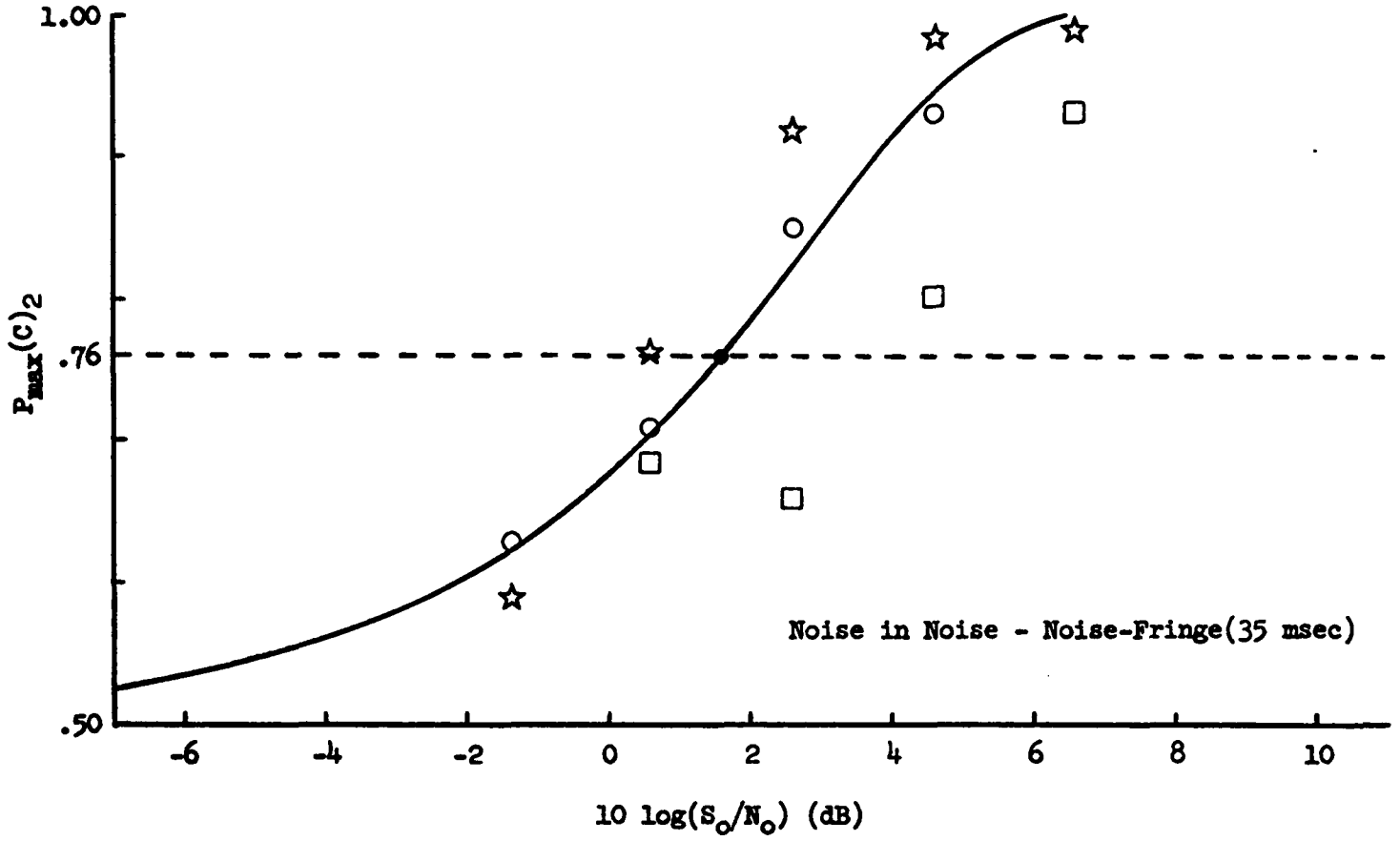
1.00
.76
.50
$P_{max}(C)_2$
-6
-4
-2
0
2
4
6
8
10
10 log(S_o/N_o) (dB)
Noise in Noise - Noise-Fringe(35 msec)

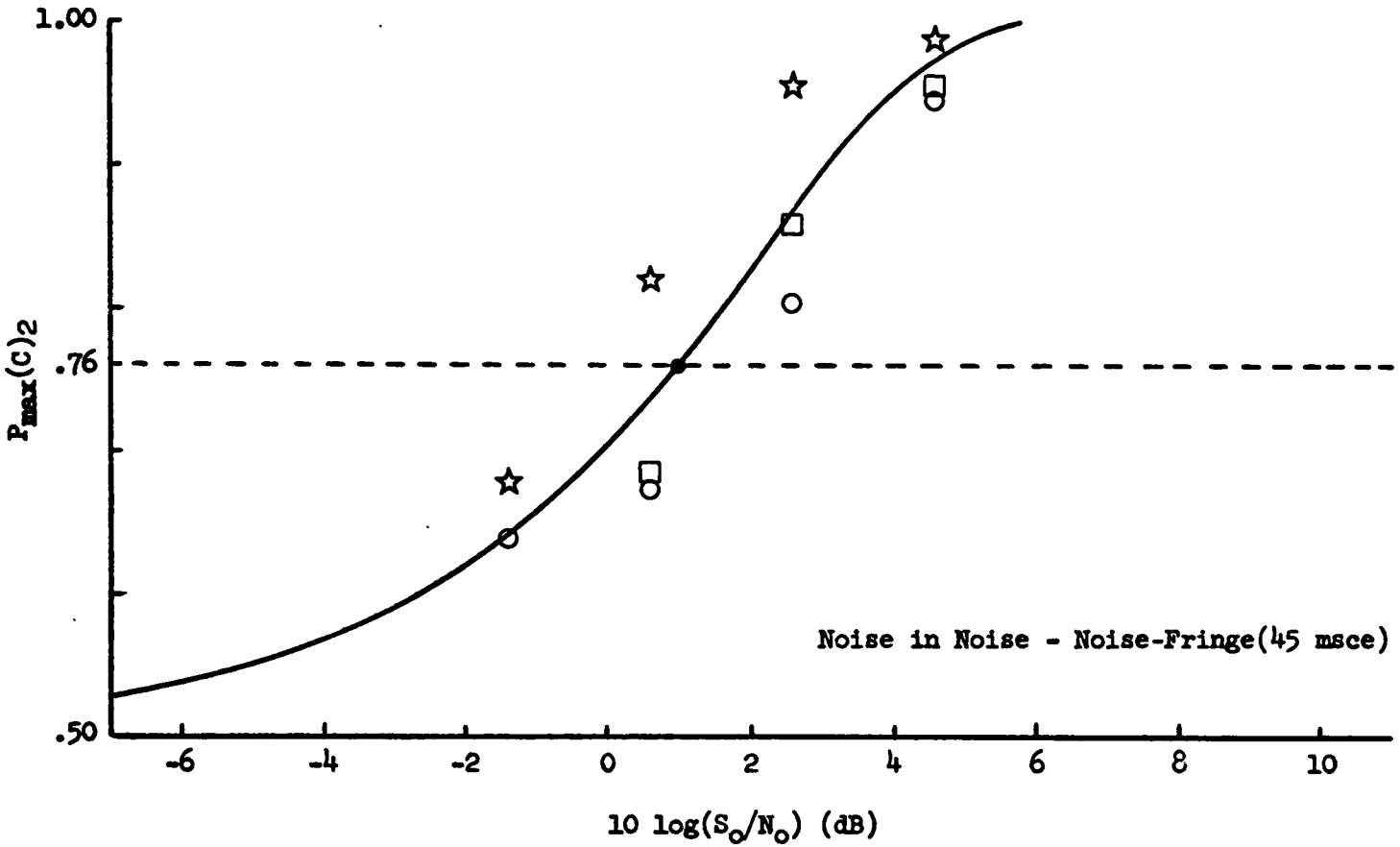
1.00
.76
.50
$P_{max}(C)_2$
-6
-4
-2
0
2
4
6
8
10
10 log(S_o/N_o) (dB)
Noise in Noise - Noise-Fringe(45 msce)

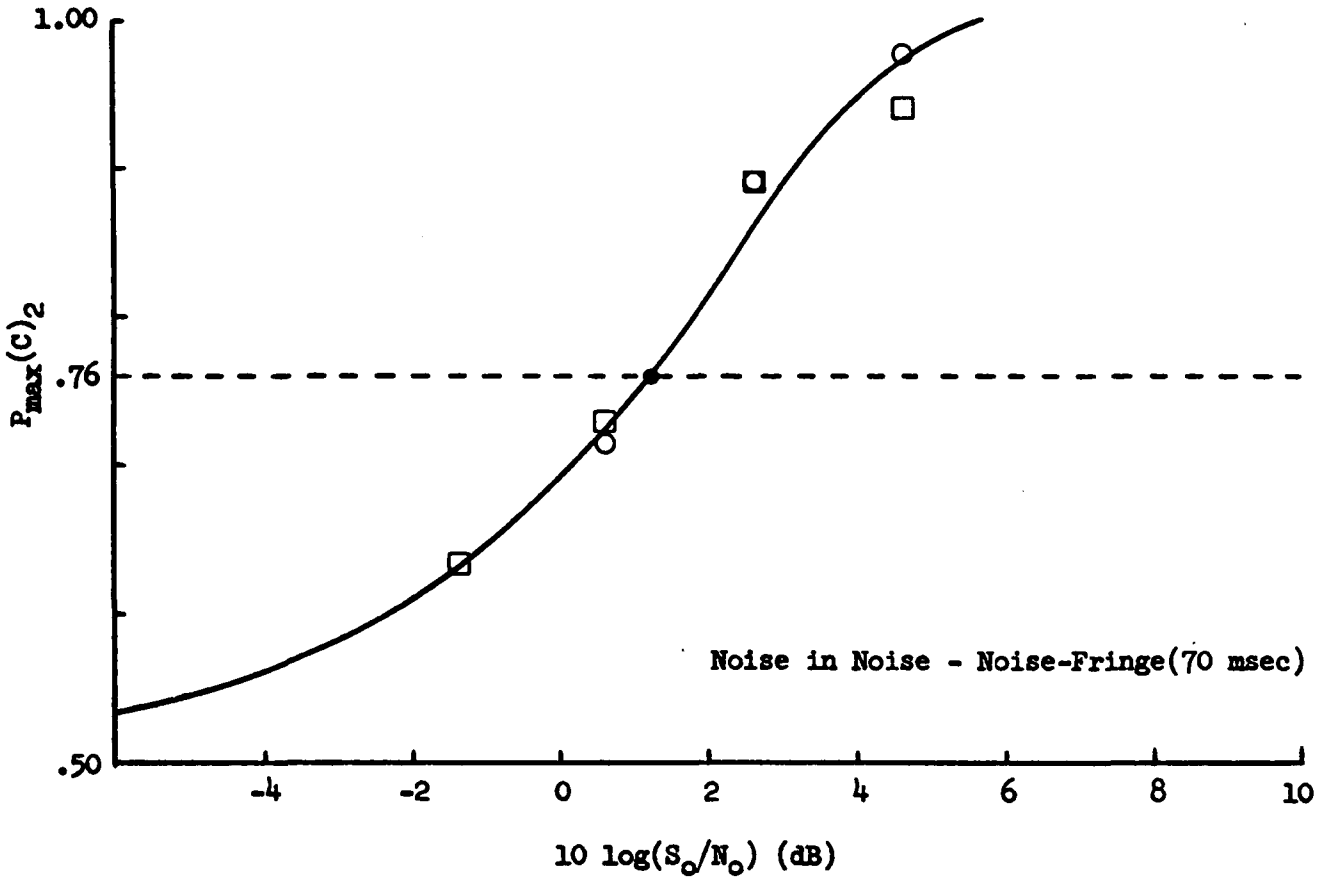
1.00
.76
.50
$P_{max}(C)_2$
-4
-2
0
2
4
6
8
10
10 log(S_o/N_o) (dB)
Noise in Noise - Noise-Fringe(70 msec)

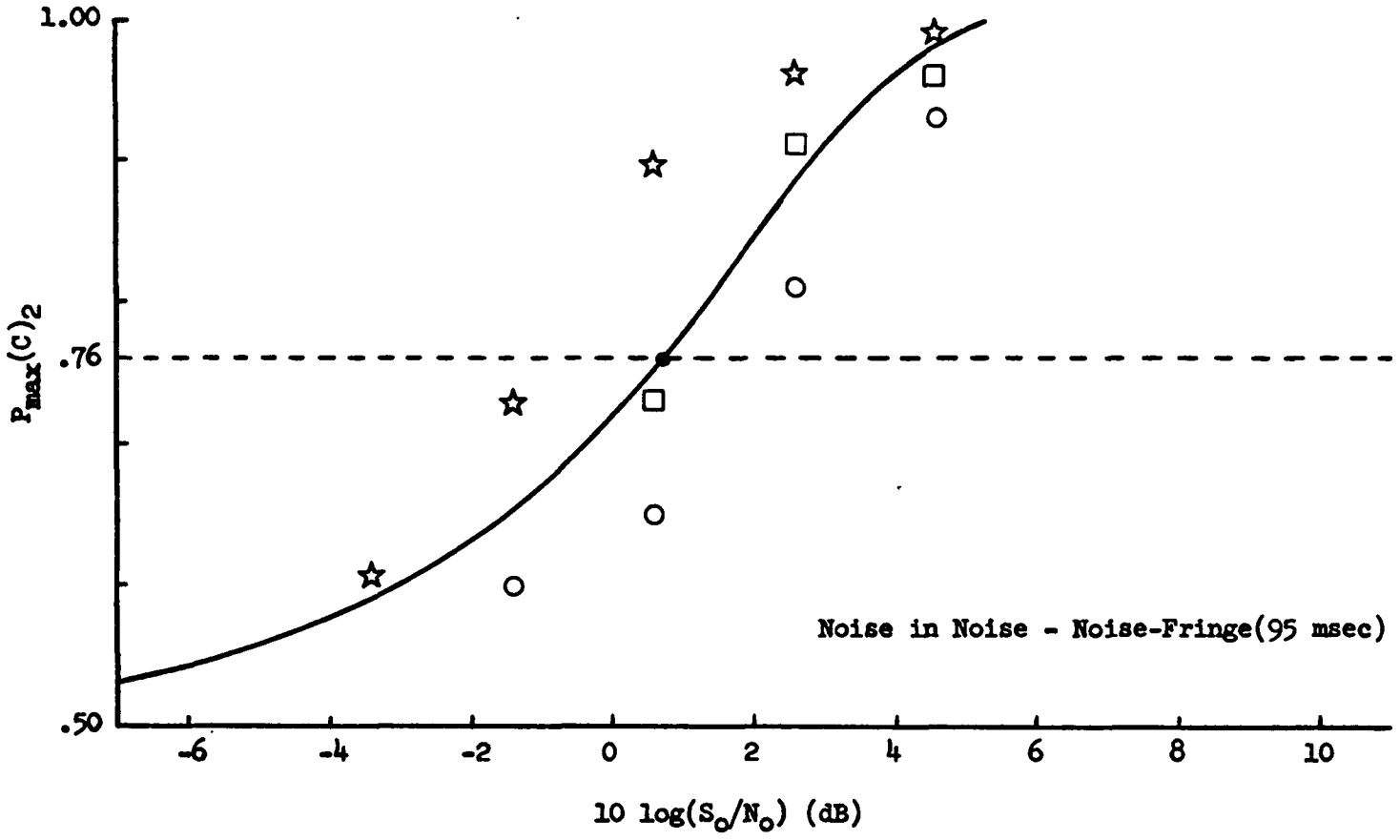
1.00
.76
.50
$P_{max}(c)_2$
-6
-4
-2
0
2
4
6
8
10
10 log(S_o/N_o) (dB)
Noise in Noise - Noise-Fringe(95 msec)

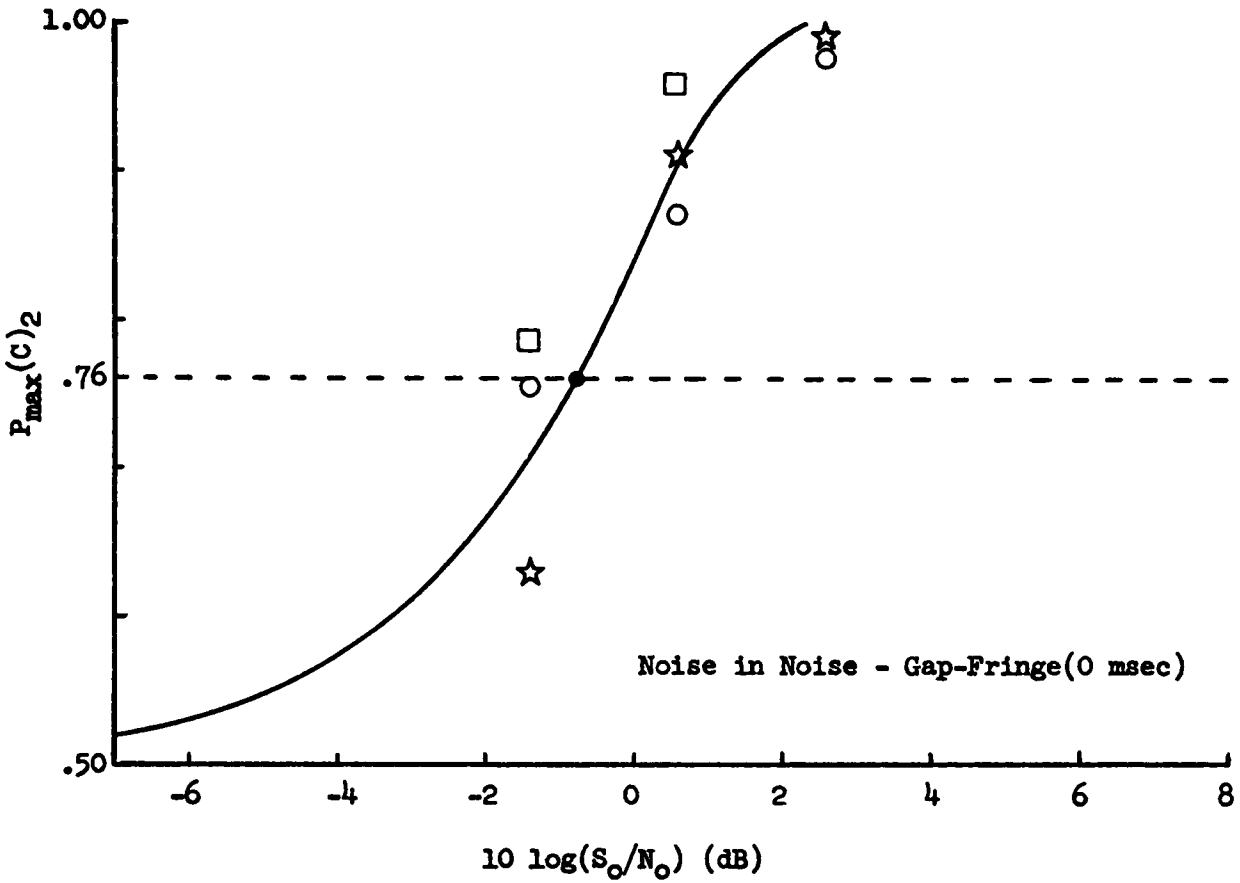
1.00
.76
.50
$P_{max}(c)_2$
-6
-4
-2
0
2
4
6
8
10 log(S_o/N_o) (dB)
Noise in Noise - Gap-Fringe(0 msec)

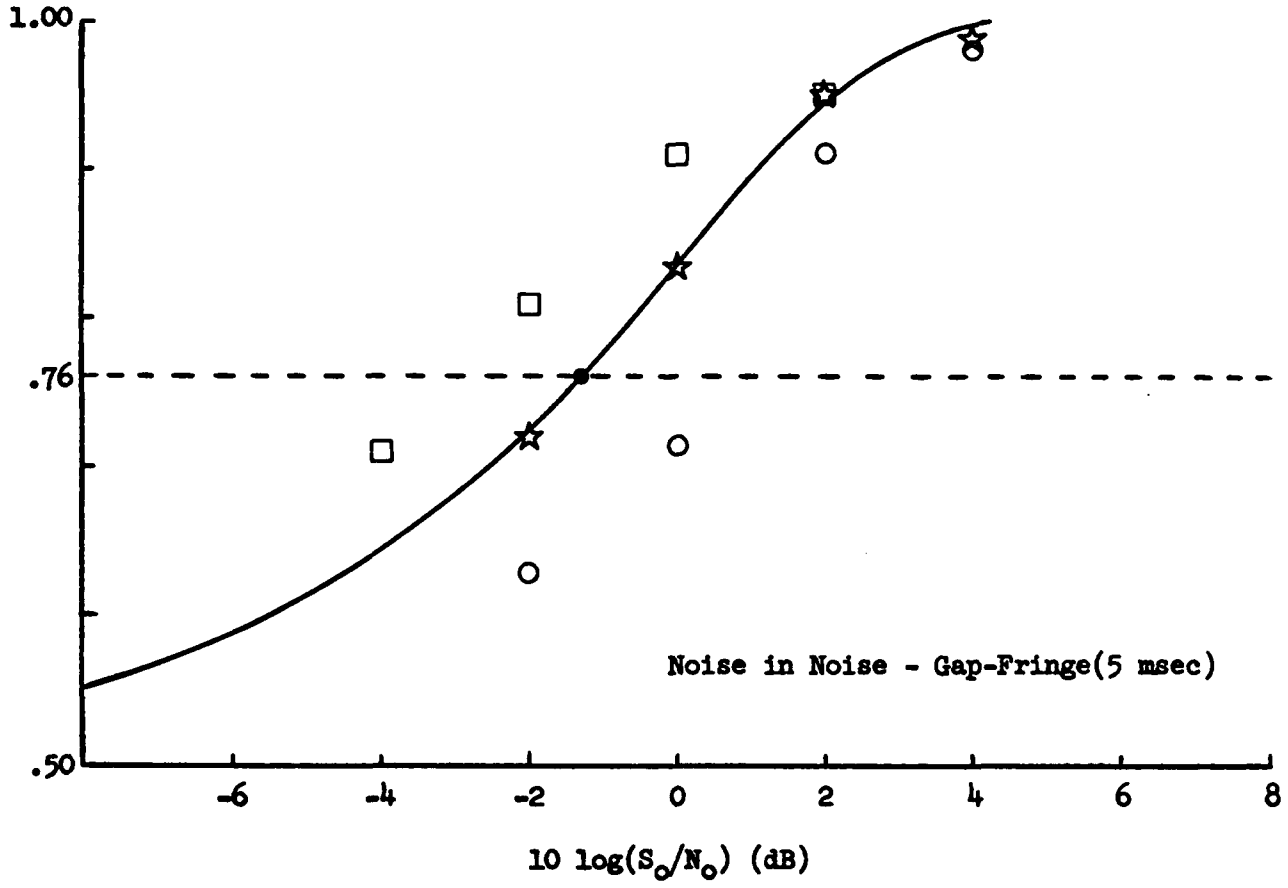
1.00
.76
.50
-6
-4
-2
0
2
4
6
8
Noise in Noise - Gap-Fringe(5 msec)
10 log(S$_o$/N$_o$) (dB)

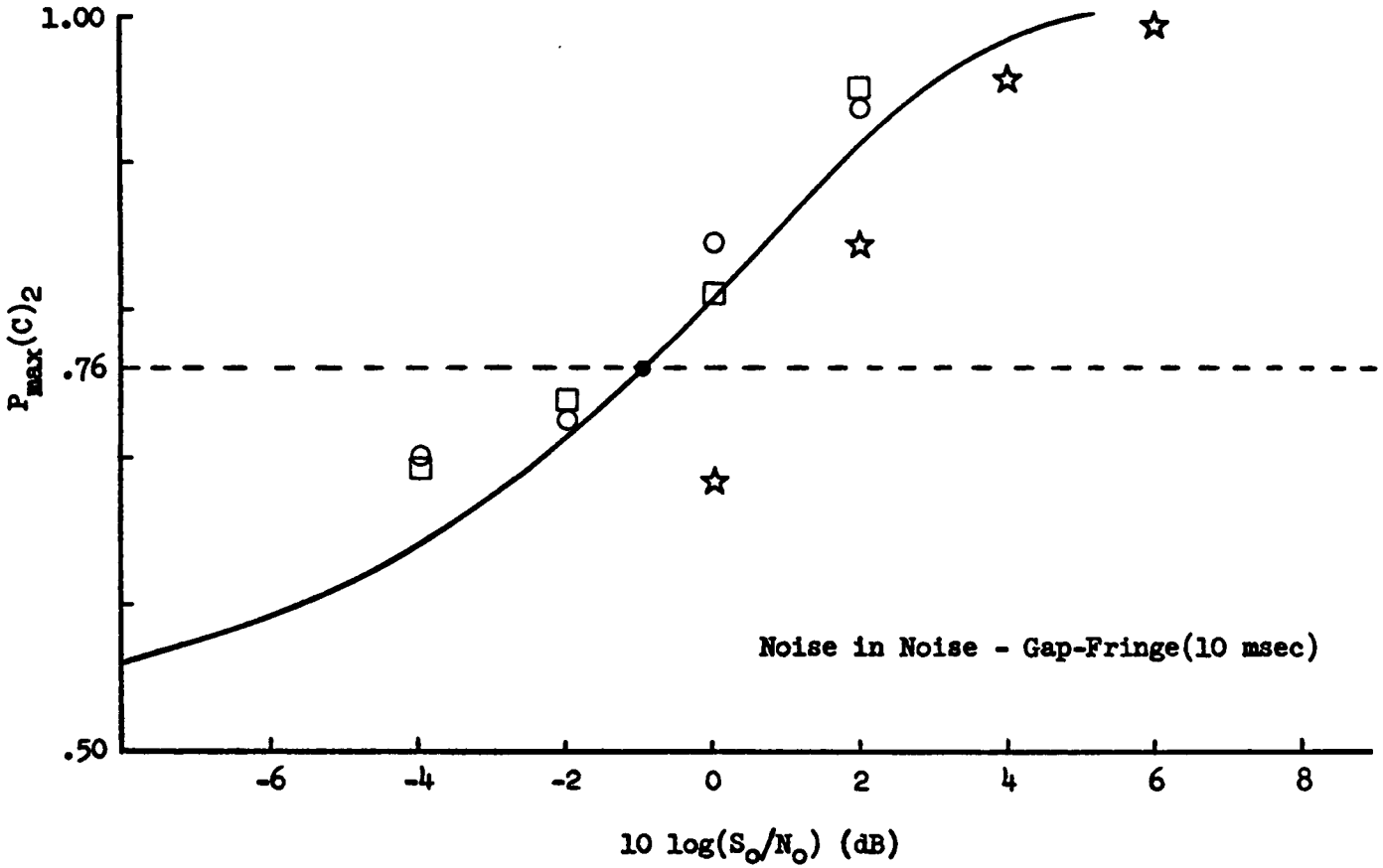
1.00
.76
.50
$P_{max}(C)_2$
-6
-4
-2
0
2
4
6
8
10 log(S_o/N_o) (dB)
Noise in Noise - Gap-Fringe(10 msec)

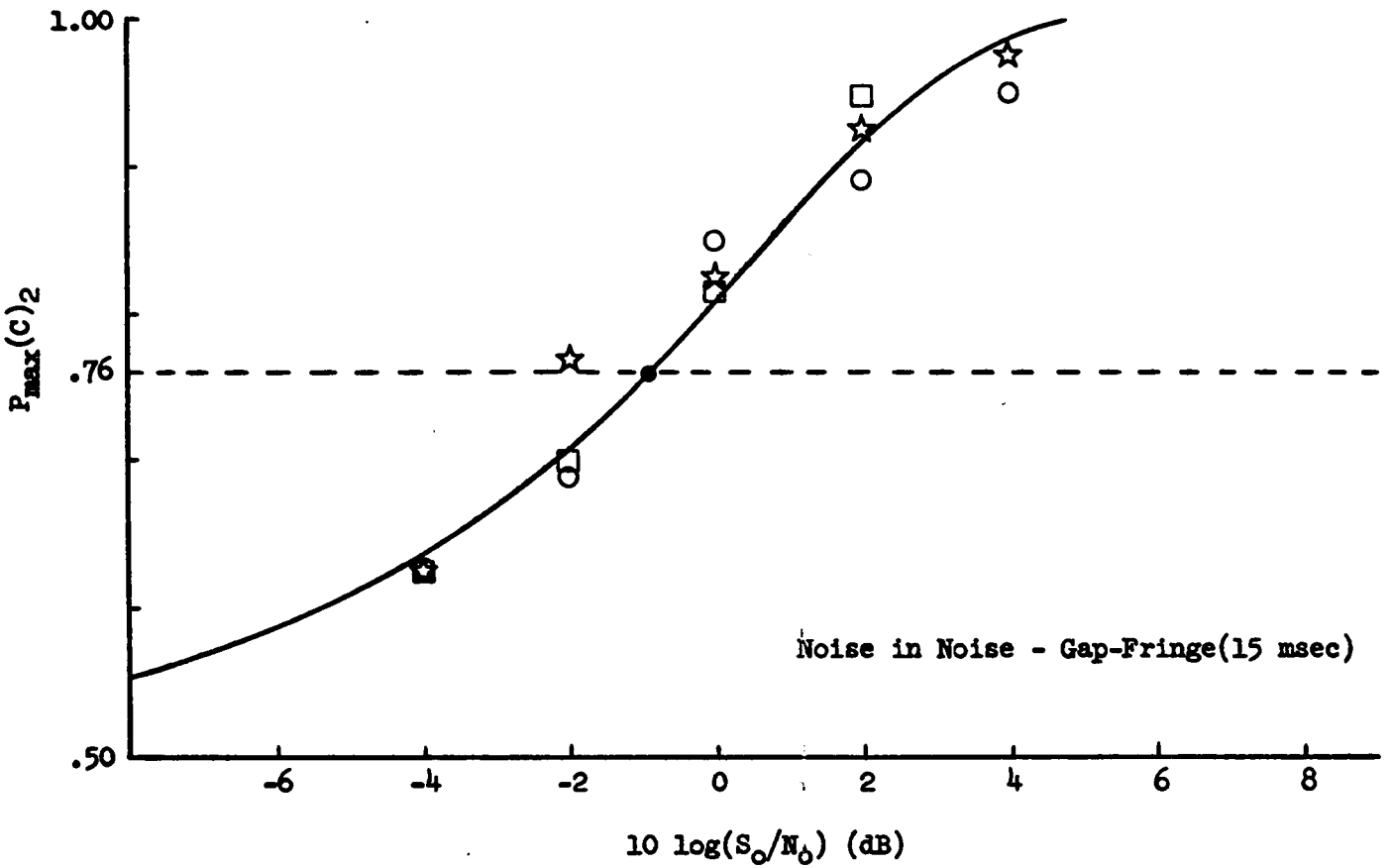
1.00
.76
.50
$P_{max}(C)_2$
-6
-4
-2
0
2
4
6
8
10 log(S_o/N_o) (dB)
Noise in Noise - Gap-Fringe(15 msec)

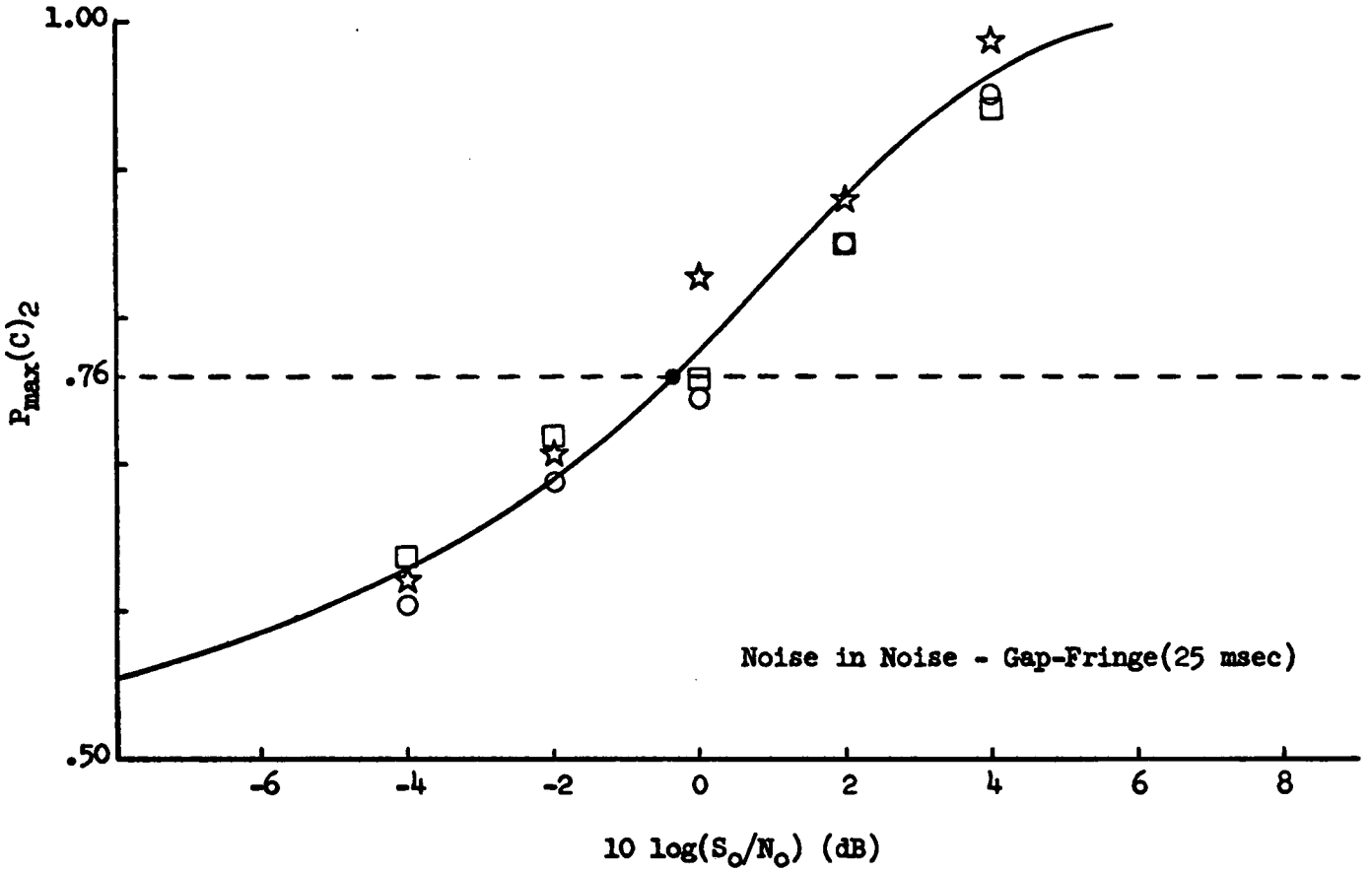
1.00
.76
.50
$P_{max}(C)_2$
-6
-4
-2
0
2
4
6
8
10 log(S_o/N_o) (dB)
Noise in Noise - Gap-Fringe(25 msec)

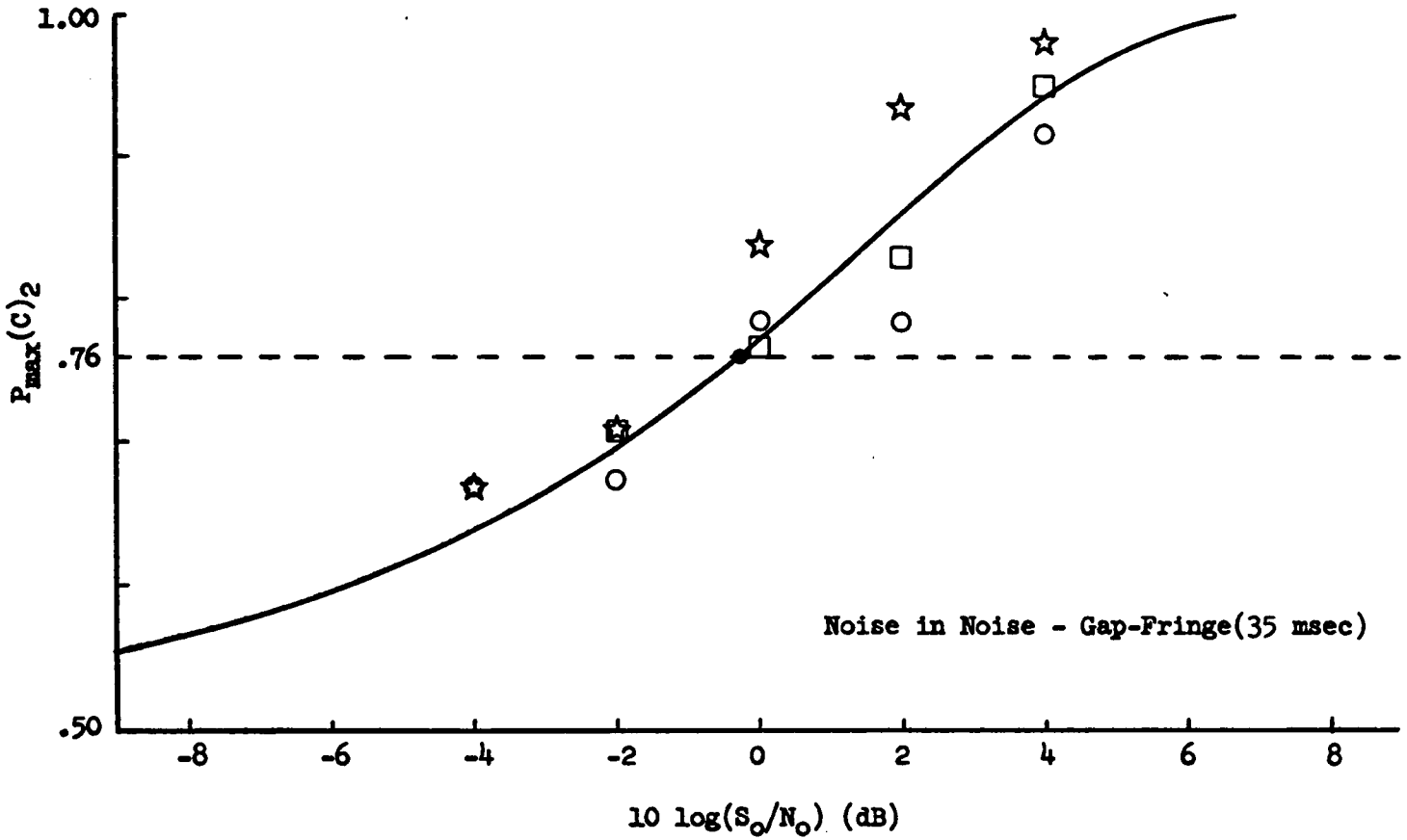
1.00
.76
.50
$P_{max}(C)_2$
-8
-6
-4
-2
0
2
4
6
8
10 log(S_o/N_o) (dB)
Noise in Noise - Gap-Fringe(35 msec)

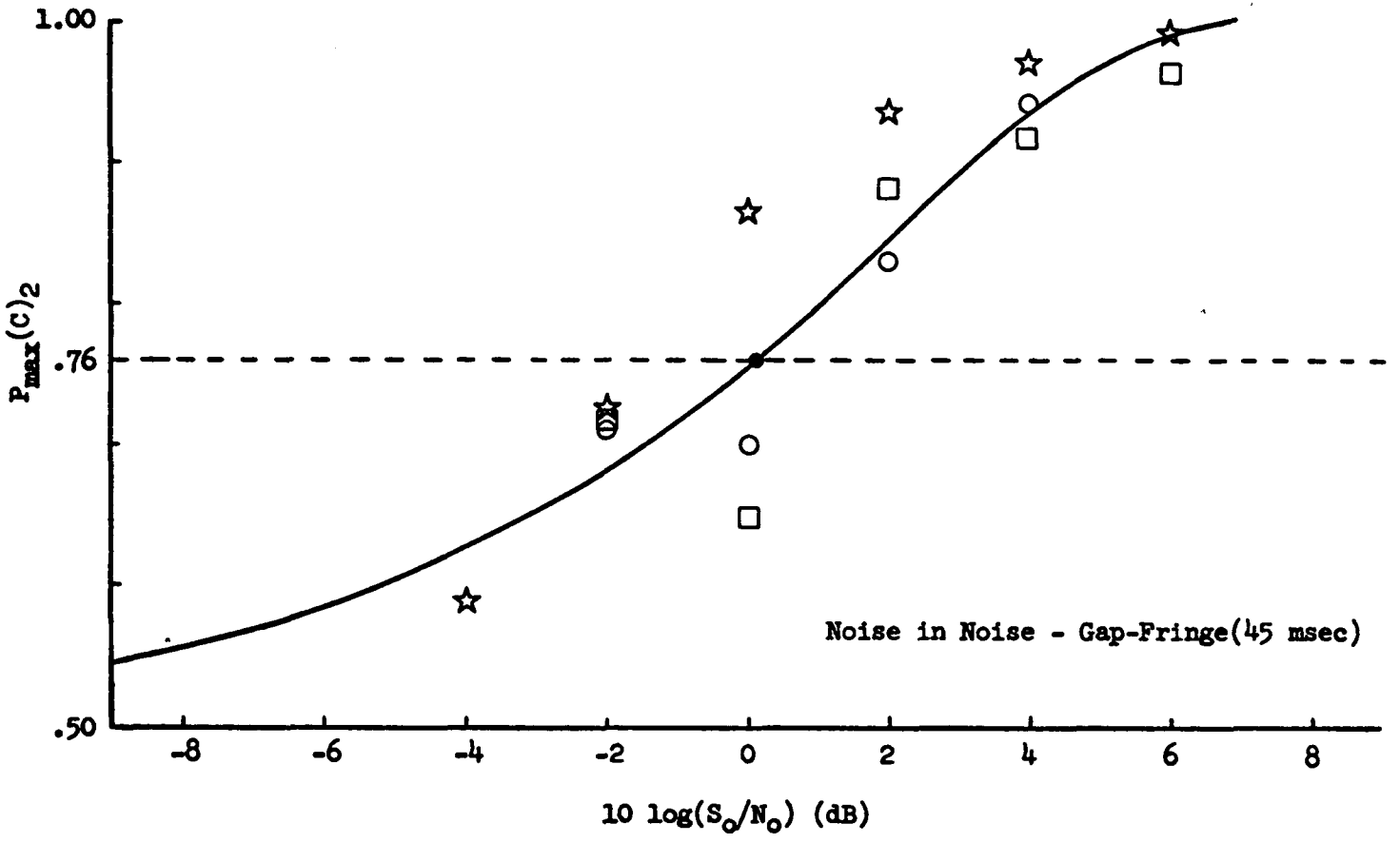
1.00
.76
.50
$P_{max}(c)_2$
-8
-6
-4
-2
0
2
4
6
8
10 log(S_o/N_o) (dB)
Noise in Noise - Gap-Fringe(45 msec)

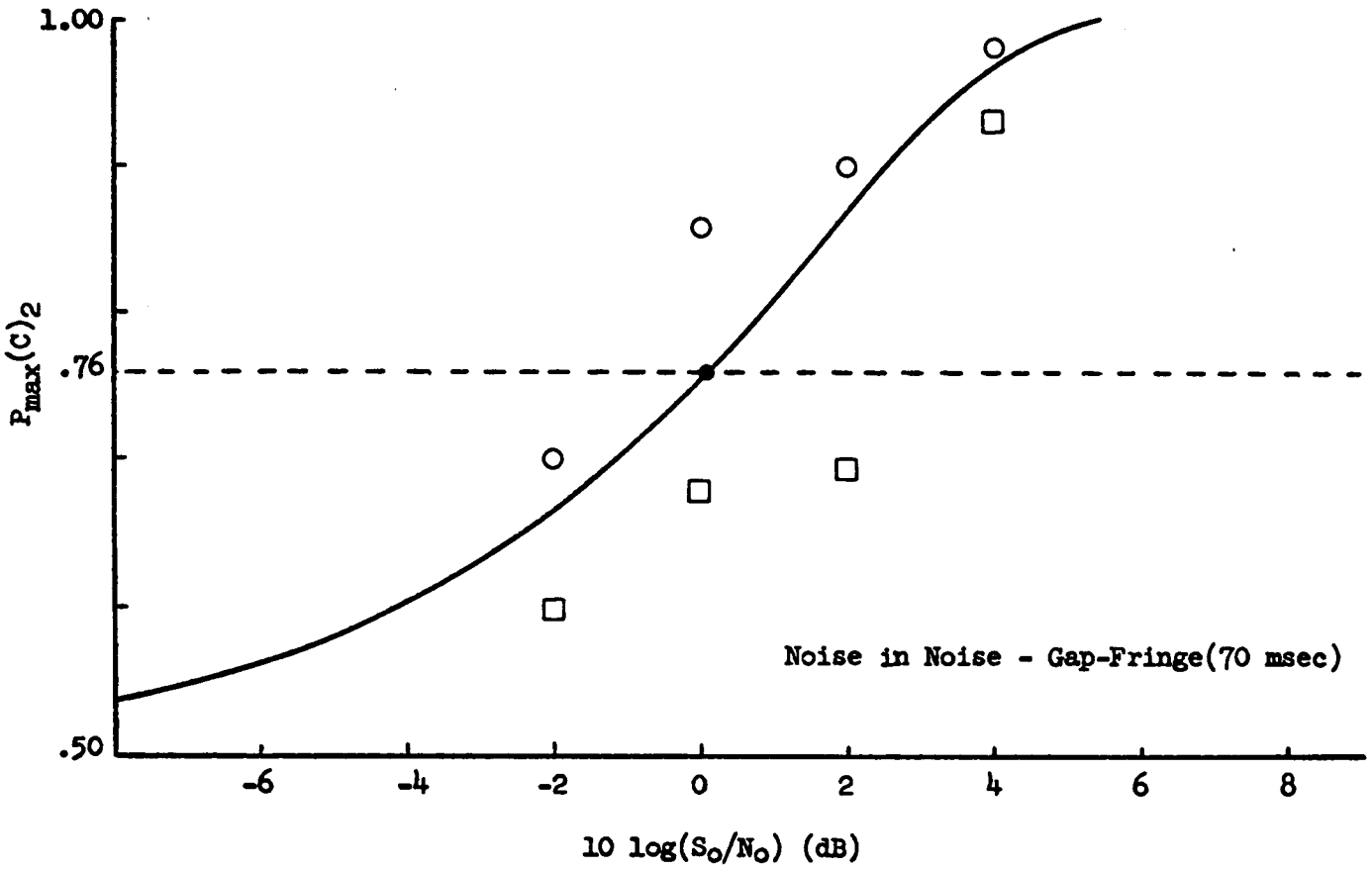
1.00
.76
.50
$P_{max}(C)_2$
-6
-4
-2
0
2
4
6
8
10 log(S_o/N_o) (dB)
Noise in Noise - Gap-Fringe(70 msec)

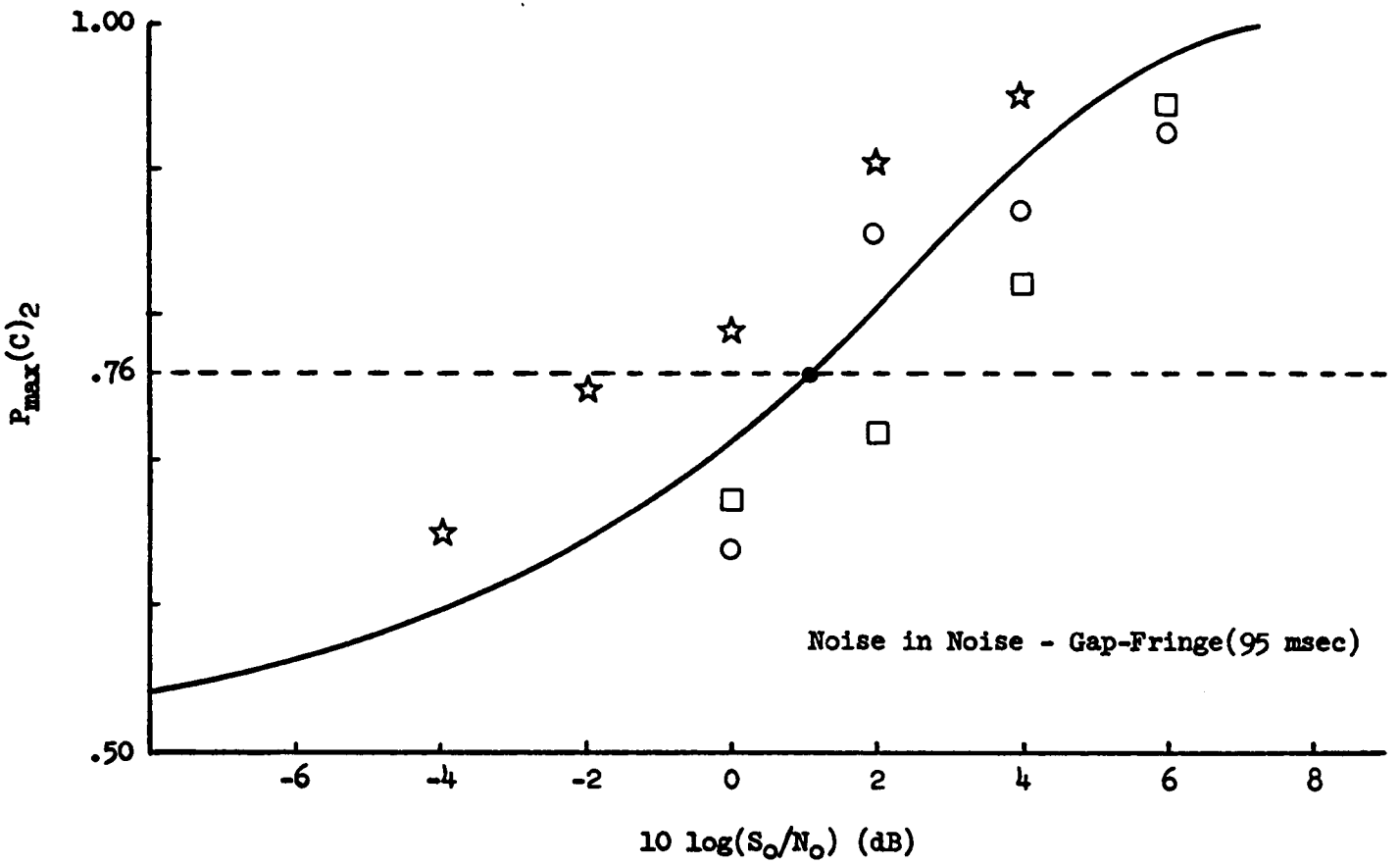
1.00
.76
.50
$P_{max}(C)_2$
-6
-4
-2
0
2
4
6
8
10 log(S_o/N_o) (dB)
Noise in Noise - Gap-Fringe(95 msec)

Table AE1. $P_{max}(C)_2$, in noise-fringe conditions, for detection of a tonal signal masked by a wideband noise (46.1 dB SPL) for variations in signal intensity levels and temporal settings, subject: PT.

Duration (msec)	10 log(E_s/N_o) (dB)												
	-1.5	0.5	2.5	3.1	4.5	5.1	6.5	7.1	8.5	9.1	10.5	11.1	13.1	15.1	17.1	19.1
0			.65		.74		.83		.90		.94					
5				.61		.74		.75		.78		.89	.95	.97		
10						.68		.74		.80		.87	.92	.98		
15						.68		.71		.84		.83	.92	.94	.98	
25								.64		.70		.87	.91	.97	.98	
35												.77	.88	.96	.99	
45												.72	.81	.88	.96	.98
70																
95								.62		.74		.87	.96	.99		

Table AE2. $P_{max}(C)_2$, in noise-fringe conditions, for detection of a tonal signal masked by a wideband noise (46.1 dB SPL) for variations in signal intensity levels and temporal settings, subject: HT.

Duration (msec)	10 log(E_s/N_o) (dB)											
	-1.5	0.5	2.5	3.1	4.5	5.1	6.5	7.1	8.5	9.1	10.5	11.1	13.1	15.1	17.1	19.1
0	.64	.74	.73		.87		.91		.93							
5				.64		.77		.78		.89		.94				
10						.67		.70		.89		.95	.98			
15						.68		.74		.77		.85	.92	.96		
25								.67		.69		.77	.91	.91	.92	
35								.67		.74		.82	.90	.91		
45								.66		.82		.86	.94			
70								.63		.71		.89	.95			
95								.60		.78		.84	.93	.98		

Table AE3. $P_{max}(C)_2$, in noise-fringe conditions, for detection of a tonal signal masked by a wideband noise (46.1 dB SPL) for varations in signal intensity levels and temporal settings, subject: SP.

	10 log(E_s/N_o) (dB)													
Duration (msec)	-1.5	0.5	2.5	3.1	4.5	5.1	6.5	7.1	8.5	9.1	10.5	11.1	13.1	15.1	17.1	19.1
0			.68		.76		.87		.90		.98					
5				.66		.74		.76		.83		.86	.94			
10						.60		.74		.70		.85	.87	.93		
15						.63		.66		.81		.81	.92	.93		
25						.60		.71		.80		.89	.96			
35								.63		.71		.87	.97			
45								.66		.67		.89	.97			
70								.61		.69		.92	.98			
95						.61		.75		.90		.97				

Table AE4. $P_{max}(C)_2$, in gap-fringe conditions, for detection of a tonal signal masked by a wideband noise (46.1 dB SPL) for variations in signal intensity levels and temporal settings, subject: PT.

Duration (msec)	10 log(E_s/N_o) (dB)									
	0.5	2.5	4.5	5.1	6.5	7.1	8.5	9.1	10.5	11.1	12.5
0				.63		.78		.94		.99	
5			.61		.76		.87		.96		
10			.71		.85		.96		.99		
15	.59	.68	.80		.82		.96		.99		
25			.73		.86		.90		.98		
35		.69	.77		.81		.93		.98		
45			.63		.77		.87		.94		.99
70											
95		.64	.72		.88		.97		.97		

Table AE5. $P_{max}(C)_2$, in gap-fringe conditions, for detection of a tonal signal masked by a wideband noise (46.1 dB SPL) for variations in signal intensity levels and temporal settings, subject: HT.

	10 log(E_s/N_o) (dB)									
Duration (msec)	0.5	2.5	4.5	5.1	6.5	7.1	8.5	9.1	10.5	11.1	12.5
0				.68		.84		.97			
5			.61		.76		.89		.98		
10		.65	.77		.92		.97				
15	.60	.70	.75		.87		.96				
25		.63	.75		.84		.87		.98		
35		.63	.71		.86		.93				
45		.64	.76		.92		.95				
70		.62	.76		.85		.85				
95		.58	.76		.79		.85		.95		

Table AE6. $P_{max}(C)_2$, in gap-fringe conditions, for detection of a tonal signal masked by a wideband noise (46.1 dB SPL) for variations in signal intensity levels and temporal settings, subject: SP.

Duration (msec)	10 log(E_s/N_o) (dB) 0.5	2.5	4.5	5.1	6.5	7.1	8.5	9.1	10.5	11.1	12.5
0				.62		.84		.96			
5		.61	.61		.86		.94		.98		
10		.66	.72		.81		.96		.99		
15		.73	.79		.92		.94				
25		.66	.74		.89		.94		.99		
35		.66	.81		.83		.95				
45		.63	.67		.81		.92		.98		
70		.65	.79		.90		.95		.98		
95		.63	.68		.83		.88		.94		

Table AE7. $P_{max}(C)_2$, in noise-fringe conditions, for detection of a noise signal masked by a wideband noise (46.1 dB SPL) for variations in signal intensity levels and temporal settings, subject: PT.

Duration (msec)	10 log(S_o/N_o) (dB)											
	-6.0	-5.4	-4.0	-3.4	-2.0	-1.4	0.0	0.6	2.0	2.6	4.0	4.6	6.6
0	.61		.69		.75		.88		.94				
5		.64		.75		.81		.91					
10						.68		.83		.92		.93	
15						.68		.83		.94		.98	.99
25				.62		.75		.82		.94		.97	
35						.59		.77		.92		.99	.99
45						.68		.82		.96		.99	
70													
95				.63		.73		.90		.96		.99	

Table AE8. $P_{max}(C)_2$, in noise-fringe conditions for detection of a noise signal masked by a wideband noise (46.1 dB SPL) for variations in signal intensity levels and temporal settings, subject: HT.

Duration (msec)	10 log(S_o/N_o) (dB)											
	-6.0	-5.4	-4.0	-3.4	-2.0	-1.4	0.0	0.6	2.0	2.6	4.0	4.6	6.6
0					.64		.79		.85		.93		
5		.62		.68		.69		.77		.85		.94	
10				.60		.71		.79		.83		.97	
15						.62		.76		.86		.92	.97
25						.60		.65		.77		.93	
35						.63		.71		.85		.93	
45						.64		.68		.81		.95	
70						.63		.73		.89		.94	
95						.60		.65		.81		.93	

Table AE9. $P_{max}(C)_2$, in noise-fringe conditions for detection of a noise signal masked by a wideband noise (46.1 dB SPL) for variations in signal intensity levels and temporal settings, subject: SP

Duration (msec)	10 log(S_o/N_o) (dB) -6.0	-5.4	-4.0	-3.4	-2.0	-1.4	0.0	0.6	2.0	2.6	4.0	4.6	6.6
0					.71		.76		.85		.90		
5								.70		.76		.87	.96
10						.67		.74		.84		.85	.98
15						.64		.71		.75		.88	.98
25								.69		.66		.80	.93
35						.59		.69		.85		.96	.97
45								.69		.86		.96	
70								.72		.89		.98	
95								.73		.91		.96	

Table AE10. $P_{max}(C)_2$, in gap-fringe conditions, for detection of a noise signal masked by a wideband noise (46.1 dB SPL) for variations in signal intensity levels and temporal settings, subject: PT.

Duration (msec)	10 log(S_o/N_o) (dB)											
	-4.0	-3.4	-2.0	-1.4	0.0	0.6	2.0	2.6	4.0	6.0
0				.63		.91		.99		
5			.72		.84		.95		.99	
10					.69		.85		.96	.99
15	.63		.77		.83		.93		.98	
25	.62		.71		.83		.88		.99	
35	.67		.71		.84		.94		.98	
45	.59		.73		.87		.94		.97	.99
70										
95	.65		.75		.79		.91		.98	

Table AE11. $P_{max}(C)_2$, in gap-fringe conditions, for detection of a noise signal masked by a wideband noise (46.1 dB SPL) for variations in signal intensity levels and temporal settings, subject: HT.

Duration (msec)	10 log(S_o/N_o) (dB)											
	-4.0	-3.4	-2.0	-1.4	0.0	0.6	2.0	2.6	4.0		6.0	
0		.59		.76		.87		.98				
5			.63		.72		.91		.98			
10	.70		.73		.85		.94					
15	.63		.69		.85		.89		.95			
25	.61		.69		.75		.85		.95			
35	.67		.68		.79		.79		.92			
45			.71		.70		.83		.94			
70			.60		.68		.80		.93			
95					.64		.86		.87		.93	

Table AE12. $P_{max}(C)_2$, in gap-fringe conditions, for detection of a noise signal masked by a wideband noise (46.1 dB SPL) for variations in signal intensity levels and temporal settings, subject: SP.

	10 log(S_o/N_o) (dB)											
Duration (msec)	-4.0	-3.4	-2.0	-1.4	0.0	0.6	2.0	2.6	4.0		6.0	
0				.79		.96						
5	.71		.81		.91		.96					
10	.69		.74		.81		.95					
15	.63		.70		.82		.95					
25	.64		.72		.76		.85		.94			
35			.71		.77		.83		.96			
45			.72		.65		.88		.92		.96	
70			.70		.86		.90		.98			
95					.68		.72		.82		.95	

BIBLIOGRAPHY

Berg, K., and Yost, W. A. (1976) "Temporal Masking of a Click by Noise in Diotic and Dichotic Listening Conditions," J. Acoust. Soc. Am. 60, 173-177.

Blodgett, H. D., Jeffress, L. A., and Taylor, R. W. (1958). "Relation of Masked Thresholds to Signal Duration for Various Interaural Phase-Combinations," Am. J. Psychol. 71, 283-290.

Campbell, R. A. (1966). "Auditory Intensity Perception and Neural Coding," J. Acoust. Soc. Am. 39, 1030-1033.

Campbell, R. A. (1969). "Threshold re Duration and Levels of a Continuous or Gated Masker," J. Acoust. Soc. Am. 46, 895-897.

Crawford, B. H. (1947). "Visual Adaptation in Relation to Brief Conditioning Stimuli," Proc. Roy. Soc. B134, 283-302.

Deatherage, B. H., and Evans, T. R. (1969). "Binaural Masking: Backward, Forward, and Simultaneous Effects," J. Acoust. Soc. Am. 46, 362-371.

De Boer, E. (1966). "Intensity Discrimination of Fluctuating Signals," J. Acoust. Soc. Am. 40, 552-560.

Dolan, T. R., and Trahiotis, C. (1972). "Binaural Interaction in Backward Masking," Percept. Psychophys. 11. 92-94.

Duifhuis, H. (1973). "Consequences of Peripheral Frequency Selectivity for Nonsimultaneous Masking," J. Acoust. Soc. Am. 54, 1471-1488.

Egan, J. P. (1965). "Masking-Level Differences as a Function of Interaural Disparities in Intensity of Signal and of Noise,"

J. Acoust. Soc. Am. 38, 1043-1049.

Egan, J. P., Lindner, W. A., and McFadden, D. (1969). "Masking-Level Differences and the Form of Psychometric Function," Percept. and Psychophys. 4, 209-215.

Elliott, L. L. (1962a). "Backward and Forward Masking of Probe Tones of Different Frequencies," J. Acoust. Soc. Am. 34, 1116-1117.

Elliott, L. L. (1962b). "Backward Masking: Monotic and Dichotic Conditions," J. Acoust. Soc. Am. 34, 1108-1115.

Elliott, L. L. (1964). "Backward Masking, Different Durations of the Masking Stimulus," J. Acoust. Soc. Am. 36, 393.

Elliott, L. L. (1965). "Changes in the Simultaneous Masked Threshold of Brief Tones," J. Acoust. Soc. Am. 38, 738-746.

Elliott, L. L. (1967). "Development of Auditory Narrow-Band Frequency Contours," J. Acoust. Soc. Am. 42, 143-153.

Elliott, L. L. (1969). "Masking of Tones before, During, and After Brief Silent Periods in Noise," J. Acoust. Soc. Am. 45, 1277-1279.

Elliott, L. L. (1971). "Backward and Forward Masking," Audiology, 10, 65-76.

Fastl, H. (1976). "Temporal Masking Effects II. Critical Band Noise Masker," Acustica, 36, 317-331.

Fletcher, H. (1940). "Auditory Patterns," Rev. Mod. Phys. 12, 47-65.

Fletcher, H. (1953). Speech and Hearing in Communication, 2nd ed. (D Van Nostrand, New York).

Garner, W. R., and Miller, G. A. (1947). "The Masked Threshold of Pure Tones as a Function of Duration," J. Exp. Psychol. 37. 293-303.

Green, D. M., Birdsall, T. G., and Tanner, W. P. Jr. (1957). "Signal Detection as a Function of Signal Intensity and Duration," J. Acoust. Soc. Am. 29, 523-531.

Green, D. M. (1960a). "Auditory Detection of a Noise Signal," J. Acoust. Soc. Am. 32, 121-131.

Green, D.M. (1960b). "Psychoacoustics and Detection Theory," J. Acoust. Soc. Am. 32, 1189-1203.

Green, D. M., and Sewall, S. T. (1962). "Effects of Background noise on Auditory Detection of Noise Bursts," J. Acoust. Soc. Am. 34, 1207-1216.

Green, D. M. (1964a). "Continuous versus Gated Masking for Noise and Sinusoidal Masker," J. Acoust. Soc. Am. 36, 2009(A).

Green, D. M. (1964b). "Consistency of Auditory Detection Judgments," Psychol. Rev. 71, 392-407.

Green, D. M. (1966). "Interaural Phase Effects in the Masking of Signals of Different Durations," J. Acoust. Soc. Am. 39, 720-724.

Green, D. M., and Swets, J. A. (1966). Signal Detection Theory and Psychophysics, (Wiley, New York).

Green, D. M. (1969). "Masking with Continuous and Pulased Sinusoids," J. Acoust. Soc. Am. 46, 939-946.

Green, D. M., and Henning, G. B. (1969). "Audition," Ann. Rev. Psychol. 20, 105-128.

Green, D. M., and McGill, W. J. (1970). "On the Equivalence of Detection Probabilities and Well-Known Statistical Quantities," Psychol. Rev. 41, 294-301.

Greenwood, D. D. (1961a). "Auditory Masking and the Critical Band," J. Acoust. Soc. Am. 33, 484-502.

Greenwood, D. D. (1961b). "Critical Bandwidth and the Frequency Coordinates of the Basilar Membrane," J. Acoust. Soc. Am. 33, 1344-1356.

Hamilton, P. M. (1957). "Noise Masked Thresholds as a Function of Tonal Duration and Masking Noise Band Width," J. Acoust. Soc. Am. 29, 506-511.

Hawkins, J. E., Jr., and Stevens, S. S. (1950). "The Masking of Pure Tones and of Speech by White Noise," J. Acoust. Soc. Am. 22, 6-13.

Helmholtz, H. L. F. (1885). The Sensation of Tone, 2nd ed. (Longrass, Green, New York).

Jeffress, L. A. (1964). "Stimulus-Oriented Approach to Detection," J. Acoust. Soc. Am. 36, 766-774.

Jeffress, L. A. (1968). "Mathematical and Electrical Models of Auditory Detection," J. Acoust. Soc. Am. 44, 187-203.

Jeffress, L. A. (1970). "Masking," In Foundations of Modern Auditory Theory Vol.I, Edited by J. V. Tobias. (Academic Press, New York). 85-114.

Jeffress, L. A. (1975). "Masking of Tone by Tone as a Function of Duration," J. Acoust. Soc. Am. 58, 399-403.

Lakey, J. R. (1976). "Temporal Masking-Level Differences: The Effect of Mask Duration," J. Acoust. Soc. Am. 59, 1434-1442.

Leshowitz, B., and Raab, D. H. (1967). "Effects of Stimulus Duration on the Detection of Sinusoids Added to Continuous Pedestals," J. Acoust. Soc. Am. 41, 487-496.

Leshowitz, B., Taub, H. B., and Raab, D. H. (1968). "Visual Detection of Signals in the Presence of Continuous and Pulsed Backgrounds," Percept. and Psychophys. 4, 207-213.

Leshowitz, B. (1969). "Receiver Operating Characteristics and Psychometric Functions Determined under Simple and Pedestal Detection Condition," J. Acoust. Soc. Am. 45, 1474-1484.

Leshowitz, B., and Cudahy, E. (1972). "Masking with Continuous and Gated Sinusoids," J. Acoust. Soc. Am. 51, 1921-1929.

Luce, R. D., and Green, D. M. (1972). "A Neural Timing Theory for Response Times and the Psychophysics of Intensity," Psychol. Rev. 79, 14-57.

Lynn, G. K., and Small, A. M. (1977). "Interactions of Backward and Forward Masking," J. Acoust. Soc. Am. 61, 185-189.

Marill, T. M. (1956). "Detection Theory and Psychophysics," Massachusetts Institute of Technology: Research Laboratories of Electronics, Technical Report No. 319.

Mathews, M. V., and Pfafflin, S. M. (1965). "Effect of Filter Type on Energy-Detection Models for Auditory Signal Detection," J. Acoust. Soc. Am. 38, 1055-1056.

McFadden, D. (1966). "Masking-Level Differences with Continuous and with Burst Masking Noise," J. Acoust. Soc. Am. 40, 1414-1419.

McGill, W. J. (1967). "Neural Counting Mechanism and Energy Detection in Audition," J. Math. Psychol. 4, 351-376.

McGill, W. J. (1968a). "Polynomial Psychometric Functions in Audition," J. Math. Psychol. 5, 369-376.

McGill, W. J. (1968b). "Variations on Marill's Detection Formula," J. Acoust. Soc. Am. 43, 70-73.

Miller, G. A. (1947). "Sensitivity to Changes in the Intensity of White Noise and its Relation to Masking and Loudness," J. Acoust. Soc. Am. 19, 609-619.

Moore, T. J., and Welsh, J. R. (1970). "Forward and Backward Enhancement of Sensitivity in the Auditory System," J. Acoust. Soc. Am. 47, 534-539.

Munson, W. A. (1947). "The Growth of Auditory Sensation," J. Acoust. Soc. Am. 19, 584-591.

Osman, E., and Raab, D. H. (1963). "Temporal Masking of Clicks by Noise Bursts," J. Acoust. Soc. Am. 35, 1939-1941.

Osman, E. (1971). "A Correlation Model of Binaural Masking Level Differences," J. Acoust. Soc. Am. 50, 1494-1511.

Osman, E., Tzuo, H., and Tzuo, P. L. (1975). "Theoretical Analysis of Detection of Monaural Signals as a Function of Interaural Noise Correlation and Signal Frequency," J. Acoust. Soc. Am. 57, 939-942.

Osman, E. (1975). "Signal-Noise Duration, Psychophysical Procedure Interaural Configuration, and the Psychometric Function," J. Acoust. Soc. Am. 58, 243-248.

Osman, E. (1980, unpublished). "Psychometric Functions for Binaural Temporal Masking of Tones by Noise,"

Osman, E., Tzuo, H., and Tzuo, P. L. (1980, unpublished) "Psychometric Function for Detection of A Brief Tone Burst in Continuous and Gated Noise Masker: Consistent Effects with Practice and Psychophysical Task,"

Patterson, R. D. (1974). "Auditory Filter Shape," J. Acoust. Soc. Am. 55, 802-809.

Patterson, R. D., and Henning, G. B. (1977). "Stimulus Variability and Auditory Filter Shape," J. Acoust. Soc. Am. 62, 649-664.

Penner, M. J., Robinson, C. E., and Green, D. M. (1972). "Critical Masking Interval," J. Acoust. Soc. Am. 52, 142.

Penner, M.J., and Cudahy, E. (1973). "Measurement of the Critical Masking Interval," J. Acoust. Soc. Am. 53, 376.

Penner, M. J., and Cudahy, E. (1973). "Critical Masking Interval: A Temporal Analog of the Critical Band," J. Acoust. Soc. Am. 54, 1530-1534.

Penner, M.J. (1974). "Effect of Masker Duration and Masker Level on Forward and Backward Masking," J. Acoust. Soc. Am. 56, 179-182.

Penner, M. J., Cudahy, E., Jenkins, G. W. (1974). "The Effect of Masker Duration on Forward and Backward Masking," Percpt. and Psychophys. 15, 405-410.

Penner, M. J. (1975). "Persistence and Integration: Two Consequences of A sliding Integrator," Percpt. and Psychophys, 18, 114-120.

Penner, M. J. (1978). "A Power Law Transformation Resulting in A Class of Short-Term Integrators That Produce Time-Intensity Trades for Noise Bursts," J. Acoust. Soc. Am. 63, 195-201.

Pfafflin, S. M., and Mathews, M. V. (1962). "Energy Detection Model for Monaural Auditory Detection," J. Acoust. Soc. Am. 34, 1842-1853.

Pickett, J. M. (1959). "Backward Masking," J. Acoust. Soc. Am. 31, 1613-1615.

Plomp, R., and Bouman, M. A. (1959). "Relation Between Hearing Threshold and Duration for Tone Pulsed," J. Acoust. Soc. Am. 31, 749-758.

Pollack, I. (1964). "Interaction of Forward and Backward Masking," J. Auditory Res. 4, 63-67.

Raab, D. H. (1961). "Forward and Backward Masking between Acoustic Clicks," J. Acoust. Soc. Am. 33, 137-139.

Raab, D. H. (1963). "Backward Masking," Psychol. Bull. 60, 118-129.

Raab, D. H., Osman, E., and Rich, E., (1963). "Effects of Wavefrom Correlation and Signal Duration," J. Acoust. Soc. Am. 35, 1942-1946.

Rayleigh, J. W. S. (1945). The Theory of Sound, Vol. 1, 2nd ed. (Dover, New York).

Robinson, D. E., and Trahiotis, C. (1972). "Effects of Signal Duration and Masker Duration on Detectability under Diotic and Dichotic Listening Conditions," Percept. and Psychophys. 12, 333-334.

Samoilova, I. K. (1959). "Masking of Short Tone Signals as a Function of the Time Interval Between Masked and Masking Sounds," Biofizika, 4, 550-558.

Schacknow, P. N., and Raab, D. H. (1976). "Noise-Intensity Discrimination: Effects of Bandwidth Conditions and Mode of Masker Presentation," J. Acoust. Soc. Am. 60, 893-905.

School, H. (1962). "Das Dynanische Verhalten des Gehors bei der Unterteilung des Schallspektrums in Frequenzgruppen," Acustica, 12, 101-107.

Siebert, W. M. (1968). "Stimulus Transformation in the Peripheral Auditory System," In Recognignizing Patterns, Edited by P. A. Kolers and M. Eden (MIT Press, Cambridge, Mass) 104-133.

Smiarouski, R. A., and Carhart, R. (1975). "Relation Among Temporal Resolution, Forward Masking, and Simultaneous Masking," J. Acoust. Soc. Am. 57, 1169-1174.

Swets, J. A. (1964). Signal Detection And Recognition by Human Observers: Contemporary Readings, (Ed.) (John Wiley and Sones, New York).

Tanner, W. P. Jr., and Birdsall, T. G. (1958). "Definition of d' and η as Psychophysical Measures," J. Acoust. Soc. Am. 30, 922-928.

Treisman, M. (1965). "Signa; Detection Theory and Crozier's Law: Derivation of a New Sensory Scaling," J. Math. Psychol. 2, 205-218.

Tucker, A., Evans, R. B., and Jeffress, L. A. (1966). "Effect of Duration Upon Detection with Gated and Continuous Noise and Signal," J. Acoust. Soc. Am. 40, 1250.

Tucker, A., Williams, P. I., and Jeffress, L. A. (1968). "Effect of Signal Duration on Detection for Gated and for Continuous Noise," J. Acoust. Soc. Am. 44, 813-816.

Viemeister, N. F. (1974). "Detection of a Noise Signal: The Effects of Duration and Masker Level," J. Acoust. Soc. Am. 88th Meeting.

Watson, C. S., and Gengel, R. W. (1969). "Signal Duration and Signal Frequency in Realtion to Auditory Sensitivity," J. Acoust. Soc. Am. 46, 989-997.

Wier, C. C., Green, D. M., Hafter, E. R., and Burkhardt, S. (1977). "Detection of a Tone Burst in Continuous-and Gated Noise Maskers; Defects of Signal Frequency, Duration, and Masker Level," J. Acoust. Soc. Am. 61, 1298-1300.

Wightman, F. L., and Green, D. M. (1966). "Effect of Duration on Detection of a Noise Signal," J. Acoust. Soc. Am. 40, 1250.

Wright, H. N. (1964a). "Temporal Summation and Backward Masking," J. Acoust. Soc. Am. 36, 927-932.

Wright, H. N. (1964b). "Backward Masking for Tones in Narrow-Band Noise," J. Acoust. Soc. Am. 36, 2217-2221.

Zwicker, E., Flottorp, G., and Stevens, S. S. (1957). "Critical Bandwidth in Loudness Summation," J. Acoust. Soc. Am. 29, 548-557.

Zwicker, E., and Wright, H. N. (1963). "Temporal Summation for Tones in Narrow-Band Noise," J. Acoust. Soc. Am. 35, 691-699.

Zwicker, E. (1965a). "Temporal Effects in Simultaneous Masking by White-Noise Bursts," J. Acoust. Soc. Am. 37, 653-663.

Zwicker, E. (1965b). "Temporal Effects in Simultaneous Masking and Loudness," J. Acoust. Soc. Am. 38, 132-141.

Zwicker, E., and Fastl, H. (1972). "On the Development of the Critical Band," J. Acoust. Soc. Am. 52, 699-702.

Zwislocki, J. (1960). "Theory of Temporal Auditory Summation," J. Acoust. Soc. Am. 32, 1046-1060.

Zwislocki, J. J. (1969). "Temporal Summation of Loudness: An Analysis," J. Acoust. Soc. Am. 46, 431-441.